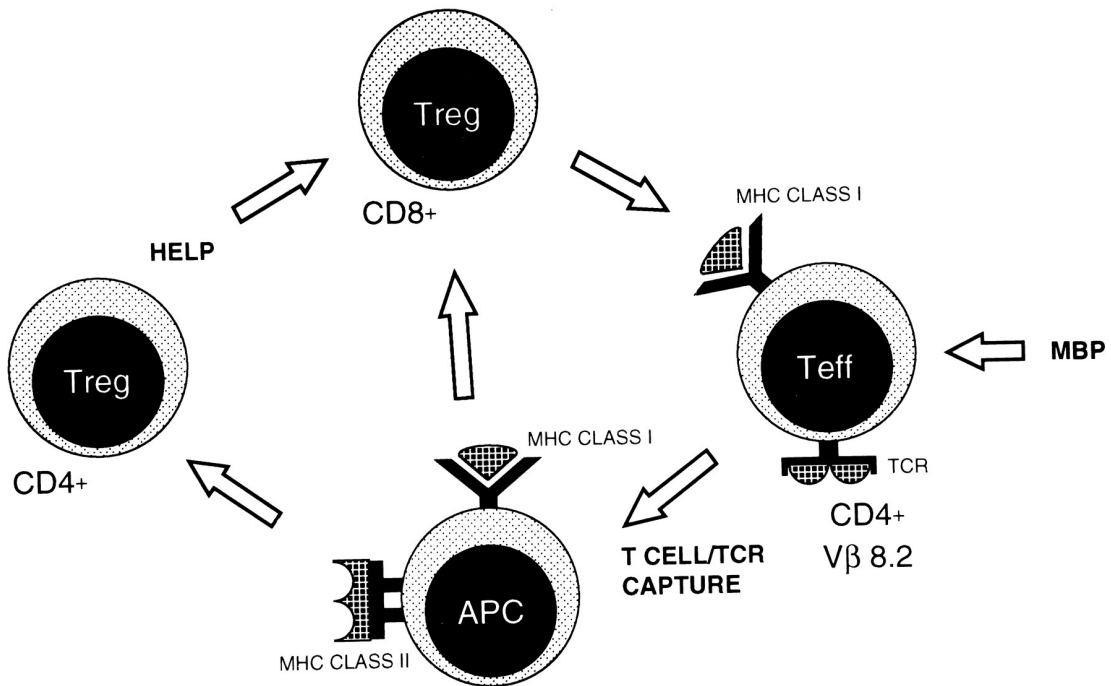


Theoretical Physiology

Rob de Boer, Theoretical Biology, UU

2006



Contents

1	Introduction	7
1.1	The simplest possible model	7
1.2	Exponential growth and decay	9
1.3	Summary	10
1.4	Exercises	11
2	Population growth	15
2.1	Birth and death	15
2.2	Density dependent death	17
2.3	Density dependent birth	18
2.4	Logistic growth	19
2.5	Stability and return time	20
2.6	Summary	22
2.7	Exercises	22
3	Interacting populations	27
3.1	Viral infection	27
3.2	Immune response	29
3.3	Exercises	31
4	Saturation functions	33
4.1	Exercises	35
5	Gene regulation	37
5.1	Separation of time scales	38
5.2	Lac-operon	38
5.3	Summary	42
5.4	Exercises	42
6	Periodic behavior	45
6.1	Circadian rhythm	46
6.2	Quasi steady state	49
6.3	Summary	51
6.4	Exercises	51

7	Chronic viral infections and immune control	55
7.1	Immune response	55
7.2	Separation of time scales	58
7.3	Summary	59
7.4	Exercises	59
8	Competitive exclusion	63
8.1	Exercises	64
9	The Hodgkin-Huxley model	67
9.1	Hodgkin-Huxley model	69
9.2	Quasi steady state	73
9.3	Exercises	75
10	T cell vaccination	79
10.1	Model	80
10.2	Steady states	82
10.3	TCV virtual experiments	84
10.4	Exercises	87
11	TCR rearrangement excision circles	89
11.1	Model	90
11.2	Homeostasis	92
11.3	Parameters	93
11.4	Exercises	94
12	Diversity of the Immune system	97
12.1	Diversity of the immune repertoire	97
12.2	MHC diversity within the individual	100
12.3	Exercises	102
13	Theoretical immunology projects	105
14	GRIND	107
14.1	Lotka Volterra model	107
14.2	Exercises	109
15	Simple Maple examples	113
16	Appendix: mathematical prerequisites	115
16.1	Sketching functions	115
16.2	Mathematical background	118
16.3	Convenient functions	119
16.4	Phase plane analysis	120
16.5	Exercises	124

CONTENTS 5

17 Answers to the exercises **127**

17 Credits **147**

Chapter 1

Introduction

This course is an introduction into Theoretical Biology for biology students. We will teach you how to read mathematical models, and how to analyze them, with the ultimate aim that you can critically judge the assumptions and the contributions of such models whenever you encounter them in your future biological research. Mathematical models are used in all areas of biology. Most models in this course are formulated in ordinary differential equations (ODEs). These will be analyzed by computing steady states, and by sketching nullclines. We will develop the differential equations by ourselves following a simple graphical procedure. Experience with an approach for writing models will help you to evaluate models proposed by others.

This first Chapter introduces some basic concepts underlying modeling with differential equations. To keep models general they typically have free parameters, i.e., letters instead of numbers. You will become familiar with the notion of a “solution”, “steady state”, “half life”, and the “expected life span”. Concepts like solution and steady state are important because a differential equation describes the *change* of the population size, rather than its *actual size*. We will start with utterly simple models that are only convenient to introduce these concepts. The later models in the course are much more challenging and more interesting.

1.1 The simplest possible model

A truly simple mathematical model is the following

$$\frac{dM}{dt} = k , \tag{1.1}$$

which says that the variable M increases at a rate k per time unit. For instance, this could describe the amount of pesticides in your body when you eat the same amount of fruit sprayed with pesticides every day. Another example is to say that M is the amount of money in your bank account, and that k is the amount of Euros that are deposited in this account on a daily basis. In the latter case the “dimension” of the parameter k is “Euros per day”. The ODE formalism assumes that the changes in your bank account are continuous. Although this is evidently wrong, because money is typically deposited on a monthly basis, this makes little difference when one considers time scales longer than one month.

This equation is so simple that one can derive its *solution*

$$M(t) = M(0) + kt , \quad (1.2)$$

where $M(0)$ is the initial value (e.g., the amount of money that was deposited when the account was opened). Plotting $M(t)$ in time therefore gives a straight line with slope k intersecting the vertical axis at $M(0)$. The slope of this line is k , which is the derivative defined by Eq. (1.1). Thus, the differential equation Eq. (1.1) gives the “rate of change” and that the solution of Eq. (1.2) gives the “population size at time t ”. Typically, differential equations are too complicated for solving them explicitly, and the solution is not available. In this course we will not consider the integration methods required for obtaining those solutions. However, having a solution, one can easily check it by taking the derivative with respect to time. For example, the derivative of Eq. (1.2) with respect to time is $\partial_t[M(0) + kt] = k$, which is indeed the right hand side of Eq. (1.1). Summarizing, the solution in Eq. (1.2) gives the amount of money at time t , and Eq. (1.1) gives the daily rate of change.

As yet, the model assumes that you spend no money from the account. Suppose now that you on average spend s Euros per day. The model then becomes $dM/dt = k - s = k'$, where $k' = k - s$ Euros per day. Mathematically this remains the same as Eq. (1.1), and one obtains exactly the same results as above by just replacing k with k' . If $k' < 0$, i.e., if you spend more than you receive, the bank account will decrease and ultimately become negative. The time to bankruptcy can be solved from the solution of Eq. (1.2): from $0 = M(0) + k't$ one obtains $t = -M(0)/k'$ provided $k' < 0$. Although our model has free parameters, i.e., although we do not know the value of k , it is perfectly possible to do these calculations.

This all becomes a little less trivial when one makes the realistic assumption that your spending is proportional to the amount of money you have. Suppose that you spend a fixed percentage, d , of your money per day. The model now becomes

$$\frac{dM}{dt} = k - dM , \quad (1.3)$$

where the parameter d is a “rate” and here has the dimension “per day”. This can be checked from the whole term dM , which should have the same dimension as k , i.e.,

“Euros per day”. Biological examples of Eq. (1.3) are red blood cells produced by bone marrow, shrimps washing onto a beach, and so on. The k parameter then defines the inflow, or production, and the d parameter the death rate. Although this seems a very simple extension of Eq. (1.1), it is much more difficult to obtain the solution

$$M(t) = \frac{k}{d} (1 - e^{-dt}) + M(0)e^{-dt}, \quad (1.4)$$

which is depicted in Fig. 1.1a. The term on the right gives the exponential loss of the initial value of the bank account. The term on the left is more complicated, but when evaluated at long time scales, e.g., for $t \rightarrow \infty$, the term $(1 - e^{-dt})$ will approach one, and one obtains the “steady state” $\bar{M} = k/d$. We conclude that the solution of Eq. (1.4) ultimately approaches the steady state $M = k/d$, which is the ratio of your daily income and daily spending. Note that this is true for any value of the initial condition $M(0)$. Finally, one can check the solution by taking the derivative $\partial_t M(t)$ giving:

$$0 + d \frac{k}{d} e^{-dt} - dM(0)e^{-dt} = [k - dM(0)]e^{-dt}, \quad (1.5)$$

which is indeed equal to the right hand side of Eq. (1.3), i.e., to $k - dM(t)$, when $M(t)$ is given by Eq. (1.4).

Fortunately, we do not always need a solution to understand the behavior of a model. This same steady state can also directly be obtained from the differential equation. Since a steady state means that the rate of change of the population is zero we set

$$\frac{dM}{dt} = k - dM = 0 \quad \text{to obtain} \quad \bar{M} = \frac{k}{d}, \quad (1.6)$$

which is the same as obtained above from the solution for $t \rightarrow \infty$. Note that a steady state also gives the population size. This steady state provides some insight in the behavior of the model, and therefore in the way people spend their money. Suppose that rich people spend the same *fraction* of their money as poor people do, and that rich people just have a higher daily income k . This means that both rich and poor people approach a steady state where their spending balances their income. Basically, this model says that people with a 2-fold higher income spend 2-fold more money, and have 2-fold more money in the bank. This is not completely trivial: if you were asked what would happen with your bank account if both your income and spending increases n -fold you might have given a different answer.

1.2 Exponential growth and decay

Consider the unfortunate case that your daily income dries up, i.e., having a certain amount of money $M(0)$ at time zero, one sets $k = 0$ and is left with $dM/dt = -dM$.

This is the famous equation for exponential decay of radioactive particles with the almost equally famous solution $M(t) = M(0)e^{-dt}$. Ultimately, i.e., for $t \rightarrow \infty$, the population size will approach zero. Plotting the natural logarithm of $M(t)$ as a function of time would give straight line with slope $-d$ per day. This equation allows us to introduce two important concepts: the half life and the expected life span. The half life is defined as the time it takes to loose half of the population size, and is found from the solution of the ODE. From

$$\frac{M(0)}{2} = M(0)e^{-dt} \quad \text{one obtains} \quad \ln \frac{1}{2} = -dt \quad \text{or} \quad t = \frac{\ln 2}{d}. \quad (1.7)$$

Since $\ln 2 \simeq 0.69$ the half life is approximately $0.69/d$ days. Note that the dimension is correct: a half life indeed has dimension time because we have argued above that d is a rate with dimension day^{-1} . The other concept is expected life span: if radioactive particles or biological individuals have a probability d to die per unit of time, their expected life span is $1/d$ time units. This is like throwing a dice. If the probability to throw a four is $1/6$, the expected waiting time to get a four is six throws. Finally, note that this model has only one steady state, $\bar{M} = 0$, and that this state is stable because it is approached at infinite time. A steady state with a population size of zero is often called a “trivial” steady state.

The opposite of exponential decay is exponential growth

$$\frac{dN}{dt} = rN \quad \text{with the solution} \quad N(t) = N(0)e^{rt}, \quad (1.8)$$

where the parameter r is known as the “natural rate of increase”. The solution can easily be checked: the derivative of $N(0)e^{rt}$ with respect to t is $rN(0)e^{rt} = rN(t)$. Biological examples of this equation are the growth of mankind, the exponential growth of a pathogen in a host, the growth of a tumor, and so on. Similar to the half life defined above, one can define a doubling time for populations that are growing exponentially:

$$2N(0) = N(0)e^{rt} \quad \text{gives} \quad \ln 2 = rt \quad \text{or} \quad t = \ln[2]/r. \quad (1.9)$$

This model also has only one steady state, $\bar{N} = 0$, which is unstable because any small perturbation above $N = 0$ will initiate unlimited growth of the population. To obtain a non-trivial (or non-zero) steady state population size in populations maintaining themselves by reproduction one needs density dependent birth or death rates. This is the subject of the next chapter.

1.3 Summary

An ordinary differential equation (ODE) describes the rate of change of a population. To know the actual population size one needs to have the solution of the ODE. These are

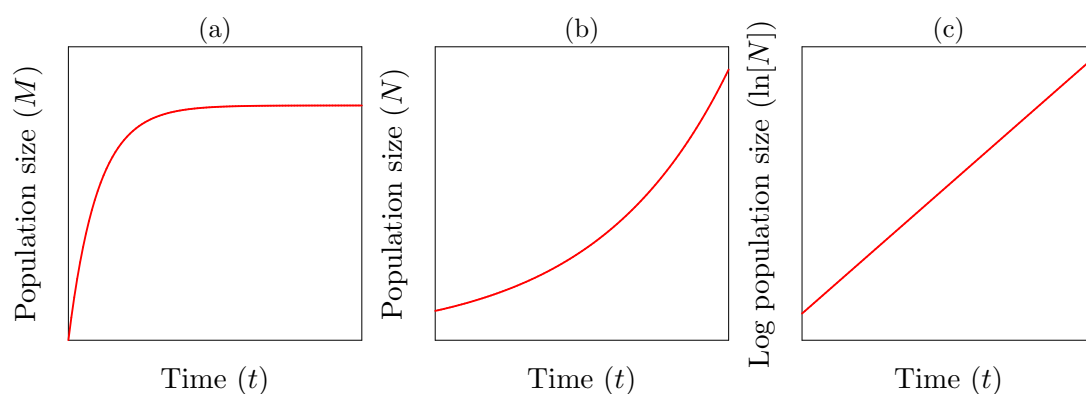


Figure 1.1: Population growth. Panel (a) depicts the solution of Eq. (1.4). Panels (b) and (c) depict exponential growth on a linear and a logarithmic vertical axis, respectively. A differential equation describes the slope of the solution for each value of the variable(s): dN/dt is the slope of the $N(t) = N(0)e^{rt}$ curve for each value of $N(t)$.

generally not available, and one typically solves the ODEs numerically on a computer to study the model behavior. Steady states are solved by setting the rate of change to zero, and do deliver the actual population size.

1.4 Exercises

Question 1.1. Red blood cells

Red blood cells are produced in the bone marrow at a rate of m cells per day. They have a density independent death rate of d per day.

- Which differential equation from this Chapter would be a correct model for the population dynamics of red blood cells?
- Suppose you donate blood. Sketch your red blood cell count predicted by this model in a time plot.
- Suppose a sportsman increases his red blood cell count by receiving blood. Sketch a time plot of his red blood cell count.

Question 1.2. SARS

Consider a deadly infectious disease, e.g., SARS, and write the following model for the spread of the disease:

$$\frac{dI}{dt} = \beta I - \delta I,$$

where I is the number of human individuals infected with SARS, β is the number of new cases each infected individual causes per day, and $1/\delta$ is the number of days an infected individual survives before he/she dies of SARS. Epidemiologists define the R_0

of a disease as the maximum number of new cases expected per infected individual. Since an infected individual here is expected to live for $1/\delta$ days, and is expected to cause β new cases per day, the R_0 of this disease is β/δ .

- a. It has been estimated that on average a SARS patient causes $R_0 = 3$ new cases, during a typical disease period of two weeks (Lipsitch *et al.*, 2003). Most patients die at the end of these two weeks. How long does it take with these parameters to infect half of the world population of 6×10^9 individuals?
- b. Do you think this is a realistic estimate? How would you extend the model to make it more realistic?

Question 1.3. Pesticides on apples

During their growth season apples are frequently sprayed with pesticides to prevent damage by insects. By eating apples you accumulate these pesticides in your body. An important factor determining the concentration of pesticides is their half life in the human body. An appropriate mathematical model is

$$\frac{dP}{dt} = \sigma - \delta P ,$$

where σ is the daily intake of pesticides, i.e., $\sigma = \alpha A$ where A is the number of apples that you eat per day and α is the amount of pesticides per apple, and δ is the rate at which the pesticides decay in human tissues.

- a. Sketch the amount of pesticides in your body, $P(t)$, as a function of your age, assuming you eat the same number of apples throughout life.
- b. How much pesticides do you ultimately accumulate after eating apples for decades?
- c. Suppose you have been eating apples for decades and stop because you are concerned about the unhealthy effects of the pesticides. How long does it take to reduce your pesticide level by 50%?
- d. Suppose you start eating two apples per day instead of just one. How will that change the model, and what is the new steady state? How long will it now take to reduce pesticide levels by 50% if you stop eating apples?
- e. What is then the decay rate if the half-life is 50 days?

Question 1.4. Injecting anesthesia

Before you undergo a minor operation they inject a certain amount of anesthesia in the muscle of your upper arm. From there it slowly flows into the blood where it exerts its sedating effect. From the blood it is picked up by the liver, where it is ultimately degraded. We write the following model for the amount of anesthesia in the muscle M , blood B and liver L :

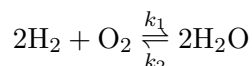
$$\frac{dM}{dt} = -eM , \quad \frac{dB}{dt} = eM - cB \quad \text{and} \quad \frac{dL}{dt} = cB - \delta L ,$$

where the parameter e is the efflux from the muscle, c is the clearance from the blood, and δ is the degradation in the liver. We assume that the degradation in the muscle and blood is negligible. The initial amount of anesthesia injected is $M(0)$: the amount in the muscle at time zero.

- Sketch the amounts of anesthesia in the muscle, $M(t)$, and in the blood, $B(t)$, as a function of time.
- How long does it take before half of the injected amount has flown from the muscle to the blood?
- Is this the right time to do the operation?
- Suppose the degradation rate is slow, i.e., let $\delta \rightarrow 0$, how much anesthesia will ultimately end up in the liver?

Question 1.5. Chemical reactions

Chemical reaction schemes can directly be translated into differential equations. For instance the reaction



is uniquely translated into

$$\frac{dz}{dt} = 2k_1x^2y - 2k_2z^2,$$

where x , y , and z are the $[\text{H}_2]$, $[\text{O}_2]$ and $[\text{H}_2\text{O}]$ concentrations. Two hydrogen molecules x have to meet one oxygen molecule y , and will form two water molecules z with reaction speed k_1 . Similarly two water molecules can dissociate into one oxygen molecule and two hydrogen molecules. Note that the speed of the reaction is proportional to the product of the concentrations x^2y of all the molecules involved. This is called the “law of mass action”.

Now consider the reaction scheme



where S , E_1 , and E_2 remain constant.

- Translate this into two differential equations for A and B .

Question 1.6. Physics (Extra exercise for cool students)

The linear ODEs used in this Chapter should be familiar to those of you having seen the famous equations for velocity and acceleration. One typically writes:

$$\frac{dx}{dt} = v \quad \text{and} \quad \frac{dv}{dt} = a,$$

where x is the total distance covered, v is the velocity, and a is the time derivative of the velocity, which is defined as the “acceleration”. Integrating dv/dt gives $v(t) = at + v(0)$, where the integration constant $v(0)$ is the velocity at time zero, and integrating $dx/dt = at + v(0)$ gives $x(t) = \frac{1}{2}at^2 + v(0)t$.

- Check the dimensions of v and a .
- Check these solutions.

- c. Now write a similar model for the amount of nitrogen deposited in a moorland by rainfall. The amount of Nitrogen in the air is increasing linearly in time because of air-pollution¹.

¹The more challenging questions are marked with an asterisk*

Chapter 2

Population growth

Ecological populations change by migration, birth and death processes. In Chapter 1 we saw that one can write simple differential equations for replicating populations, and for populations that maintain themselves by immigration. We will here study similar models explicitly from the notion of the biological birth and death processes, and will develop functions to describe how these processes may depend on the population size. Rather than taking well-known equations for granted, we will introduce an approach for “how to develop a mathematical model”. We will stress that there are always many different models for each particular situation. Models will be analyzed by computing steady states, and by sketching nulleclines. It is important to realize that all models introduced here require a number of “unrealistic assumptions”: (1) all individuals are equal, (2) the population is well-mixed, (3) the population size N is large, and (4) the parameters are constants.

2.1 Birth and death

In the previous Chapter we introduced the equation $dN/dt = rN$ for a population growing exponentially with a natural rate of increase r . This natural rate of increase is obviously a composite of birth and death rates. A more natural model for a biological population that grows exponentially is

$$\frac{dN}{dt} = (b - d)N \quad \text{with solution} \quad N(t) = N(0)e^{(b-d)t}, \quad (2.1)$$

where b is a birth rate with dimension t^{-1} , and d is the death rate with the same dimension. Writing the model with explicit birth and death rates has the advantage that the parameters of the model are strictly positive (which will be true for all parameters

in this course). Moreover one now knows the “generation time” or “expected life span” $1/d$. Since every individual has a birth rate of b new individuals per unit of time, and has an expected life span of $1/d$ time units, one knows that the expected number of offspring of an individual is $R_0 = b/d$. We will use this R_0 as the expected “fitness” of an individual. In epidemiology the R_0 is used for predicting the spread of an infectious disease: whenever $R_0 < 1$ a disease will not be able to spread in a population. One infected host is then on average expected to be replaced by less than one newly infected host.

In this book we will give solutions of differential equations whenever they are known, but for most ecological models the solution is not known. We will not explain how these solutions are obtained. The textbook by Adler (1997) gives an overview of methods of integration. You can also use Maple or Mathematica to find the explicit solution of some of the differential equations used here. The solution can easily be checked: the derivative of $N(0)e^{(b-d)t}$ with respect to t is $N(0)(b-d)e^{(b-d)t} = (b-d)N(t)$.

A non-replicating population increasing with an external influx and a density independent death rate, e.g., Eq. (1.3) or Eq. (2.2), will ultimately approach a steady state where the influx balances the death. This is not so for this model with density independent *per capita* birth and death rates: the only equilibrium of Eq. (2.1) is $N = 0$. If $b > d$, i.e., if the fitness $R_0 > 1$, this equilibrium is unstable because introducing the smallest number of individuals into the $N = 0$ state leads to exponential growth. If $R_0 < 1$ this equilibrium is stable because every population will ultimately go extinct (i.e., for $t \rightarrow \infty$ the solution $N(0)e^{(b-d)t} \rightarrow 0$). Note that one could argue that Eq. (2.1) also has a steady state when $b = d$. However, this is a rare and strange condition because the birth rate and the death rate would have to be exactly the same over long time scales.

Biological examples of Eq. (2.1) are mankind, the exponential growth of algae in a lake, and so on. Similarly, the natural rate of increase $r = b - d$ yields a “doubling time” solved from $2N(0) = N(0)e^{rt}$ giving $t = \ln[2]/r$ time units. A famous example of the latter is the data from Malthus (1798) who investigated the birth records of a parish in the United Kingdom and found that the local population had a doubling time of 30 years. Solving the natural rate of increase r per year from $30 = \ln[2]/r$ yields $r = \ln[2]/30 = 0.0231$ per year, which can be expressed as a growth rate of 2.31% per year. More than 200 years later the global human growth rate is still approximately 2% per year. Simple exponential growth therefore seems a fairly realistic model for the complicated growth of the human population.

Eq. (2.1) describes a “replicating” population. A simple density-independent model for a “non-replicating” population is

$$\frac{dN}{dt} = s - dN \quad \text{with solution} \quad N(t) = \frac{s}{d} \left(1 - e^{-dt}\right) + N(0)e^{-dt}, \quad (2.2)$$

where s is a production rate (individuals t^{-1}) and d is a death rate (t^{-1}). This model

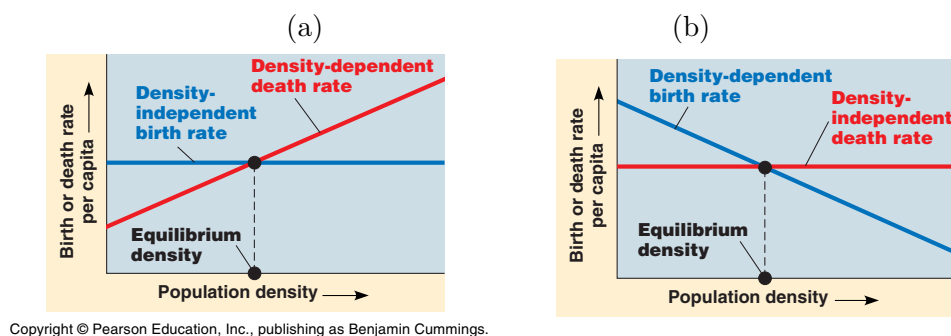


Figure 2.1: Graphs of the *per capita* birth and death rates. Equilibrium points correspond to the intersection points where the birth rate equals the death rate. From: Campbell & Reece (2008)52.14.

has a steady state of $\bar{N} = s/d$ individuals that is found by solving $dN/dt = 0$. Thus, this non-replicating population has a (stable) steady state in the absence of density dependent processes. Biological examples of such non-replicating populations are seeds blowing into a field, and so on. There is no typical doubling time, and the R_0 is not defined because small populations always expand. The expected life span remains $1/d$ time units, and the individual half life remains $\ln[2]/d$ time units.

Birth and death rates are typically not fixed because the processes of birth and death often depend on the population size. Due to competition at high population densities birth rates may become lower and death rates higher when the population size increases (see Fig. 2.1). This is called density dependence. We here wish to develop models that are realistic in the sense that we understand which biological process is mechanistically responsible for the regulation of the population size. A good procedure for developing such models is to decide beforehand which process, i.e., birth or death, is most likely to be subjected to density-dependent effects. The next step is to sketch a functional relationship between the biological process and the population density.

2.2 Density dependent death

If the death rate increases with the population size one could, for example, propose a simple linear increase of the *per capita* death rate with the population size (see Fig. 2.1a). This linear increase need not be realistic, but is certainly a natural first extension of a model where the death rate fails to depend to the population size. A simple mathematical function for the graph in Fig. 2.1a is $f(N) = d(1 + N/k)$, where d is the normal death rate that is approached when the population size is small, and where k determines the slope with which the death rate increases with N . To incorporate the death rate of Fig.

2.1a into our model one simply replaces the *parameter* d in Eq. (2.1) with the *function* $f(N) = d(1 + N/k)$:

$$\frac{dN}{dt} = [b - d(1 + N/k)]N . \quad (2.3)$$

The dimension of the parameter k is biomass, or individuals, and its exact interpretation is that the death rate has doubled when $N = k$. At low population sizes the expected life span of the individuals approaches $1/d$ time units, and they always have a birth rate b per time unit. The fitness of individuals obeying Eq. (2.3) therefore equals $R_0 = b/d$. The R_0 is always a maximum fitness, i.e., is computed for an individual under optimal conditions, which here means $N \rightarrow 0$.

To search for steady states of Eq. (2.3) one sets $dN/dt = 0$, cancels the trivial $N = 0$ solution, and solves from the remainder

$$b - d = dN/k \quad \text{that} \quad \bar{N} = k \frac{b - d}{d} = k(R_0 - 1) \quad (2.4)$$

is the non-trivial steady state population size. In ecology such a steady state is called the “carrying capacity”. A simple linear density dependent death rate is therefore sufficient to deliver a carrying capacity. The carrying capacity depends strongly on the fitness of the population, i.e., doubling $(R_0 - 1)$ doubles the population size.

To test whether these steady state are stable one could study the solution of Eq. (2.3) to see what happens when $t \rightarrow \infty$. Although this solution is known, we prefer to introduce a graphical method for determining the stability of a steady state. Fig. 2.1a sketches the *per capita* birth and death rates as a function of the population size in one graph. When these lines intersect the birth and death rates are equal and the population is at steady state. To check the stability of the non-trivial state state, one can study what happens when the population size is somewhat increased. Increasing N from the equilibrium density \bar{N} makes $dN/dt < 0$ because the death rate exceeds the birth rate. This forces the population back to its steady state value. Similarly, decreasing N makes $dN/dt > 0$ which pushes the population back to the steady state. We conclude that the non-trivial steady state is stable. The instability of the trivial steady state $N = 0$ can also be checked from Fig. 2.1a: increasing N from $\bar{N} = 0$ makes $dN/dt > 0$ whenever $b > d$, i.e., whenever the fitness $R_0 > 1$.

2.3 Density dependent birth

Alternatively, one may argue that the *per capita* birth rate b should decrease with the population size. Fig. 2.2 shows some experimental evidence supporting this for two natural populations. The simplest functional relationship between the *per capita* birth rate and the population size is again a linear one (see Fig. 2.1b), and a simple

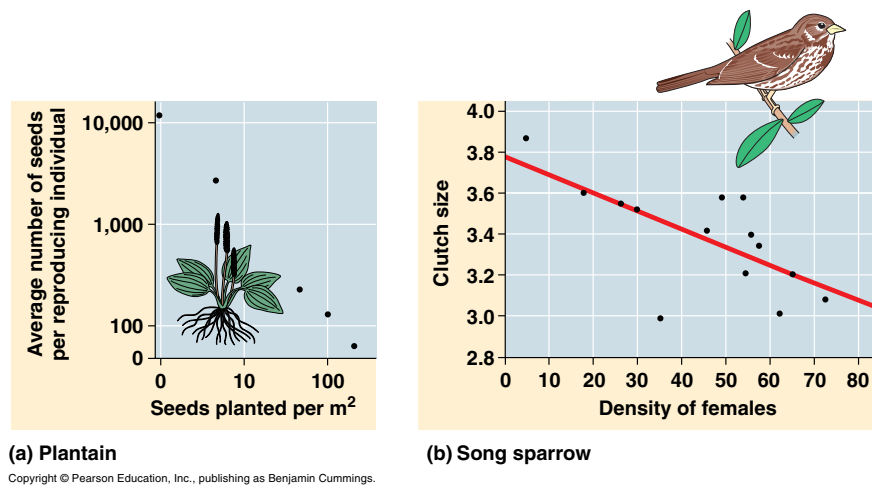


Figure 2.2: Panels (a) and (b) show for a plant species and a bird species that the *per capita* reproduction rate depends on the population size. From: Campbell & Reece (2008)52.15.

mathematical description is $f(N) = b(1 - N/k)$. Replacing the b parameter by this linear function the model becomes

$$\frac{dN}{dt} = [b(1 - N/k) - d]N . \quad (2.5)$$

The dimension of the parameter k is again biomass, or individuals, and its exact interpretation now is that the birth rate becomes zero when $N = k$. At low population sizes the fitness of individuals obeying Eq. (2.5) remains $R_0 = b/d$, which is natural because at a sufficiently low population size there should be no difference between the two models. The steady states now are $N = 0$ and solving

$$b - d = b \frac{N}{k} \quad \text{yields} \quad \bar{N} = k(1 - d/b) = k(1 - 1/R_0) . \quad (2.6)$$

A simple linear density dependent birth term therefore also allows for a carrying capacity. However, this carrying capacity approaches the value of k and is fairly independent of the fitness whenever $R_0 \gg 1$. By the same procedure as illustrated above one can test graphically from Fig. 2.1b that the carrying capacity is stable, and that $N = 0$ is unstable.

2.4 Logistic growth

We have seen that the carrying capacity of a population with density dependent death depends strongly on the fitness of its individuals, whereas with density dependent birth

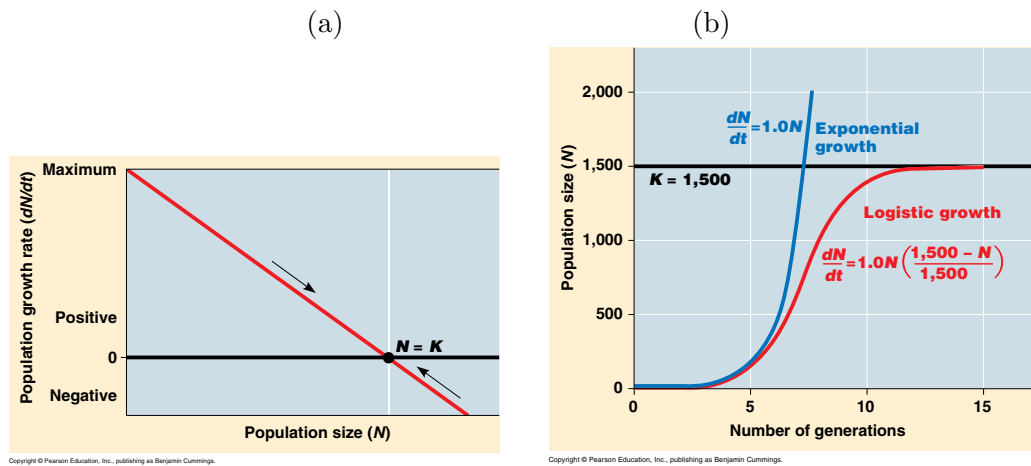


Figure 2.3: Logistic growth. From: Campbell & Reece (2008)52.11/12. Note that the label of the vertical axis in (a) should have been the *per capita* rate $[dN/dt]/N$.

this is much less so. Mathematically, one can rewrite both models as the classical “logistic equation” however:

$$\frac{dN}{dt} = rN(1 - N/K), \quad \text{with solution} \quad N(t) = \frac{KN(0)}{N(0) + e^{-rt}(K - N(0))}, \quad (2.7)$$

with a natural rate of increase of $r = b - d$, and where K is the carrying capacity of the population. In the exercises you will be asked to rewrite Eqs. (2.3 & 2.5) into Eq. (2.7), but you can easily see that all three are of the same form because they all have a positive linear and a quadratic negative term. The behavior of the three models is therefore the same: starting from a small initial population the growth is first exponential, and later approaches zero when the population size approaches the carrying capacity (see Fig. 2.3). Starting from a large initial population, i.e., from $N(0) > K$, the population size will decline until the carrying capacity is approached.

2.5 Stability and return time

The steady states $N = 0$ in Fig. 2.1 are not stable because small perturbations increasing N makes $dN/dt > 0$ which further increases N . The non-trivial steady states in Fig. 2.1 are stable because increasing N makes $dN/dt < 0$. It appears that steady states are stable when $\partial_N[dN/dt] < 0$, and unstable when this slope is positive (see Fig. 2.4).

Mathematically one can linearize any function $f(x)$ at any value of x by its local derivative:

$$f(x + h) \simeq f(x) + \partial_x f h, \quad (2.8)$$

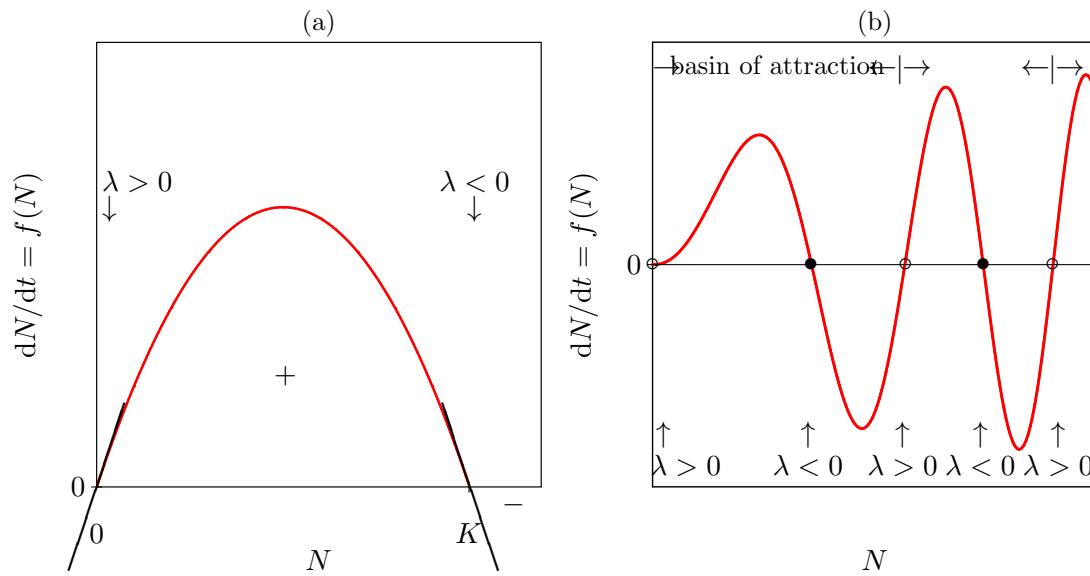


Figure 2.4: The stability of steady state is determined by the local derivative (slope) of the growth function at the steady state. Panel (a) depicts the logistic growth function $f(N) = rN(1 - N/K)$ and Panel (b) depicts an arbitrary growth function.

where h is a small distance (see Fig. 16.3 in the Appendix). To apply this to our stability analysis one rewrites $f(N)$ into $f(\bar{N} + h)$ where \bar{N} is the steady state population size and h is a small disturbance. Following Eq. (2.8) one obtains

$$\frac{d\bar{N} + h}{dt} = f(\bar{N} + h) \simeq f(\bar{N}) + \partial_N f h = 0 + \partial_N f h = \lambda h, \quad (2.9)$$

where $\lambda = \partial_N f$ is the derivative of $f(N)$ with respect to N . For the $f(N) = s - dN$ of Eq. (2.2) one obtains $\lambda = -d$, and for the logistic equation one obtains $\lambda = r - 2rN/K$, which still depends on the population size N . At the carrying capacity of the logistic equation, i.e., at $N = K$, the local tangent is $\lambda = -r$ and at $N = 0$ we obtain $\lambda = r$ (see Fig. 2.4a). Because $d(\bar{N} + h)/dt = dh/dt$ we obtain

$$\frac{dh}{dt} = \lambda h \quad \text{with solution} \quad h(t) = h(0)e^{\lambda t}, \quad (2.10)$$

for the behavior of the disturbance around the steady state. Thus, whenever the local tangent λ at the equilibrium point is positive, small disturbances grow; whenever $\lambda < 0$ they decline, and the equilibrium point is stable. For an arbitrary growth function this dependence on the slope λ is illustrated in Fig. 2.4b. This Figure shows that the unstable steady states, here saddle points, separate the basins of attraction of the stable steady states.

The stability of a steady state can be expressed as a “Return time”

$$T_R = -\frac{1}{\lambda}, \quad (2.11)$$

i.e., the more negative λ the faster perturbations die out. For example, consider the return time of the logistic growth equation around its carrying capacity. Above we derived that at $\bar{N} = K$ the tangent $\lambda = -r$. This means that $T_R = 1/r$, i.e., the larger r the shorter the return time. Populations that grow fast are therefore more resistant to perturbations. The paradigm of r -selected and K -selected species is built upon this theory. Finally, note that the dimensions are correct: because r is a rate with dimension “time⁻¹”, T_R indeed has the dimension “time”.

2.6 Summary

A stable non-trivial population size is called a carrying capacity. Replicating populations will only have a carrying capacity when the *per capita* birth and/or death rate depends on the population density. For non-replicating populations is this not so. A steady state is stable if the local derivative of the growth function is negative. The steeper this derivative, the shorter the return time.

2.7 Exercises

Question 2.1. Density dependent growth

A density dependent birth rate need not decline linearly with the population density. Consider a population with a density dependent growth term:

$$\frac{dN}{dt} = (bf(N) - d)N \quad \text{with} \quad f(N) = \frac{1}{1 + N/h}.$$

- a. Sketch how the *per capita* birth rate depends on the population density N .
- b. Sketch how the birth rate of the total population depends on the population density N .
- c. Compute the steady states of the population.
- d. What is the R_0 and express the steady state in terms of the R_0 ?
- e. Is $f(N)$ a Hill function (see Chapter 16)?

Question 2.2. Density dependent death

Consider a replicating population where most of the death is due to competition with

other individuals, i.e., let $f(N) = cN$ in a model where $dN/dt = (b - f(N))N$.

- Sketch the *per capita* death rate as a function of N .
- Sketch the *per capita* net growth rate as a function of N .
- Compute the steady state.
- Why is the R_0 not defined?
- What is the return time in the non-trivial steady state?

Question 2.3. Growth of insects

Consider an insect population consisting of larvae L and adults A :

$$\frac{dL}{dt} = aA - dL(1 + eL) - cL \quad \text{and} \quad \frac{dA}{dt} = cL - \delta A .$$

- Interpret all terms of the model.
- Sketch the nullclines and the vector field (see Section 16.4).
- Determine the stability of the steady state(s).

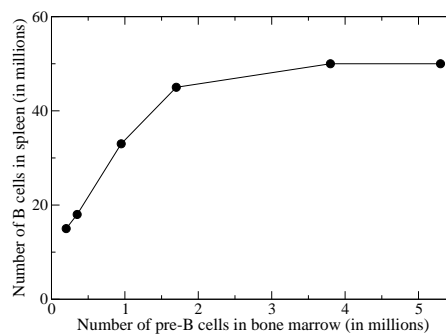
Question 2.4. Stem cells

Stem cells are maintained by continuous division. A fraction of the daughter cells differentiate and obtains other phenotypes. A convenient model for stem cell growth is the logistic equation $dS/dt = rS(1 - S/k)$.

- Expand the model with differentiation of stem cells
- Write a simple model for the differentiated cells
- Analyze the model by nullclines and determine the stability of the steady states (see Section 16.4).

Question 2.5. Freitas

Agnes *et al.* (1997) at the Pasteur Institute manipulated the number of cells in the bone marrow (pre-B cells) producing naive B cells (e.g., in the spleen), and found the following:



The simplest model for the naive B cell population is $dB/dt = m - dB$ where m is the

bone marrow production, and $1/d$ is the average life span of naive B cells. The rate of naive B cell production is proportional to the number of pre-B cells, i.e., $m = \alpha P$, where P is the number of pre-B cells.

- a. Is this simple model compatible with the data?
- b. If not, how would you extend the model?
- c. Do the data require homeostasis, i.e., density dependent regulation?
- d. Is $dB/dt = m - dB$ accounting for homeostasis?

Question 2.6. Negative birth

The *per capita* birth rate function $f(N) = b(1 - N/k)$ of Eq. (2.5) is not completely correct because the birth rate becomes negative when $N > k$. This can be repaired by writing $f(N) = \max[0, b(1 - N/k)]$ which equals zero when $b(1 - N/k) \leq 0$. Will this change the steady states analyzed in this Chapter?

Question 2.7. Logistic growth

Logistic growth $dN/dt = rN(1 - N/K)$ is a popular equation for describing a replicator population with a maximum population size (see Fig. 2.3).

- a. What is the maximum population size?
- b. Show that Eq. (2.5) can be rewritten as a logistic growth.
- c. Show that Eq. (2.3) can be rewritten as a logistic growth.

Question 2.8. Red blood cells

Red blood cell production in the bone marrow is regulated by the erythrocyte numbers in the periphery. Erythrocyte production is stimulated by the hormone *erythropoietin* that is produced by renal epithelial cells when the blood delivers insufficient oxygen. On average the human body produces 3×10^9 new erythrocytes per kg of body weight per day. Because the bone marrow of the long bones becomes fatty in adults, the total amount of bone marrow producing erythrocytes decreases with age. Nevertheless, the number of peripheral red blood cells remains fairly constant.

- a. Write a mathematical model, i.e., a growth equation, assuming that red blood cells have a finite life span of about 120 days, and that the production in the bone marrow is regulated by the erythrocyte density.
- b. Compute the steady state.
- c. Does this model explain the observation that erythrocyte numbers are fairly independent of the age of an individual? Hint: the effect of *erythropoietin* is sigmoidal with a high Hill-coefficient (Belair *et al.*, 1995).

Question 2.9. Naive T cell renewal

Data suggest that naive T cells expand by cell division when densities are low.

- a. Write a simple growth model assuming that naive T cells divide when densities are low.
- b. Check the feasibility of the model by computing the steady state.

Question 2.10. Tumor growth

Consider a small melanoma growing as a flat disk. Assume that the tumor cells are dividing only at the tumor boundary because of a lack of blood supply inside. Assume that cell death occurs uniformly throughout the tumor mass. Hint: the surface area of a circle is πr^2 while its circumference is $2\pi r$. Thus, if N is the total number of cells in the tumor, the number of cells at the surface is proportional to \sqrt{N} .

- a. Write a growth model for the total number of cells in the tumor.
- b. What is the steady state?
- c. Sketch the per capita growth as a function of the tumor mass.
- d. How would you extend this to a three-dimensional tumor growing as a ball?

Chapter 3

Interacting populations

Our mission in this Chapter is to study properties of models in which several populations interact. We will focus on the negative interaction of pathogens onto their target cells, and the negative control that an immune response has on infected cells. Here the models will be analyzed with nullclines and steady state analysis. In Chapter 7 similar models will be combined into a larger, more complicated models, that will be analyzed in terms of their steady states.

3.1 Viral infection

Consider the infection of a population of target cells T by cells I infected by some virus. This could be a hepatitis infection where HBV or HCV infects liver cells, or HIV infecting CD4⁺ T cells. Measuring time in units of days a natural model to write is

$$\frac{dT}{dt} = \sigma - \delta_T T - \beta T I \quad \text{and} \quad \frac{dI}{dt} = \beta T I - \delta_I I, \quad (3.1)$$

where σ is the daily production of target cells, uninfected target cells have a half life of $\ln[2]/\delta_T$ days, and infected cells have a half life of $\ln[2]/\delta_I$ days. One can set $\delta_I > \delta_T$ to allow for cytopathic effects of the virus. Uninfected cells can become infected by meeting with infected cells at a rate β /day per infected cell.

The model assumes an absence of homeostasis in the target cell population. The healthy steady state is solved from setting $I = 0$ and $dT/dt = 0$, i.e., $\bar{T} = \sigma/\delta_T$ cells. This represents the normal size of the target cell population (e.g., the normal size of the liver). In Chapter 2 we have seen the solution of this growth model in Eq. (2.2). During an infection we have to solve the steady state from the whole system Eq. (3.1). Starting

with the simplest equation we set $dI/dt = 0$ to find $\bar{I} = 0$ and $\bar{T} = \delta_I/\beta$. Apparently, the equilibrium number of uninfected target cells becomes independent of their production and life span, but is solely determined by the infection parameters β and δ_I . Next we set $dT/dt = 0$ to find

$$\bar{I} = \frac{\sigma}{\beta\bar{T}} - \frac{\delta_T}{\beta} = \frac{\sigma}{\delta_I} - \frac{\delta_T}{\beta}, \quad (3.2)$$

when $\bar{T} = \delta_I/\beta$ is substituted. The full model therefore has two steady states: the uninfected state ($\bar{T} = \sigma/\delta_T, \bar{I} = 0$) and the infected state ($\bar{T} = \delta_I/\beta, \bar{I} = \frac{\sigma}{\delta_I} - \frac{\delta_T}{\beta}$). In the uninfected state the number of uninfected target cells is proportional to their daily production, in the infected state the production σ determines the number of infected cells; \bar{T} is totally independent of their production σ .

We have seen in Chapter 2 that it is convenient to define the maximum per capita growth, R_0 , of the infection. In this two-dimensional system the R_0 of the infection is defined as the per capita growth over a whole generation at maximum target cell availability $T = \sigma/\delta_T$. Multiplying the maximum daily per capita growth $\sigma\beta/\delta_T$ with the generation time $1/\delta_I$ yields $R_0 = \frac{\sigma\beta}{\delta_I\delta_T}$. The infection can only spread in the target cell population if $R_0 > 1$. This can also be seen from requiring that $dI/dt_{\max} = I(\sigma\beta/\delta_T - \delta_I) > 0$ which also yields the requirement $R_0 > 1$. The infected steady state can be written in terms of the R_0 as

$$\hat{T} = \frac{\sigma}{\delta_T} \frac{1}{R_0} \quad \text{and} \quad \hat{I} = \frac{\sigma}{\delta_I} \left(1 - \frac{1}{R_0}\right), \quad (3.3)$$

which shows that the degree of depletion of target cells from the healthy steady state $\bar{T} = \sigma/\delta_T$ is proportional to R_0 , and that $\hat{I} \simeq \sigma/\delta_I$ whenever $R_0 \gg 1$. The latter would imply that the infection rate β hardly influences the steady state number of infected cells.

We continue by drawing nullclines. Setting $dI/dt = 0$ already yielded $I = 0$ and $T = \delta_I/\beta$, corresponding to two straight nullclines in the phase space. Setting $dT/dt = 0$ already yielded $I = \frac{\sigma}{\beta T} - \frac{\delta_T}{\beta}$. It is therefore most convenient to construct a phase space having I on the vertical axis and T as the horizontal variable. Plotting $I = \frac{\sigma}{\beta T} - \frac{\delta_T}{\beta}$ is the same as plotting a function $y = p/x - q$ (where $p = \sigma/\beta$ and $q = \delta_T/\beta$). For the intersections with the axes one finds that $I = 0$ when $T = \sigma/\delta_T$, which is obvious because it is the uninfected steady state found above. Letting $T \rightarrow \infty$ yields $I = -\delta_T/\beta$ as the horizontal asymptote, and $T \rightarrow 0$ gives the vertical axis as the vertical asymptote. Thus, in the positive domain, the $dT/dt = 0$ nullcline is the hyperbolic function depicted in Fig. 3.1. There are two possibilities: if $\delta_I/\beta < \sigma/\delta_T$ (i.e., $R_0 = \frac{\sigma\beta}{\delta_I\delta_T} > 1$) there is a non-trivial steady state corresponding to a chronic infection. If $R_0 < 1$ the infection cannot expand in the healthy steady state $\bar{T} = \sigma/\delta_T$ cells (Fig. 3.1b).

The stability of the steady state can be studied by means of the vector field. We chose extreme regions in the phase space to determine the signs of dT/dt and dI/dt . Left of the $dT/dt = 0$ nullcline the target cells increase because the production σ exceeds the

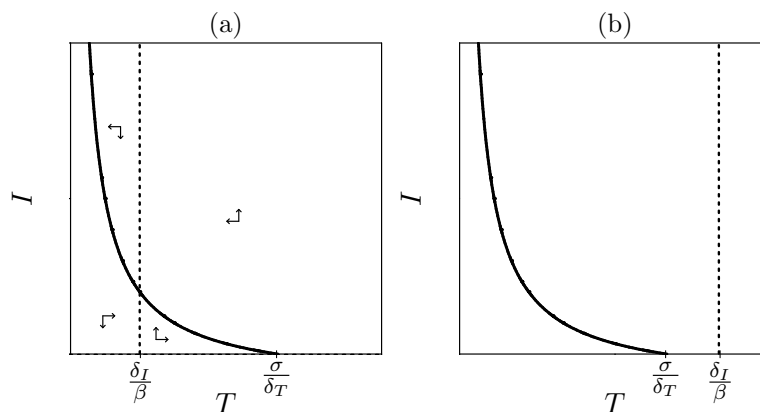


Figure 3.1: The phase space with nullclines of Eq. (3.1).

loss $dT + \beta TI$ when $T \rightarrow 0$. Left of the $dI/dt = 0$ nullcline $dI/dt < 0$ because $\beta T < \delta_I$. In Fig. 3.1b the healthy steady state $\bar{T} = \sigma/\delta_T$ is stable because the vector field points toward in all directions. The healthy steady state is unstable in Fig. 3.1a because the vertical direction points upwards. Thus, in Fig. 3.1a ($\bar{T} = \sigma/\delta_T, \bar{I} = 0$) is a saddle point. The stability of the infected state is more difficult to determine from the vector field. Since the vector field does not have a stable and unstable direction the point cannot be a saddle point. Because there is no local positive feedback from the variables onto themselves (cf. Chapter 2), i.e., increasing T around the steady state decreases dT/dt and increasing I decreases dI/dt , we conclude the steady state is stable.

3.2 Immune response

Virus infections typically evoke immune responses composed of antibodies and $CD8^+$ cytotoxic T cells. One interpretation of the model written above in Eq. (3.1) is that the effect of antibody response, and/or the cellular immune response is reflected in the clearance rate δ_I of infected cells. We can also extend the model with an explicit immune response by writing

$$\frac{dT}{dt} = \sigma - \delta_T T - \beta TI, \quad \frac{dI}{dt} = \beta TI - \delta_I I - kIE, \quad \text{and} \quad \frac{dE}{dt} = \alpha EI - \delta_E E, \quad (3.4)$$

where the kIE term reflects the killing of infected cells by the immune effectors E , and the αEI represents the clonal expansion of immune effectors in response to antigen.

The steady state of the model is found by solving the equations from the simplest to the most complicated. Solving $dE/dt = 0$ yields $\bar{E} = 0$, which is the steady state considered

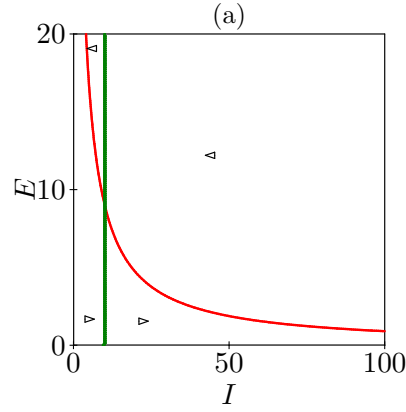


Figure 3.2: Nullclines of Eq. (3.7) with the non-trivial steady state. Parameters: $\alpha = 0.001$, $\beta = 0.1$, $\delta_E = 0.01$, $\delta_I = 0.1$, $\delta_T = 0.1$, $k = 1$ and $\sigma = 100$.

above, and $\bar{I} = \delta_E/\alpha$. Solving $dT/dt = 0$ yields

$$\bar{T} = \frac{\sigma}{\delta_T + \beta\bar{I}} = \frac{\sigma}{\delta_T + \beta\delta_E/\alpha}. \quad (3.5)$$

Solving $dI/dt = 0$ yields $\bar{I} = 0$ which is the uninfected state, and

$$\bar{E} = \frac{\beta}{k}\bar{T} - \frac{\delta_I}{k} = \frac{\beta\alpha\sigma}{k(\alpha\delta_T + \beta\delta_E)} - \frac{\delta_I}{k}. \quad (3.6)$$

Note that for the non-trivial solution, we now solve \bar{I} from $dE/dt = 0$ and \bar{E} from $dI/dt = 0$. Further note that the steady state infected cells is now only determined by the immune response parameters α and δ_E .

One can simplify this model to better focus on the interaction between the immune response and the infected cells by eliminating the target cell equation by making the quasi steady state assumption $dT/dt = 0$. Substituting $T = \sigma/(\delta_T + \beta I)$ into dI/dt yields for the interaction between the immune response and the infected cell a two-dimensional model

$$\frac{dI}{dt} = \frac{\sigma\beta I}{\delta_T + \beta I} - \delta_I I - kIE, \quad \text{and} \quad \frac{dE}{dt} = \alpha EI - \delta_E E. \quad (3.7)$$

The non-trivial nullclines of this model are $I = \delta_E/\alpha$ for $dE/dt = 0$, and $E = \frac{\sigma\beta}{k(\delta_T + \beta I)} - \frac{\delta_I}{k}$ for $dI/dt = 0$, which is of the form $y = a/(b + x) - c$. Thus in a phase space with the immune response on the vertical axis and the infected cells on the horizontal axis we again obtain a vertical “parasite” $dE/dt = 0$, and a hyperbolic “host” nullcline between a vertical asymptote at $I = -\delta_T/\beta$ and a horizontal asymptote approaching $E = -\delta_I/k$. This looks like Fig. 3.1 except for the fact that the hyperbolic nullcline crosses the vertical axis having its asymptote at a negative value of I (Fig. 3.2). Because

the vector field is also similar to that in Fig. 3.1 the non-trivial steady state is again stable. In Fig. 3.2 we only plot the nullcline configuration where the nullclines intersect, i.e., where the immune response exists. When $E = 0$ we have to consider Eq. (3.1) with Fig. 3.1.

3.3 Exercises

Question 3.1. Lotka Volterra model

Redo the analysis of the infection model Eq. (3.1) for a target cell population that grows logistically rather than by an independent production term.

- Write the equations and define the R_0 of the infection.
- Compute the steady states.
- Sketch the nullclines and determine the stability of the steady states.

Question 3.2. Seals

Assume that seals in the Waddenzee have a density dependent birth rate and a density independent death. Healthy seals S live on average $1/d$ days, and can become infected with a virus carried by infected seals I . Infected seals die after a short period averaging about $1/\delta$ days. We write the following model:

$$\frac{dS}{dt} = bS(1 - S/k) - dS - \beta SI \quad \text{and} \quad \frac{dI}{dt} = \beta SI - \delta I \quad \text{where} \quad \delta \gg d .$$

- What is the steady state of healthy seal population?
- What is the R_0 of the seals?
- Express the steady state from **a.** in terms of this R_0 .
- Suppose that pollution with PCBs halves the birth rate of the seals. What is the steady state of the seal population under polluted circumstances?
- How many healthy seals S are there in a population chronically infected with this deadly virus?
- How is this healthy seal population size in the infected steady state changing by water pollution with PCBs?
- Sketch the nullclines of the model and determine the stability of all the steady states.
- Sketch the nullclines of the model in the presence and the absence of PCBs in one picture.

Question 3.3. Solving the steady state

Find the non-trivial steady state concentration of molecule B in the following reaction chain assuming that all species are present:

$$\frac{dA}{dt} = a - bA - cAB, \quad \frac{dB}{dt} = cAB - dB - eBC, \quad \frac{dC}{dt} = eBC - fC .$$

Question 3.4. Viral fitness

Viruses have high mutation rates and short generation times, and can hence adapt rapidly to escape from drugs or the immune response. Some of these escape mutations are associated with a high fitness cost. In the model of Eq. (3.1) one would write

$$\frac{dT}{dt} = \sigma - \delta_T T - f\beta TI \quad \text{and} \quad \frac{dI}{dt} = f\beta TI - \delta_I I ,$$

where the fitness $f \leq 1$.

- a. Compute the steady state of this model.
- b. How does the steady state viral load depend on the viral fitness?
- c. How can this be? What is the major effect of a loss in fitness?

Chapter 4

Saturation functions

The infection term in the previous Chapter was a simple mass action term. At high target cell densities one would expect that infected cells approach some maximum rate at which they can infect target cells, however. This can be done by replacing the mass action term by one of the saturation functions defines in Chapter 16.

Consider again the infection of a population of target cells T by cells I infected by some virus, and now assume that the infection term is saturated, i.e., at high concentrations of target cells, each infected cell infects some maximum number of target cells per day. For simplicity now consider a target cell population that is maintained by logistic growth:

$$\frac{dT}{dt} = rT(1 - T/K) - \frac{\beta IT}{h + T} \quad \text{and} \quad \frac{dI}{dt} = \frac{\beta IT}{h + T} - \delta_I I, \quad (4.1)$$

where h is the target cell density at which the infection proceeds at half of its maximum rate. The parameter β now has the interpretation of the maximum infection rate at maximum target cell availability. We have employed a simple Hill-function to define the saturation function.

The nullclines of the target cells are $T = 0$ or

$$r(1 - T/K) = \frac{\beta I}{h + T} \quad \text{or} \quad I = (r/\beta)(h + T)(1 - T/K), \quad (4.2)$$

which is a parabola crossing the $I = 0$ axis at $T = -h$ and $T = K$, and having its maximum at $T = (K - h)/2$ (see Fig. 4.1a-c). The nullclines of the infected cells is $I = 0$ and $T = \delta_I h / (\beta - \delta_I)$, which is the vertical line in Fig. 4.1a-c. Because of the saturation, one can now consider the maximum per capita virus growth per generation at optimal, i.e., infinite, target cell availability. This yields $R_0 = \beta / \delta_I$. Thus the $dI/dt = 0$ nullcline is located at $T = h / (R_0 - 1)$. The target cells increase below the parabola, and

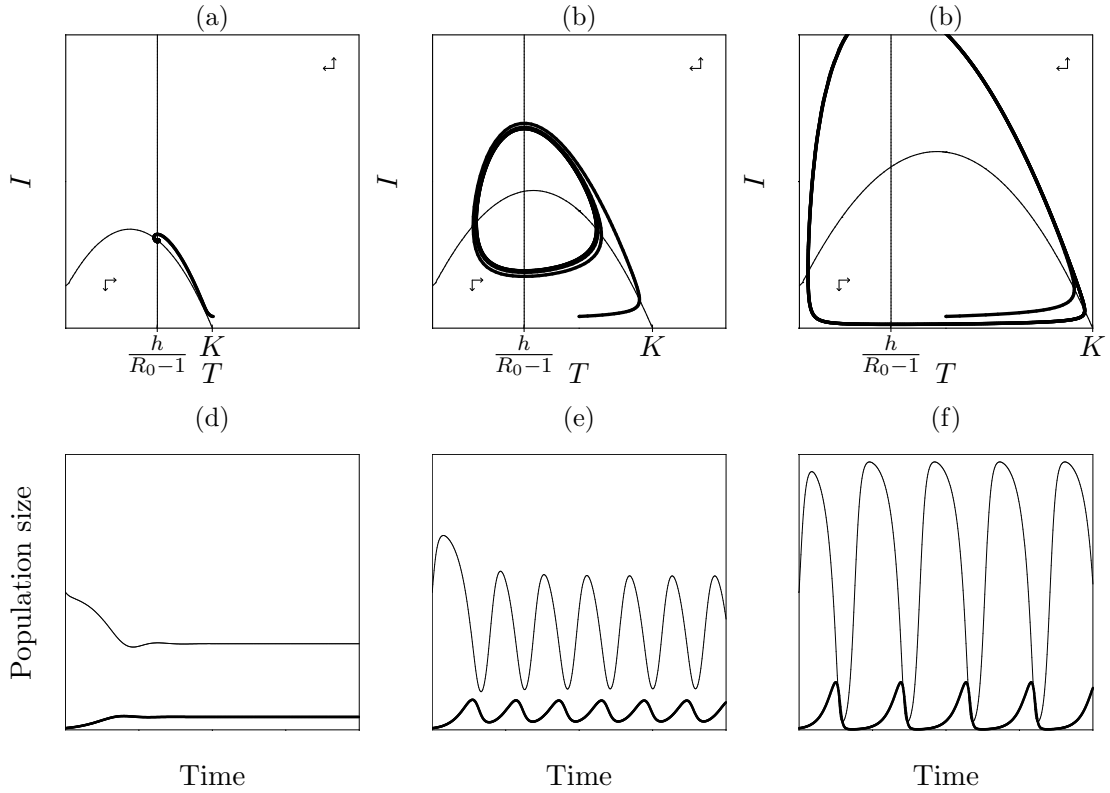


Figure 4.1: The nullclines and trajectories of Eq. (4.1) for $h/R_0 - 1 > (K - h)/2$ (a) and $h/(R_0 - 1) < (K - h)/2$ (b & c). The non-trivial steady state is stable in (a) and unstable in (b) and (c). The carrying capacity K is indicated. The nullcline of the immune response is the vertical line located at $R = h/(R_0 - 1)$. From left to right the carrying capacity increases. In the two panels on the right the model behavior approaches a stable limit cycle. The heavy line in the time plots denotes the target cells.

infected cells increase at the right side of the vertical line. When $h/R_0 - 1 > K$ we obtain Fig. 4.1a where the uninfected state is stable. When $(K - h)/2 < h/(R_0 - 1) < K$ the nullclines intersect at the right side of the top of the parabola. From the vector field one can see that the steady state is not a saddle. Increasing T in the steady state decreases dT/dt , while increasing I keeps $dI/dt = 0$. Because there is no positive feedback the equilibrium is stable. In Fig. 4.1c, where $h/(R_0 - 1) < (K - h)/2$, the nullclines intersect left of the top. The local vector field is the same, except for the fact that increasing T increases dT/dt . Due to this positive feedback the steady state is unstable. The behavior now is a stable limit cycle (Fig. 4.1e & f). Such a limit cycle can account for relapsing diseases (see Chapter 10), and/or periodic fevers. Periodic behavior will be addressed further in Chapter 6.

4.1 Exercises

Question 4.1. Host-parasite models

The target cells in Eq. (4.1) grow logistically, and having a saturated infection term, we obtained the parabolic nullcline for the target cells.

- a. Replace the logistic growth by a fixed source and a density-independent death term. Sketch the nullclines.
- b. Replace the fixed source by a density-dependent source. Sketch the nullclines.
- c. Is the “humped” host nullcline that so easily leads to periodic behavior a general phenomenon?

Question 4.2. Immune control

Consider anti-retroviral therapy in the immune control model defined by Eq. (3.4).

- a. What do you expect in the long run for the viral load I from a therapy that decreases β ?
- b. Would such a treatment have any positive effect for the patient?

Question 4.3. Oscillations

During primary infections with the measles virus transient oscillations in the viral load and the immune response have been observed.

- a. Can that be explained with the model in this Chapter?
- b. Do you really require the saturated infection term of this model, or would the model with a mass action infection term also explain this?

Chapter 5

Gene regulation

Protein synthesis depends on DNA transcription making mRNA molecules and translation of mRNA into proteins. Some proteins inhibit the transcription of their own mRNA. Let us model this by a declining Hill function $1/(1+x)$ (see Chapter 16), and assume that mRNA molecules M and proteins P have turnover rates d and δ respectively:

$$\frac{dM}{dt} = \frac{c}{1+P} - dM \quad \text{and} \quad \frac{dP}{dt} = lM - \delta P, \quad (5.1)$$

where c is the maximum transcription rate, and l is the translation rate. When $P = 0$ the gene is “on”, when $P \rightarrow \infty$ the gene is “off” and the transcription rate becomes zero. To analyse this model we draw nullclines. Setting $dM/dt = 0$ the simplest function to obtain is $M = \frac{c/d}{1+P}$, which is an inverse Hill function with maximum c/d when $P = 0$ (see Fig. 5.1). Solving $dP/dt = 0$ for M yields the straight line $M = (\delta/l)P$ (see Fig. 5.1). The nullclines intersect in only one steady state. The vector field around the steady state shows that the point is a stable node.

To allow for swift gene regulation mRNA has to be short lived. Assuming that transcription is a much faster process than translation, the mRNA concentration will typically be close to its steady state value for each protein concentration. This so-called “quasi steady state” is obtained by solving M from $dM/dt = 0$, which we already did for drawing the nullcline. Substituting $M = \frac{c/d}{1+P}$ into dP/dt yields the quasi steady state model

$$\frac{dP}{dt} = \frac{\pi}{1+P} - \delta P, \quad (5.2)$$

where $\pi = lc/d$ is the maximum production rate.

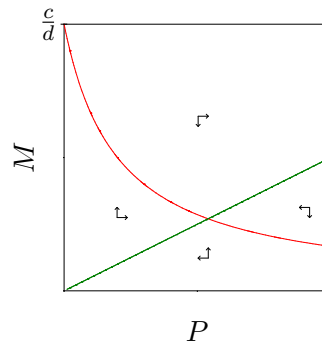


Figure 5.1: The nullclines of Eq. (5.1): qualitatively there is only one possible phase space with one stable steady state.

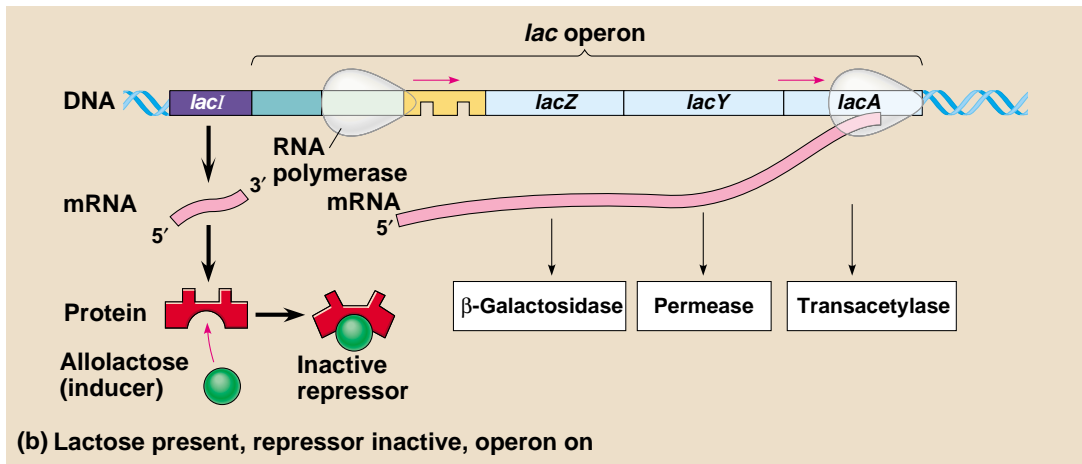
5.1 Separation of time scales

One often simplifies models by distinguishing slow and rapid time scales. This is a very important technique. For fast variables one can do a “quasi steady state” (QSS) approximation. This means that the QSS variable is in steady state with the rest of the system, i.e., with the slow part of the system. When the slow part changes the QSS variable walks along. By a QSS approximation one basically replaces a differential equation with an algebraic equation. A simple example of a QSS approximation would be the position of a fast fighter jet that is following a slow Boeing 747. If the pilot of the fighter jet has the order to tail the Boeing, one can describe the location of the fighter jet as a short distance behind the Boeing. Whenever the Boeing changes course, the rapid fighter jet will immediately follow. If the fighter jet were a slow plane, this would not be a valid assumption. This story was originally told by Lee Segel from Israel. He was the “father of the quasi steady state assumption” (Segel, 1988; Borghans *et al.*, 1996), and a great story teller.

Conversely, variables that are much slower than the other variables of a model can be approximated by constants that do not change at all on the time scale of interest. One example will be the assumption that the immune response is not changing during anti-retroviral therapy in Chapter 7. In this course we will use both techniques in order to obtain natural simplifications of our models.

5.2 Lac-operon

Bacteria can use several external substrates for cellular growth and switch the corresponding intra-cellular pathways on and off depending on the available resources. One



Copyright © Pearson Education, Inc., publishing as Benjamin Cummings.

Figure 5.2: The *lac* operon: regulated synthesis of inducible enzymes. From: Campbell & Reece (2008) 18.22.

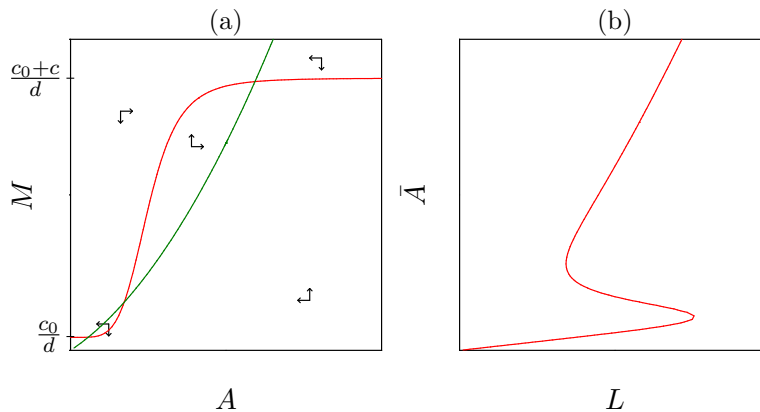


Figure 5.3: Nullclines of Eq. (5.3). Parameters: $L = c = d = v = 1$, $c_0 = 0.05$, $h = 2$, $m = 5$, and $\delta = 0.2$.

of the possible substrates is the sugar lactose, and the regulation of the “Lac-operon” was one of the first circuits of gene regulation that was revealed (Jacob & Monod, 1961). Regulation of the Lac-operon involves a positive feedback because the sugar allolactose, A , activates gene expression by deactivating a repressor R . Allolactose is an isomer of lactose that is formed in small amounts from lactose. The intracellular lactose concentration is determined by an enzyme permease that is produced by this gene complex. The gene complex also codes for the enzyme β -galactosidase that hydrolyzes the disaccharide

allolactose into glucose and galactose. This can be summarized into the following model

$$\begin{aligned} R &= \frac{1}{1 + A^n}, \\ \frac{dM}{dt} &= c_0 + c(1 - R) - dM = c_0 + \frac{cA^n}{1 + A^n} - dM, \\ \frac{dA}{dt} &= ML - \delta A - \frac{vMA}{h + A}, \end{aligned} \quad (5.3)$$

where $0 < R \leq 1$ a sigmoid Hill function representing the “concentration” of active repressor, M is the mRNA concentration, L is a parameter representing the extracellular lactose concentration, and A is allolactose. The allolactose concentration increases when the gene complex is active, i.e., when permease is present, and extracellular lactose L is transported from the extra-cellular to the intra-cellular environment. This is formulated as a simple “mass action term” of the external lactose concentration, L , and the permease M . The substrate allolactose is degraded according to a Michaelis-Menten enzyme substrate reaction, with maximum rate v and Michaelis-Menten constant h (see the exercises). This reaction depends on the enzyme β -galactosidase, the concentration of which is assumed to be proportional to the activation of the gene complex, i.e., to the amount of mRNA M . Overall there is a positive feedback because increasing M , increases A , and increases M (Griffith, 1968).

To analyze the model we draw nullclines. Setting $dM/dt = 0$ yields

$$M = \frac{c_0}{d} + \frac{(c/d)A^n}{1 + A^n}, \quad (5.4)$$

which is a sigmoid Hill function with an offset $M = c_0/d$ when $A = 0$ (see Fig. 5.3a). One obtains the vector field by noting that $dM/dt > 0$ and $dA/dt < 0$ when A is large and M is small. The $dA/dt = 0$ nullcline is solved from

$$M \left(L - \frac{vA}{h + A} \right) = \delta A \quad \text{or} \quad M = \frac{\delta A}{L - \frac{vA}{h + A}}. \quad (5.5)$$

Approximating this for $A \rightarrow 0$ yields $M \simeq (\delta/L)A$, which increases with A . Depending on the parameters v , h , and L there can be a vertical asymptote along which the curve goes to infinity (Fig. 5.3a). When the concentration of mRNA is high, and that of allolactose A is low, the allolactose concentration increases ($dA/dt > 0$). In Fig. 5.3a the nullclines intersect in three steady states. The vector field shows that the one in the middle is a saddle point, and that the two at the boundaries are stable nodes.

For one specific concentration of lactose, L , the operon can therefore be “on” or “off”, i.e., in one of the two stable steady states. The effect of the lactose concentration can better be visualized by again making a quasi steady state assumption for mRNA equation. Substituting Eq. (5.4) into dA/dt in Eq. (5.3) yields a very complicated expression. Using the computer program GRIND (see Chapter 14) we plot this complicated $dP/dt = 0$

nullcline as a function of the lactose concentration in Fig. 5.3b. The curve in Fig. 5.3b is basically a bifurcation diagram: it depicts the steady state allolactose concentration, \bar{A} , as a function of a parameter, the extra-cellular lactose concentration L . The upper and lower branches are stable and the branch in the middle is unstable. Bacteria growing in an environment that is extremely poor in lactose are in a state with low levels of allolactose, because the Lac-operon is off. Bacteria growing in an environment rich in lactose have an active Lac-operon and high intracellular allolactose concentrations. Bacteria growing in environment with an intermediate lactose concentration can be in either of these two states however (Novick & Weiner, 1957; Ozbudak *et al.*, 2004; Van Hoek & Hogeweg, 2006). At these concentrations the bacteria have “alternative stable states” (May, 1977; Scheffer *et al.*, 2001; Ozbudak *et al.*, 2004), and it depends on the history of the bacteria in which state they will be. Moreover the curve in Fig. 5.3b implies a form of “hysteresis”. If one decreases the extra-cellular lactose concentration from very high to very low, one follows the upper branch. At a critical lactose concentration, L_1 , the bacteria suddenly switch to the state with a closed operon. On the other hand, if one increases the lactose concentration from low to high, one switches from bacteria with a repressed operon to an expressed operon at lactose concentration L_2 . Fig. 5.3b shows that $L_2 > L_1$. Thus, the system has a form of memory, and tends to remain in the state where it was. This is called hysteresis.

The two transition points are catastrophic bifurcations. The system has a discontinuity and jumps to an alternative attractor. The bifurcations in Fig. 5.3b are called “saddle-node” bifurcations because a saddle point and a stable node merge and annihilate each other. In the Nonlinear system courses given by our group you can learn a lot more about bifurcation theory.

Models of gene regulation have recently attracted much more attention because one can nowadays read the activity of thousands of genes in a single RNA-chip experiment. To understand the properties of complicated networks of genes influencing each other, people are studying models composed of many equations, one for each of the genes in the network. A simple phenomenological ODE for a gene producing protein “one”, P_1 , that is downregulating its own transcription, but is upregulated by another gene product, P_2 , one could write something like

$$\frac{dP_1}{dt} = c \frac{h_1}{h_1 + P_1} \frac{P_2}{h_2 + P_2} - dP_1, \quad (5.6)$$

where one uses simple Hill functions for the stimulatory and inhibitory effects the proteins P_1 and P_2 have on the production of protein one. This model can obviously be extended for the influence of many different proteins on the transcription of one of them. Writing ODEs for all of the proteins, one obtains a model of a large gene network. Another exciting recent development is to experimentally record the gene expression of single genes, and fit these data to mathematical models (Golding *et al.*, 2005; Golding & Cox, 2006; Raj *et al.*, 2006). This work has demonstrated that transcription occurs in bursts, which may be stochastic.

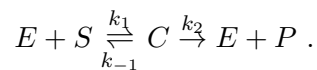
5.3 Summary

Positive feedback loops account for alternative steady states and hysteresis. Simple models for gene activity allow for complicated networks of regulatory interactions.

5.4 Exercises

Question 5.1. Michaelis-Menten

The Michaelis-Menten term used in Eq. (5.3) comes from a quasi steady assumption. Consider the following reaction for the formation of some product P from a substrate S . The enzyme E catalyzes the reaction, i.e.,



Because the enzyme is released when the complex dissociates one writes a conservation equation

$$E + C = E_0 .$$

- a. Write the differential equations for the product P and the complex C . Use the conservation equation!
- b. Assume that the formation of the complex is much faster than that of the product, i.e., make the quasi steady state assumption $dC/dt = 0$.
- c. Write the new model for the product. Simplify by defining new parameters.
- d. Sketch the rate at which the product is formed (dP/dt) as a function of the substrate concentration S .
- e. Write an ODE for the substrate, and note that you can add dC/dt to simplify dS/dt because $dC/dt = 0$.

Question 5.2. mRNA

Rewrite the mRNA protein model of Eq. (5.1) assuming that the inhibition follows a sigmoid Hill function.

- a. Sketch the nullclines
- b. Determine the stability of the steady state(s)
- c. Assume that the mRNA kinetics are much faster than those of the protein molecules, and write a model for dP/dt .

Question 5.3. Lac-operon

Simplify the model for the Lac-operon by removing the degradation of allolactose by

β -galactosidase.

- a. Sketch the nullclines
- b. Determine the stability of the steady state(s)
- c. Assume that the mRNA kinetics are much faster than those of the protein molecules, and write a model for dA/dt .

Chapter 6

Periodic behavior

In Chapter 4 we have seen that predators and prey can coexist by a stable oscillation. This rhythmic or periodic behavior originated from destabilizing a stable spiral point at a Hopf bifurcation (see Fig. 4.1). Periodic behavior is a typical element of living systems. Table 6.1 coming from the book on biological rhythms by Goldbeter (1996) lists a number of them. In this Chapter we will continue with gene regulation by studying the transcription factors determining the circadian rhythm.

Rhythm	Period
Neural rhythm	0.01 to 10 sec
Heart rhythm	1 sec
Calcium oscillations	1 sec to minutes
Biochemical oscillations	1 min to 20 min
Mitotic cell division	10 min to 24 hour
Hormonal rhythms	10 min to hours
Circadian (day-night) rhythm	24 hour
Ovulation cycle	28 days
Seasonal rhythms	1 year
Epidemiological and ecological behavior	years

Table 6.1: A number of biological rhythms ranked by their period. From: Goldbeter (1996).

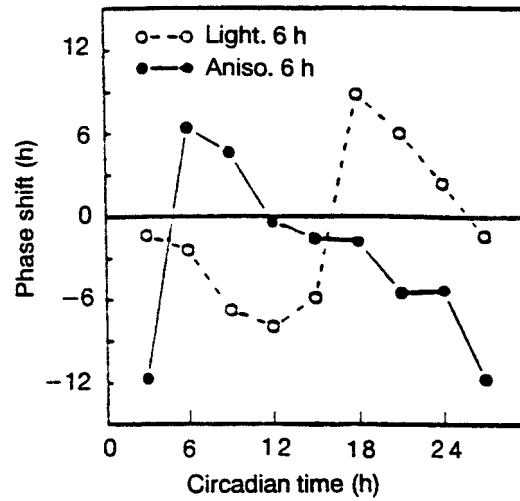


Figure 6.1: Phase response curves obtained in chick pineal cell cultures for 6h pulses of light (and anisomycin (Aniso.), an inhibitor of protein synthesis). Pineal cells produce melatonin in response to signals from the suprachiasmatic nucleus (SCN) in the hypothalamus. Protein concentrations in the pineal gland cycle with a 24 hour rhythm. When cells are exposed to light for 6 hours, the peaks of this rhythm shift forward or backward in time. Exposing cells to light at different time-points during the original cycle, and measuring the corresponding shift in clock-time, one can depict the so-called “phase-shift” as a function of time. From Figure 11.1 in Goldbeter (1996).

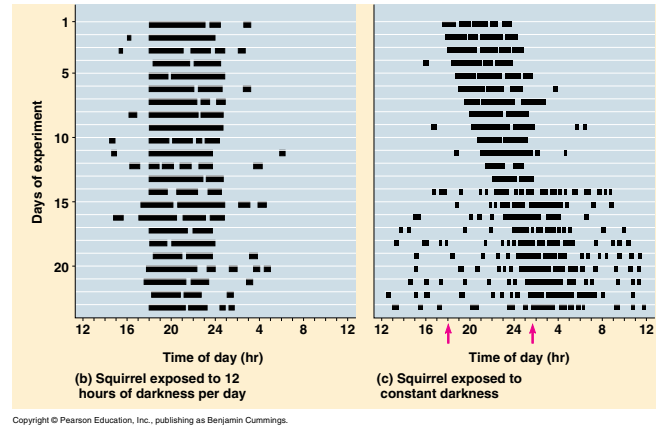


Figure 6.2: Circadian rhythms in a nocturnal mammal. From: Campbell & Reece (2008)48.25.

6.1 Circadian rhythm

The notion of a biological clock is typically used for the 24 hour cycle of the day/night rhythm. This is an autonomous cycle which persists under constant circumstances (i.e.,

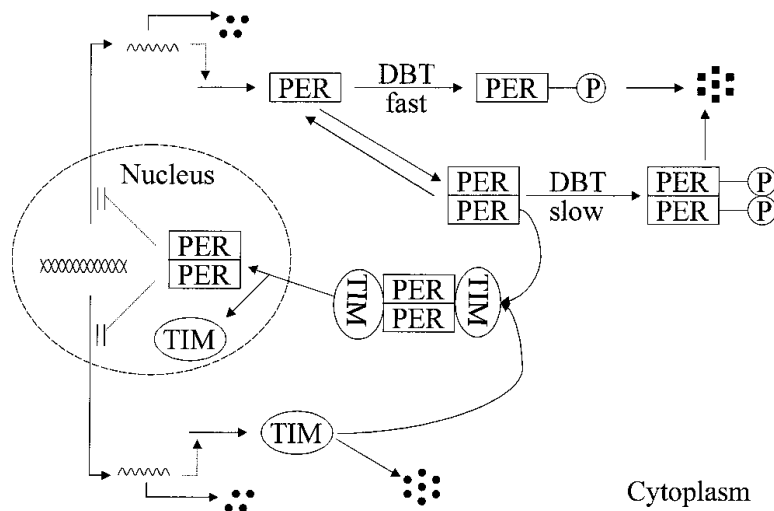


Figure 6.3: A simple molecular mechanism for the circadian clock in *Drosophila*. PER and TIM proteins (rectangle and oval, respectively) are synthesized in the cytoplasm, where they may be destroyed by proteolysis or they may combine to form relatively stable hetero-dimers. Heteromeric complexes are transported into the nucleus, where they inhibit transcription of *per* and *tim* mRNA. We assume that PER monomers are rapidly phosphorylated by DBT (a kinase encoded by the *double-time* gene) and then degraded. Dimers, we assume, are poorer substrates for DBT. From Figure 1 in Tyson *et al.* (1999).

under continuous light or darkness). Human volunteers living for half a year in the absence of a natural day/night rhythm develop a circadian rhythm of about 25 hours (Winfrey, 1986). This autonomous behavior is also obvious when we experience jet lag. Exposure to light, or even to short flashes of light, during the right part of the cycle can reset the clock, i.e., leads to a phase shift. An example of clock resetting is shown in Fig. 6.1 where cultured pineal cells are exposed to flashes of light, or to an inhibitor of protein synthesis. Depending on the timing of the light pulse the internal clock of the cells is shifted forwards or backwards. This dependence of the circadian rhythm to light allows the autonomous rhythm to adjust to the day/light cycle. This adjustment is called entrainment.

Circadian rhythms are common in plants and animals. Flowers opening early in the morning continue to do so when they are placed in total darkness. In vertebrates it has been shown that small group of neurons in the hypothalamus functions as a pacemaker for the circadian rhythm. Many other processes are influenced by this daily rhythm, e.g., hormone levels vary during the day.

The molecular basis of the circadian rhythm has been heavily studied in *Drosophila*. Fruit flies keep an 24 hour rhythm in complete darkness, and over a very wide range of temperatures (from 18–33 °C) (Barkai & Leibler, 2000; Vilar *et al.*, 2002; Goldbeter, 2002). Particular point mutations in the so-called *per*-gene (*per* = *period*) however

lead to different periods of the rhythm. Point mutations in another gene, *timeless* or *tim*, destroy the rhythm. The *tim*-gene encodes a protein (TIM) which binds the PER-protein. The PER-protein and *per*-mRNA concentrations oscillate with a period of 24 hours, where the protein concentrations rise 4–6 hours later than those of the mRNA. The PER-protein forms dimers that bind the TIM-protein. The PER-TIM complexes are transported to the nucleus where it binds transcription factors (see Fig. 6.3).

In the nucleus the PER-protein inhibits transcription by binding another protein (CLOCK-CYC) (Goldbeter, 2002) that activates *per* and *tim* gene expression. Thus, there is a negative feedback that acts by a counteracting gene activation. This negative feedback is the basis of most mathematical models for the circadian rhythm (Goldbeter, 1996, 2002). A negative feedback is not enough to have oscillations however. We have seen in the predator prey model (Fig. 4.1) that a positive feedback tends to destabilize the steady state, which by a Hopf bifurcation may give rise to a stable limit cycle. We will here present the model of Tyson *et al.* (1999), which has a positive feedback because PER and TIM complexes are more resistant to turnover than their monomers. There are alternative models that obtain periodic behavior without a positive feedback by the incorporation of “time delays” due to a number of phosphorylation events of the PER-protein (Goldbeter, 1996, 2002).

PER-protein is phosphorylated by DBT-kinase, after which it is rapidly degraded (see Fig. 6.3). The model of Tyson *et al.* (1999) assumes that PER/TIM dimers are phosphorylated at a much slower rate than the monomers. By this assumption dimers are more stable, i.e., have a longer expected life span, than monomers. This is a positive feedback because an increase in the concentrations of PER and TIM leads to a slower decay, which further increases the concentrations. Because PER and TIM-protein are subjected to similar interactions in the cell, Tyson *et al.* (1999) lump them together into one variable called P (for protein). This protein exists in the form of monomers P_1 or dimers P_2 . Assuming that protein concentrations in the cytosol remain proportional to those in the nucleus, Tyson *et al.* (1999) write the following three equations

$$\frac{dM}{dt} = \frac{c}{1 + (P_2/P_c)^2} - \delta_M M, \quad (6.1)$$

$$\frac{dP_1}{dt} = lM - \frac{\rho_1 P_1}{h + P_1 + 2P_2} - \delta_P P_1 - 2k_a P_1^2 + 2k_d P_2, \quad (6.2)$$

$$\frac{dP_2}{dt} = k_a P_1^2 - k_d P_2 - \frac{\rho_2 P_2}{h + P_1 + 2P_2} - \delta_P P_2, \quad (6.3)$$

where $\rho_2 \ll \rho_1$ such that dimers have a much slower phosphorylation rate than monomers. Transcription (i.e., mRNA production) decreases as a function of the PER/TIM dimers, P_2 , according to a sigmoid Hill function (when $P_2 = P_c$ transcription is half-maximal). For the phosphorylation Tyson *et al.* (1999) assume a Michaelis-Menten saturation where both the monomers and dimers are substrates competing for access to the DBT-kinase (see the Exercises). The h parameter is the Michaelis-Menten constant: when $P_1 + 2P_2 =$

h the proteins are phosphorylated at the half maximal rate. The behavior of the model is depicted in Fig. 6.4a: the concentrations of mRNA and total protein ($T = P_1 + 2P_2$) indeed oscillate on a limit cycle where the protein concentration T lags a few hours behind the mRNA concentration M .

6.2 Quasi steady state

To simplify the model into two ODEs, Tyson *et al.* (1999) assume that dimerization and dissociation is much faster than all other processes of the model, i.e., they assume that k_a and k_d are fast parameters. If this is the case, then at any point in time the total dimerization should approximately equal the total dissociation, i.e., $k_a P_1^2 \simeq k_d P_2$, or $P_2 \simeq K P_1^2$ where $K = k_a/k_d$. Knowing the P_2 and P_1 ratio, one can rewrite the model in terms of the total concentration of PER-protein. Because there are two PER-molecules in one P_2 dimer we define $T = P_1 + 2P_2$. Since $P_2 = K P_1^2$ we have $T = P_1 + 2K P_1^2$ such that we can solve P_1 from this quadratic equation, i.e.,

$$P_1 = \frac{-1 + \sqrt{1 + 8KT}}{4K}, \quad (6.4)$$

(check for yourself that the negative root of the quadratic equation has to be ignored because it yields a negative solution for P_1). The differential equation for the total PER-protein concentration is obtained by summing Eqs. 6.2 and 6.3:

$$\frac{dT}{dt} = lM - \frac{\rho_1 P_1 + 2\rho_2 P_2}{h + T} - \delta_P T, \quad (6.5)$$

where P_1 is defined by Eq. (6.4) and $P_2 = K P_1^2$. Together with Eq. (6.1) this defines a 2-dimensional model, which is analyzed by nullclines in Fig. 6.5.

The form of the total PER-protein nullcline $dT/dt = 0$ is determined by a complicated function (see Eq. (6.5)) and has the form of a third order equation with a minimum and a maximum (see Fig. 6.5). In the top left corner of the phase space, with a lot of mRNA M and little PER-protein T , protein is produced by translation (lM is large) and there is little loss by phosphorylation (because $T = P_1 + 2P_2$ is small). Thus, above the T -nullcline $dT/dt > 0$. The valley in the T -nullcline is due to the positive feedback: this is the region where increasing T decreases the turnover of the PER-protein. The mRNA nullcline has a much simpler form because it is a Hill function. As long as $P_2 \ll P_c$ the nullcline approaches $M = c/\delta_M = 10$. Above this steady state $dM/dt < 0$, i.e., the mRNA concentration decrease above the nullcline and increases below it. When the PER-protein concentration increases the mRNA nullcline curves to the bottom. The parameters are chosen such that the two nullclines intersect in the unstable part of the PER nullcline.

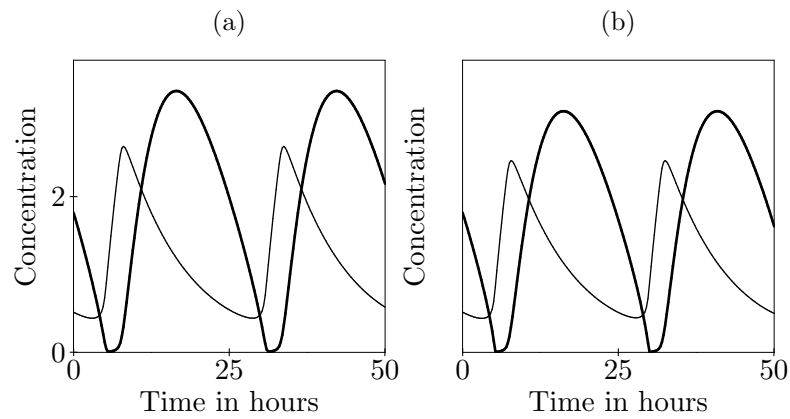


Figure 6.4: The behavior of the 3-dimensional (a) and the 2-dimensional Tyson *et al.* (1999) model. Parameters: $h = 0.05$, $k_a = 2000$, $k_d = 10$ ($K = 200$), $\delta_M = 0.1/\text{hour}$, $\rho_1 = 10$, $\rho_2 = 0.03$, $\delta_P = 0.1/\text{hour}$, $P_c = 0.1$, $c = 1$ and $l = 0.5$.

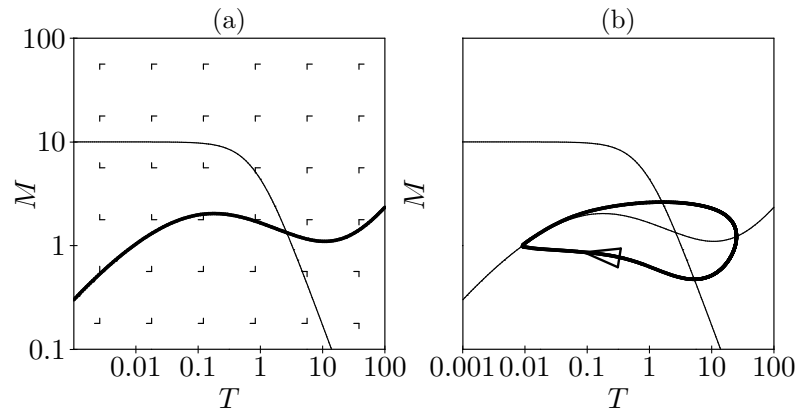


Figure 6.5: The nullclines and trajectories of the 2-dimensional model defined by Eq. (6.1) and Eq. (6.5). (a) nullclines and (b) nullclines with the stable limit cycle. The heavy line in (a) is the $dT/dt = 0$ nullcline and the light line the $dM/dt = 0$ nullcline. The heavy line in (b) is a trajectory approaching the stable limit cycle. Parameters as in Fig. 6.4 (see (Tyson *et al.*, 1999)).

From the vector field we read that increasing total protein, T , makes $dT/dt > 0$, which is a local positive feedback. Increasing M makes $dM/dt < 0$. Because of the positive feedback the non-trivial steady state is likely to be unstable. Tyson *et al.* (1999) choose parameters such that the steady state is unstable, and the behavior of the model is the limit cycle shown in Fig. 6.4 and Fig. 6.5. Parameters were chosen such that the cycle has a period of about 24 hours (Tyson *et al.*, 1999). The curves in Fig. 6.4 give the behavior of the 3-dimensional and the 2-dimensional model. The assumption that $P_2 = KP_1^2$ is apparently reasonable for the current parameter values, i.e., $k_a = 2000$ and $k_d = 10$ ($K = 200$). In the computer exercises you can study other choices for the time scale of the dimerization k_a and dissociation k_d , while keeping overall the same

parameters, i.e., $K = 200$.

The paper by Tyson *et al.* (1999), the book by Goldbeter (1996) and his review in *Nature* (Goldbeter, 2002) provide an excellent background to the material covered in this chapter.

6.3 Summary

Periodic behavior is easily observed in simple models. Possible mechanisms accounting for periodic behavior are time delays and positive feedback loops. Intuitively, it is difficult to understand why steady states would become unstable and then be surrounded by a new attractor taking the form of a stable limit cycle.

6.4 Exercises

Question 6.1. Tyson model

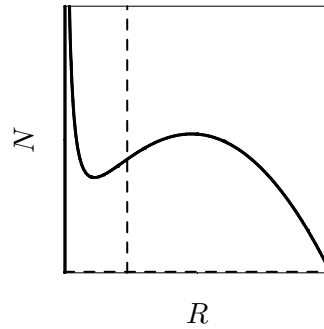
Consider Fig. 6.5 with the phase space of the Tyson *et al.* (1999) model.

- a. Shift the mRNA-nullcline horizontally such that the steady state is located on three qualitatively different regions of the PER-nullcline.
- b. Determine the stability of the steady state for each situation.
- c. Sketch for each situation a representative trajectory.

Two extra exercises for the most interested students:

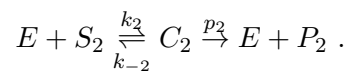
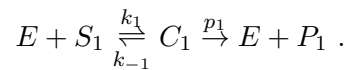
Question 6.2. Goldbeter, Nature, 2002 (Extra exercise for cool students)

Read the review paper by Goldbeter on biological rhythms published in *Nature* in 2002. The Figure in Box 1 depicts a bifurcation diagram. Sketch a similar bifurcation diagram by varying the R_0 of the predator in the sigmoid predator prey model with a nullcline configuration:



Question 6.3. Michaelis-Menten (Extra exercise for cool students)

Extend the Michaelis-Menten term to allow for two substrates competing for access to the enzyme. Thus, consider the following reaction for the formation of some product P_i from a substrate S_i . The enzyme E catalyzes the reaction, i.e.,



Because the enzyme is released when the complex dissociates one writes a conservation equation

$$E + C_1 + C_2 = E_0 .$$

- Write the differential equations for the substrates and the complexes. Use the conservation equation!
- Assume that the formation of the complexes is much faster than that of the product, i.e., make the quasi steady state assumptions $dC_1/dt = dC_2/dt = 0$. Note that you can add dC_i/dt to simplify dS_i/dt .
- Write the new model for the substrates. Simplify by defining new parameters.
- Compare your result with the phosphorylation term in the Tyson *et al.* (1999) model.

Question 6.4. Computer exercise: Circadian rhythm

The Tyson *et al.* (1999) model for the circadian rhythm is available as a GRIND model in the files `tyson.*`.

- Draw the nullclines of Fig. 6.5 by reading the `tyson.txt` parameter file.
- The circadian rhythm of *Drosophila* hardly depends on the temperature. Assume that temperature mainly determines the K parameter and study how this affects the stability of the steady state and the period of the limit cycle.
- Point mutations in the PER-protein do influence the period of the limit cycle. Assume that mutated forms of the PER-protein are phosphorylated at different rates, and

study how that influences the stability of the steady state and the period of the cycle.

- d.** Make a phase response curve as in Fig. 6.1 by perturbing the protein concentration P .

Chapter 7

Chronic viral infections and immune control

Our mission in this Chapter is to study models with so many differential equations that one can no longer use nullcline analysis. Only in the exercises we will again draw nullclines after simplifying the model by separating its time scales.

We consider the epidemiology of a chronic viral infection within one individual. A chronic viral infection consists of many viral generations where the virus infects target cells that produce novel virus particles. The damage caused by the virus occurs by lysis of the target cells, for so-called cytolytic viruses, or by the killing of infected cells by the host immune response (e.g., by $CD8^+$ cytotoxic T cells). Recent modeling work in virology has revealed a number of new insights into chronic viral infections like HIV infection, hepatitis, and human leukemia viruses like HTLV-1 (Ho *et al.*, 1995; Wei *et al.*, 1995; Nowak & Bangham, 1996; Nowak & May, 2000). Previously, it was thought that chronic viral infections were due to “slow viruses”, but now one realizes that a chronic infection is a (quasi) steady state where a rapidly reproducing virus is controlled by the host (probably by the host immune response). HIV-1 and HTLV-1 have $CD4^+$ T cells as the major target cell and hepatitis viruses infect liver cells. The availability of target cells may also play a role in limiting the chronic infection.

7.1 Immune response

Virus infections typically evoke immune responses composed of antibodies and $CD8^+$ cytotoxic T cells. A natural model for target cells T , infected cells I , virus particles V , and a cellular immune response E , would be

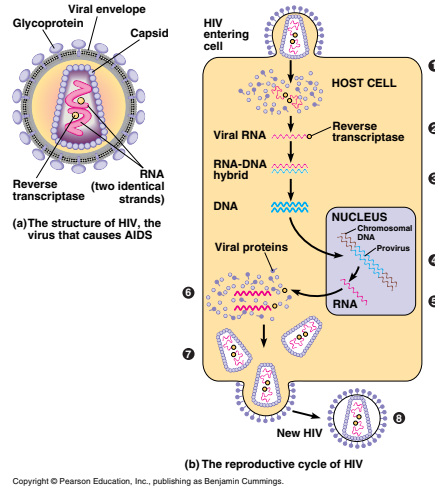


Figure 7.1: HIV-1 infection of a target cell. From: Campbell & Reece (2008)18.10.

$$\begin{aligned}
 \frac{dT}{dt} &= \sigma - \delta_T T - \beta TV, \\
 \frac{dI}{dt} &= \beta TV - \delta_I I - kEI, \\
 \frac{dV}{dt} &= pI - \delta_V V, \\
 \frac{dE}{dt} &= \alpha EI - \delta_E E,
 \end{aligned} \tag{7.1}$$

where σ is the daily production of target cells, uninfected target cells have a half life of $\ln[2]/\delta_T$ days, and infected cells have a half life of $\ln[2]/\delta_I$ days. One can set $\delta_I > \delta_T$ to allow for cytopathic effects of the virus. Uninfected cells can become infected by meeting with infected cells at a rate β /day per infected cell. The kEI term reflects the killing of infected cells by the immune effectors E , and the αEI represents the clonal expansion of immune effectors in response to antigen.

The non-trivial steady states of this model should correspond to the situation of a chronic viral infection. These steady states are found by solving the equations from the simplest to the most complicated. Solving $dE/dt = 0$ yields the solutions $\bar{E} = 0$ or $\bar{I} = \delta_E/\alpha$. Proceeding with the latter, i.e., considering the case with an immune response, one solves $dV/dt = 0$ to find that $V = (p/\delta_V)I$. Next, one can solve $dT/dt = 0$ and finally one solves $dI/dt = 0$ to find:

$$\bar{I} = \frac{\delta_E}{\alpha}, \quad \bar{V} = \frac{p}{\delta_V} \bar{I} = \frac{p\delta_E}{\alpha\delta_V}, \quad \bar{T} = \frac{\sigma}{\delta_T + \beta\bar{V}} = \frac{\alpha\sigma\delta_V}{\alpha\delta_T\delta_V + p\beta\delta_E}, \tag{7.2}$$

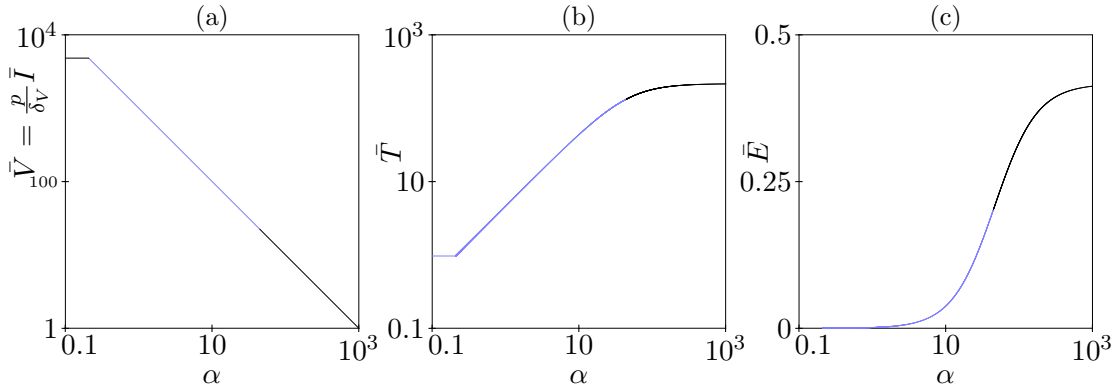


Figure 7.2: The steady state of Eq. (7.2) as a function of the immune activation parameter α . When α becomes too small the immune response cannot maintain itself, and the virus is controlled by target cell availability. This new steady state for low α can be computed by solving the steady state of Eq. (7.1) for $E = 0$, and is therefore independent of α . Parameters: $\beta = 0.01$ per virion per day, $\delta_E = \delta_I = 0.1$ per day, $\delta_T = 0.01$ per day, $\delta_V = 3$ per day, $k = 1$ per cell per day, $p = 100$ per day and $\sigma = 10$ cells per day.

and

$$\begin{aligned} \bar{E} &= \frac{p\beta}{k\delta_V}\bar{T} - \frac{\delta_I}{k} \\ &= \frac{p\beta\alpha\sigma}{k(\alpha\delta_T\delta_V + p\beta\delta_E)} - \frac{\delta_I}{k}, \end{aligned} \quad (7.3)$$

which is a saturation function of α (see Fig. 7.2c).

From these steady state one can read that the size of the target cell population declines with the viral load \bar{V} , i.e., the extend of liver damage, or of $CD4^+$ T cell depletion, increases with the viral load. Surprisingly, the steady state number of infected cells, $\bar{I} = \delta_E/\alpha$, only depends on immune response parameters (Nowak & Bangham, 1996), which suggests that target cell availability cannot have any contribution to the viral load.

During the chronic phase HIV-1 infected patients have a quasi steady state viral load called the “set point” (see Fig. 7.3). Different patients have enormously different set points, i.e., more than a 1000-fold variation between patients. Patients with a high set point tend to have a much faster disease progression (Mellors *et al.*, 1996). According to this model the steady state number of infected cells $\bar{I} = \delta_E/\alpha$. Because the expected life span of effector cells is not expected to vary much between people, 1000-fold variations in \bar{I} can only be explained by 1000-fold variations in α , see Fig. 7.2 (Nowak & Bangham, 1996; Müller *et al.*, 2001). The corresponding variation in the immune response \bar{E} is saturation function of α , however. Patients differing n -fold in the set point are not expected to differ n -fold in the immune response \bar{E} (see Fig. 7.2). This explains the

paradoxical observation that patients with low and high virus loads of HTLV-I tend to have the same level of the CD8⁺ T cell response (Nowak & Bangham, 1996; Nowak & May, 2000). Although the immune activation parameter, α , completely determines the steady state viral load, it apparently has less effect on the magnitude of the immune response.

7.2 Separation of time scales

For several viral infections it has been established that the kinetics of free viral particles is much faster than that of infected cells. For instance, for both HCV and HIV-1 infections we know that $\delta_V \gg \delta_I$ (Perelson *et al.*, 1996; Neumann *et al.*, 1998). It is therefore quite reasonable to assume that the virus equation is at quasi steady state. Setting $dV/dt = 0$ we employ that $V = (p/\delta_V)I$, i.e., the virus load becomes proportional to the concentration of infected cells. Substituting $V = (p/\delta_V)I$ into the model yields

$$\begin{aligned}\frac{dT}{dt} &= \sigma - \delta_T T - \beta' T I, \\ \frac{dI}{dt} &= \beta' T I - \delta_I I - k E I, \\ \frac{dE}{dt} &= \alpha E I - \delta_E E,\end{aligned}\tag{7.4}$$

where $\beta' \equiv p\beta/\delta_V$. The technique by which we have simplified the 4-dimensional model into a 3-dimensional model is called ‘‘separation of time scales’’. Here we have removed the fastest time scale by a quasi steady state assumption. Note that the virus concentration is not assumed to remain constant: rather it is assumed to be proportional to the infected cells.

There is another time scale in the model that we can eliminate under certain circumstances. After the immune response E has been established it probably changes on a very slow time scale. For instance, during therapy of chronically infected patients, the stimulation of the immune effector cells will drop, because αI decreases, but due to memory effects the effector population may remain large. One could account for such memory effects by allowing the immune effectors E to have a very long half-life $\ln[2]/\delta_E$, i.e., by making δ_E a small parameter. If the immune effector cells are long-lived their decline during therapy should be negligible, i.e., one can simplify the model during therapy by the approximation that E remains constant. This fixed value of E is given by Eq. (7.3). Thus, the simplified model where we have removed the fastest and the slowest time scale becomes

$$\frac{dT}{dt} = \sigma - \delta_T T - \beta' T I, \quad \frac{dI}{dt} = \beta' T I - \delta I,\tag{7.5}$$

where $\beta' \equiv p\beta/\delta_V$ and $\delta \equiv \delta_I + kE$.

This is a model that you are familiar with. It is a host-parasite model with a fixed production term (see the “Malaria” exercise in Chapter 3). So you know the reproductive ratio of the infection and its steady state:

$$R_0 = \frac{\beta' \sigma}{\delta_T \delta} \quad \text{such that} \quad \bar{T} = \frac{\sigma}{\delta_T R_0} = \frac{K}{R_0} \quad \text{and} \quad \bar{I} = \frac{\sigma}{\delta} \left(1 - \frac{1}{R_0} \right), \quad (7.6)$$

where K is the “carrying capacity” of the target cells. Since most viruses have rapid growth rates, i.e., typically $R_0 \gg 1$, this reveals that the steady state density of infected cells, and hence the viral load, remains fairly independent of β' (Bonhoeffer *et al.*, 1997).

The 2-dimensional model of Eq. (7.5) can be used to fit the data from HIV-1 or HCV infected patients under anti-retroviral treatment. Current treatments consist of nucleoside analogs that block *de novo* infections, and of protease inhibitors blocking production of infectious virus particles. This basically means that the drugs reduce the infection parameter β . Thus the model for infected cells under treatment becomes $dI/dt = -\delta I$, which has the simple solution $I(t) = I(0)e^{-\delta t}$. By plotting the decline of the virus load during treatment on a logarithmic scale, and fitting the data by linear regression, one therefore obtains estimates for the half life $\ln[2]/\delta$ of productively infected cells. For HIV-1 this has been done (Ho *et al.*, 1995; Wei *et al.*, 1995), and these now classical studies estimate half lives of 1–2 days for cells productively infected with HIV-1. Similar results have been obtained with HBV (Nowak & Bangham, 1996) and HCV (Neumann *et al.*, 1998). Thus, chronic viral infections are not slow, and involve hundreds of viral generations over the host life time. This is a fine example where mathematical modeling has increased our understanding of chronic viral infections.

7.3 Summary

Models of viral infections and immune reactions strongly resemble ecological models. Intuitively one cannot predict which parameters are most important in controlling the virus load. The large difference between patients with a low and a high viral load can only be explained by large differences in immune response parameters, which need not result in very different magnitudes of the actual immune response. The fact that the viral generation time can be estimated by a simple linear regression proves that simple models sometimes allow for important new interpretations.

Nowak & May (2000) have published a very readable book on modeling viral infections.

7.4 Exercises

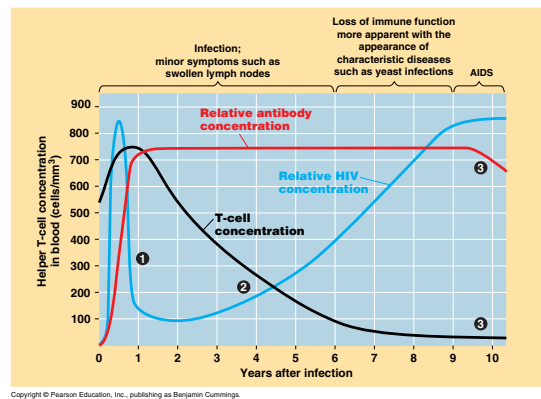


Figure 7.3: The time course of an HIV-1 infection. Figure 43.20 in Campbell & Reece (2002).

Question 7.1. $CD4^+$ T cells

HIV-1 infected patients die from the immunodeficiencies that are brought about by their low $CD4^+$ T cell counts. A form of treatment that has been tried is to give immunostimulatory medication to increase the $CD4^+$ T cell counts. Suppose that $CD4^+$ are the most important target cells of HIV-1.

- Incorporate an immunostimulatory treatment in Eq. (7.5).
- What is the effect that you expect from this treatment?
- What alternative treatment is in fact suggested by this model?
- How would this alternative treatment affect the number of uninfected $CD4^+$ T cells?

Question 7.2. Rebound

Patients treated with anti-retroviral medication (i.e., reverse transcriptase inhibitors) sometimes have a rebound in their viral load even before the virus evolves drug resistance (see Fig. 7.4). In the models developed here this form of treatment can be modeled by reducing β . Investigate the expected effects of treatment by analyzing the phase space of Eq. (7.5).

- Sketch the nullclines before and after treatment in one phase space.
- Sketch the trajectory corresponding to this treatment in the same figure (also do this with Madonna or GRIND (see Chapter 14)).
- Sketch the same behavior as a function of time.
- Is drug resistance necessary for the observed viral rebound?

Question 7.3. Immune control

Consider anti-retroviral therapy in the immune control model defined by Eq. (7.1).

- What do you expect in the long run for the infected cell load I from a therapy that decreases β ?
- Would such a treatment have any positive effect for the patient?

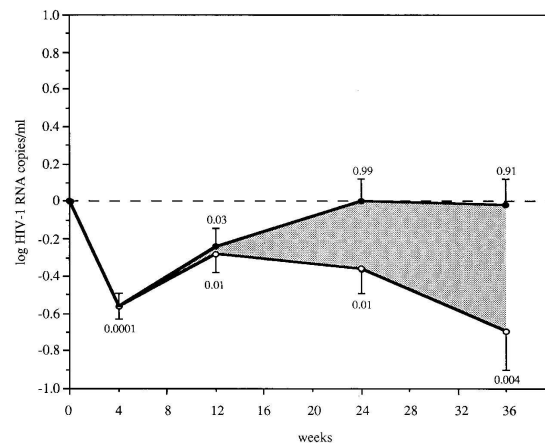


Figure 7.4: Mean changes from baseline (\pm SE) in the total HIV-1 RNA load (\bullet), and 70 wild-type HIV-1 RNA (\circ). Absolute copy numbers of 70 wild-type RNA were calculated from total serum HIV-1 RNA load by using the percentages of 70 wild-type RNA, as detected by the point mutation assay. Numbers above and underneath error bars indicate P values of the changes (paired two-tailed t test). The shaded area represents the contribution of 70 mutant HIV-1 RNA to changes in total HIV-1 RNA load. From: De Jong *et al.* (1996).

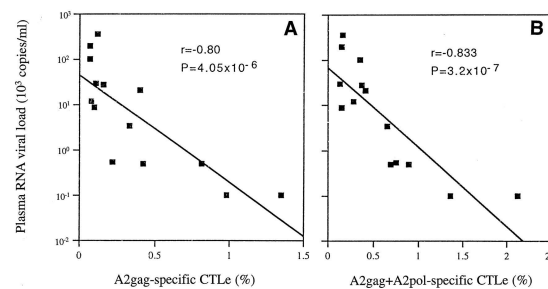


Figure 7.5: The viral load as a function of the size of the $CD8^+$ T cell immune response. There is an excellent negative correlation for two different proteins of the virus (gag and pol). From: Ogg *et al.* (1998).

Question 7.4. Ogg *et al.* (1998)

Although this is now controversial, Ogg *et al.* (1998) found an excellent negative correlation between the size of the $CD8^+$ T cell immune response and the viral load depicted in Fig. 7.5. The same authors have also argued that the large variations in the viral set points between HIV-1 infected patients have to be due to differences in the immune reactivity parameter α (Nowak & Bangham, 1996). Study whether these two interpretations are consistent by analyzing the following model

$$\frac{dI}{dt} = \beta V - \delta_I I - \alpha k EI, \quad \frac{dV}{dt} = pI - \delta_V V, \quad \frac{dE}{dt} = \alpha EI - \delta_E E,$$

where we have omitted the target cells for simplicity.

a. Remove the fastest time scale by a quasi steady state assumption.

- b. Sketch the nullclines of the simplified model.
- c. Write expressions for the non-trivial steady state of the model.
- d. Assume that patients differ in the immune reactivity parameter α , what kind of correlation do you expect between the viral load V and the immune response E ?*

Question 7.5. Competitive exclusion

Reconsider the full model Eq. (7.4) and let there now be two immune responses to the infected cells, i.e.,

$$\frac{dT}{dt} = \sigma - \delta_T T - \beta T I, \quad \frac{dI}{dt} = \beta T I - \delta_I I - k_1 I E_1 - k_2 I E_2, \quad (7.7)$$

$$\frac{dE_1}{dt} = \alpha_1 E_1 I - \delta_E E_1 \quad \text{and} \quad \frac{dE_2}{dt} = \alpha_2 E_2 I - \delta_E E_2. \quad (7.8)$$

For the sake of the argument let E_1 be the clone with the highest binding affinity of this antigen, i.e., let $\alpha_1 > \alpha_2$.

- a. What is the steady state of dE_1/dt ?
- b. What is the steady state of dE_2/dt ?
- c. Can both be true when $\alpha_1 > \alpha_2$?
- d. Substitute your answer of **a.** into dE_2/dt , and simplify. What do you expect for the second immune response when the first is at steady state?

You have discovered a concept from ecology called “competitive exclusion” (see Chapter 8): two immune responses cannot co-exist on the same resource (antigen). Since one can have several co-existing immune responses to several epitopes of the same virus during chronic immune reactions, one would have to argue that there is intra-specific competition in the immune system (De Boer *et al.*, 2001).

Chapter 8

Competitive exclusion

Competitive exclusion is a very general outcome of mathematical models. It occurs when two species compete for the same resource, e.g., when two viruses compete for the same target cells, or when two ecological species compete for the same niche. In Exercise 7.5 you showed that there can be no two immune response controlling one virus in steady state.

To illustrate the concept in its most general form consider some “resource” R that is used by two populations N_1 and N_2 . For simplicity we scale the maximum resource density to one. An example would be the total amount of nitrogen in a lake, which is either available for algae to grown on, or is unavailable being part of the algal biomass. A simple Lotka-Volterra like model is:

$$R = 1 - N_1 - N_2, \quad \frac{dN_1}{dt} = N_1(b_1R - d_1), \quad \frac{dN_2}{dt} = N_2(b_2R - d_2), \quad (8.1)$$

where R is the amount of nitrogen available for growth of the algae. The two populations have an R_0 of b_1/d_1 and b_2/d_2 , respectively. Substitution of $R = 1 - N_1 - N_2$ into dN_1/dt yields

$$\frac{dN_1}{dt} = N_1 (b_1(1 - N_1 - N_2) - d_1), \quad (8.2)$$

which has nullclines $N_1 = 0$ and

$$N_2 = 1 - \frac{1}{R_{0_1}} - N_1. \quad (8.3)$$

Similarly the $dN_2/dt = 0$ nullcline is found by substituting the amount of resource, R , into $dN_2/dt = 0$ and has nullclines $N_2 = 0$ and

$$N_2 = 1 - \frac{1}{R_{0_2}} - N_1. \quad (8.4)$$

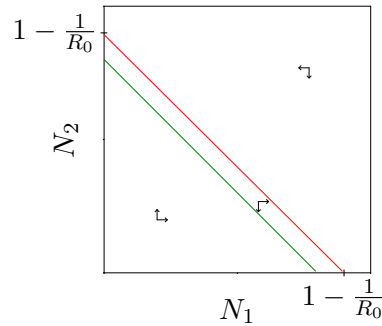


Figure 8.1: The parallel nullclines of Eq. (8.1).

Thus, plotting N_2 as a function of N_1 the two nullclines run parallel with slope -1 . The fact that they are parallel means that there is no steady state in which the two populations coexist. The intersects with the vertical N_2 axis are located at $N_2 = 1 - 1/R_0$. Thus the species with the largest fitness, R_0 , has the “highest” nullcline, and wins the competition (Fig. 8.1).

Competitive exclusion is a paradoxical result because many biological systems are characterized by the co-existence of many different species that seem to survive on very few resources. Examples are the incredible number of different bacterial species living in the ground, the number of algae species living in water, and the millions of lymphocyte clones comprising the adaptive immune system.

8.1 Exercises

Question 8.1. Saturated proliferation

Consider two immune responses to the same pathogen, and assume that the immune responses reduce the pathogen concentration to

$$A = 1 - kE_1 - kE_2 .$$

The maximum proliferation rate is a saturation function (i.e., a Hill function) of the pathogen concentration. Thus, let the immune responses be described by

$$\frac{dE_1}{dt} = \frac{pE_1A}{h_1 + A} - dE_1 \quad \text{and} \quad \frac{dE_2}{dt} = \frac{pE_2A}{h_2 + A} - dE_2 ,$$

where $h_2 > h_1$ means that the second response requires a higher pathogen concentration for obtaining the same proliferation rate. Because the proliferation is saturated it seems that exclusion would be less likely.

- a. Draw the nullclines in a phase space of E_1 and E_2 .
- b. Can the two responses coexist?
- c. What is the difference with Fig. 8.1?

Question 8.2. Competitive proliferation

Consider two immune responses to the same pathogen, and assume that the immune responses reduces the pathogen concentration to

$$A = 1 - kE_1 - kE_2$$

and let the immune responses be described by

$$\frac{dE_1}{dt} = \frac{pE_1A}{1 + c_1E_1} - dE_1 \quad \text{and} \quad \frac{dE_2}{dt} = \frac{pE_2A}{1 + c_2E_2} - dE_2 ,$$

where $c_2 > c_1$ means that the second response has a stronger intra-specific competition.

- a. Draw the nullclines in a phase space of E_1 and E_2 .
- b. Can the two responses coexist?
- c. What is the difference with Fig. 8.1?

Question 8.3. Virus competition experiments (Extra exercise for cool students)

To determine the relative fitness of two variants of a virus one typically grows them together in conditions under which they grow exponentially. Thus, consider two variants of a virus that grows exponentially according to

$$\frac{dV_1}{dt} = rV_1 \quad \text{and} \quad \frac{dV_2}{dt} = r(1 + s)V_2 ,$$

where s is the conventional selection coefficient. One way to represent the data is to plot how the fraction $f \equiv V_2/(V_1 + V_2)$ evolves in time. To compute how the fraction $f(t)$ changes on needs to employ the quotient rule of differentiation: $[f(x)/g(x)]' = (f(x)'g(x) - f(x)g(x)')/g(x)^2$. Thus, using $'$ to denote the time derivative, one obtains for df/dt :

$$\begin{aligned} \frac{df}{dt} &= \frac{V_2'(V_1 + V_2) - (V_1' + V_2')V_2}{(V_1 + V_2)^2} , \\ &= \frac{V_2'V_1 - V_1'V_2}{(V_1 + V_2)^2} , \\ &= \frac{r(1 + s)V_2V_1 - rV_1V_2}{(V_1 + V_2)^2} , \\ &= r(1 + s)(1 - f)f - rf(1 - f) , \\ &= rsf(1 - f) , \end{aligned}$$

which is the logistic equation with growth rate rs and steady states $f = 0$ and $f = 1$. Thus one expects a sigmoidal replacement curve of the two variants.

- a.** Now write a differential equation of the ratio $\rho = V_2/V_1$ of the two populations.
- b.** Virologists plot the logarithm of the ratio in time to determine the relative fitness (Holland *et al.*, 1991). What is the slope of $\ln[\rho]$ plotted in time?

Chapter 9

The Hodgkin-Huxley model

This Chapter explains the Hodgkin-Huxley model (1952) for the generation of an action potential in neurons. This is a complicated model. We introduce it because it is the most famous model in Theoretical Biology (Hodgkin and Huxley were honored with the Nobel prize for this work), and because it gives you an idea what a large realistic model can look like. The Hodgkin-Huxley model resulted from detailed experiments with the giant squid neuron, which was combined with electrophysics and computational work on mechanical calculators. The power of the model is that it can predict the outcome of experiments. We will explain the full model and then show how simplification by separation of time scales can help to obtain a better understanding. Mathematical models are commonly used in neurophysiology.

An action potential is generated at the cell body of a neuron and then travels along the axon to a synapse where the electrical signal is transmitted to the receiving cell. An action potential is generated by the opening and closing of voltage-sensitive gates (see Fig. 9.2). The intracellular and extracellular concentrations of a number of ions, like sodium (Na^+) and potassium (K^+), are different. These differences in the ion concentrations are responsible for a voltage of -70mV over the cell membrane, which is called the resting potential (see Fig. 9.1). The flux of ions over a membrane is influenced both by diffusion due to concentration differences, and by the electrical field. The latter influence is described by a simple equation of the form $f(V) = zV/(e^{zV} - 1)$ where z is the valence of the ion, and V is the voltage. This function is depicted in Fig. 9.3: the current in one particular direction is zero when the valence has the same sign as the voltage, and becomes proportional to the voltage when they have opposite signs. Note, that this is quite a neat function that we could add to our families of Hill functions and exponential functions for modeling a process that smoothly switches on around some value of x and then approaches a linear dependence on x .

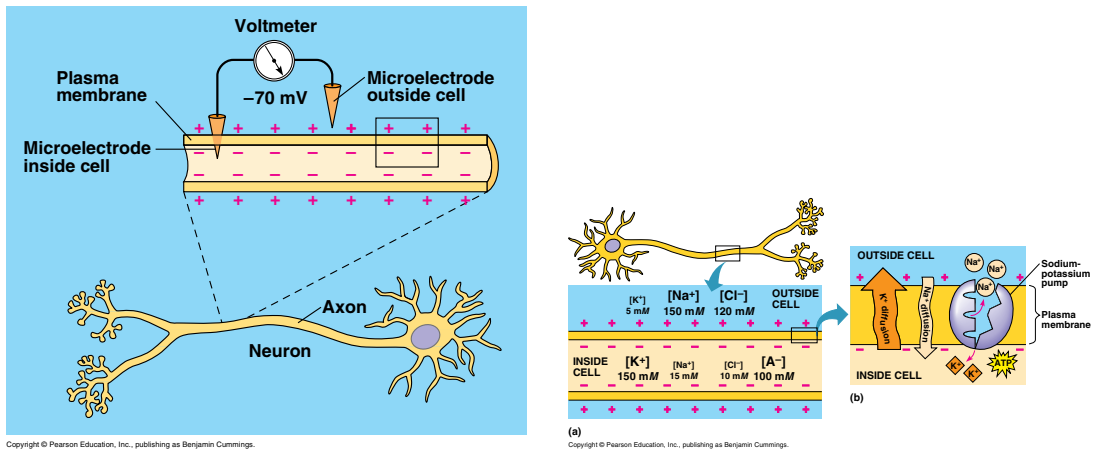


Figure 9.1: The resting membrane potential. Figures 48.6a and 48.7 in Campbell & Reece (2002) and 48.9 and 48.10 in Campbell & Reece (2005).

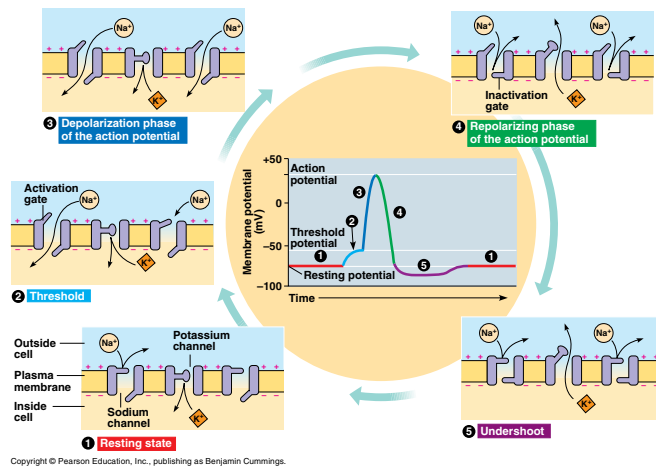


Figure 9.2: Voltage sensitive gates open and close to generate an action potential. From: Campbell & Reece (2008)48.13.

To model the flux, or current, of ions across a membrane one writes the so-called Nernst equation composed of the inward and outward flux. For the voltage dependence, the Nernst equation uses the function $f(V) = zV/(e^{zV} - 1)$ for the inward direction and hence

$$f(-V) = \frac{-zV}{e^{-zV} - 1} = \frac{-zVe^{zV}}{1 - e^{zV}} = \frac{zVe^{zV}}{e^{zV} - 1} \tag{9.1}$$

for the outward direction. For instance for the K⁺ ion (which has valence $z = 1$) the

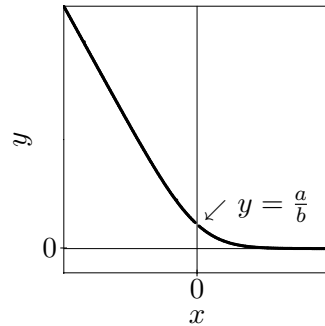


Figure 9.3: The shape of the influx function $y = ax/(e^{bx} - 1)$ in Eq. (9.2). To know the value at $x = 0$ one uses the l'Hopital rule: $\lim_{x \rightarrow a} f(x)/g(x) = \lim_{x \rightarrow a} f'(x)/g'(x)$. Thus, $\lim_{x \rightarrow 0} ax/(e^{bx} - 1) = \lim_{x \rightarrow 0} a/(be^{bx}) = a/b$.

current I_K across the membrane is given by:

$$\begin{aligned}
 I_K &= \text{inward} - \text{outward} \\
 &= pK_o f(V) - pK_i f(-V) \\
 &= pK_o \frac{zV}{e^{zV} - 1} - pK_i \frac{zV e^{zV}}{e^{zV} - 1} \\
 &= (K_o - K_i e^{zV}) \frac{pzV}{e^{zV} - 1}, \tag{9.2}
 \end{aligned}$$

where K_o and K_i give the outside and inside K^+ concentrations, respectively. (This voltage V is scaled with the temperature T , the Faraday constant F , and the gas constant R .) The equilibrium voltage \bar{V} , i.e., the concentrations at which the current I_K becomes zero, can be solved from Eq. (9.2) as

$$\bar{V}_K = \frac{1}{z} \ln \frac{K_o}{K_i}. \tag{9.3}$$

Any concentration difference, or ratio K_o/K_i , therefore functions as a “battery” of \bar{V}_K mV. This steady state voltage is called the Nernst equilibrium potential. The other ions, e.g., Na^+ and Ca^{2+} , also function as such a “battery”, and therefore contribute to the resting potential of the neuron. These different contributions are combined in the famous Goldman equation.

9.1 Hodgkin-Huxley model

The total current I over the membrane is the sum of the currents of the different ions. Because $I = V/R$ the current of every ion is given by the resistance R over the membrane and the potential difference between the equilibrium voltage \bar{V} and the membrane

potential V . For the current of sodium (Na^+), potassium (K^+) and a rest-group of ions, one therefore writes:

$$I = g_N(\overline{V}_N - V) + g_K(\overline{V}_K - V) + g_R(\overline{V}_R - V) \quad (9.4)$$

where g_N, g_K , and g_R are the conductances (i.e., $g = 1/R$), and where $\overline{V}_N, \overline{V}_K$, and \overline{V}_R are the Nernst equilibrium potentials for sodium, potassium and the rest-group, respectively. Because $dV/dt = I/C$, where C is the capacity of the membrane, the change in the membrane potential V obeys

$$\frac{dV}{dt} = \frac{1}{C} [g_N(\overline{V}_N - V) + g_K(\overline{V}_K - V) + g_R(\overline{V}_R - V)] . \quad (9.5)$$

Voltage sensitive channels in the cell membrane specifically regulate the transport of ions through the membrane (see Fig. 9.2). The conductances g_N and g_K are therefore complex functions of the voltage V . Hodgkin and Huxley were able to measure the current of ions through these channels by “voltage-clamp” experiments with the axon of the giant squid. In voltage-clamp experiments one fixes the voltage by means of a thin silver thread within the axon. With micro-electrodes one can register the current of the ions over time for any (change in) voltage. One can distinguish sodium from potassium channels by depleting sodium or potassium from the medium.

To describe the voltage dependence of g_N and g_K , measurements were done to see how fast the current through the channels changes, and what equilibrium the current ultimately approaches when the voltage is kept at a certain value (see Fig. 9.4). In the Hodgkin Huxley model the voltage is scaled such that the resting potential corresponds to $V = 0$. Moreover, in the model an action potential is a sharp decrease of the voltage (from $V = 0$ to $V \simeq -110$, see Fig. 9.5), whereas normally one defines the voltage such that it increases (see Fig. 9.2). Anyway, Hodgkin and Huxley defined three variables, m , n and h , which are three fitted voltage sensitive channel proteins. The m variable corresponds to the opening of the sodium channel, h to the inhibition (closure) of the sodium channel, and n to the opening of the potassium channel. The channels open and close at a certain rate determined by the membrane potential V , and are —like our Hill functions— scaled between zero and one (see Fig. 9.4). For the sodium channel they wrote

$$\frac{dm}{dt} = 0.1(1 - m) \frac{V + 25}{e^{(V+25)/10} - 1} - 4me^{V/18} = \alpha_m(1 - m) - \beta_m m , \quad (9.6)$$

$$\frac{dh}{dt} = 0.07(1 - h)e^{V/20} - \frac{h}{e^{(V+30)/10} + 1} = \alpha_h(1 - h) - \beta_h h , \quad (9.7)$$

and for the potassium channels

$$\frac{dn}{dt} = 0.01(1 - n) \frac{V + 10}{e^{(V+10)/10} - 1} - 0.125ne^{V/80} = \alpha_n(1 - n) - \beta_n n . \quad (9.8)$$

These three differential equations seem very complicated but are basically simple functions fitted to the data in Fig. 9.4. For instance the opening of m has the form

$y = ax/(e^{bx} - 1)$ that we already depicted in Fig. 9.3. The closure of h has a function $1/(e^{ax} + 1)$ which is a sigmoid function vanishing to zero when $x \rightarrow \infty$.

Substitution of the m , h , and n variables into the conductance terms of Eq. (9.5), together with the estimated maximum of each term, finally gives the Hodgkin-Huxley equation for the change of the voltage

$$\frac{dV}{dt} = \frac{1}{C} [120m^3h(\bar{V}_N - V) + 36n^4(\bar{V}_K - V) + 0.3(\bar{V}_R - V)] , \quad (9.9)$$

with the three scaled Nernst equilibrium potentials $\bar{V}_N = -115$, $\bar{V}_K = 12$, and $\bar{V}_R = -10.5989$. This mathematical model has one stable steady state where $V \simeq 0$, $m \simeq 0.05$, $h \simeq 0.6$ and $n \simeq 0.3$. A sufficiently large decrease of the resting potential in this steady state triggers a model behavior that very realistically resembles an action potential (see Fig. 9.5).

Having the Hodgkin Huxley model at hand one can understand what happens after decreasing the resting potential, i.e., after exciting the membrane:

1. Due to the decrease in voltage, sodium changes m open (see Fig. 9.4) and a minor current of Na^+ ions leaks inwards. Because the conductance for Na^+ is now much larger than that for the other ions, the voltage approaches the Nernst equilibrium potential for sodium $\bar{V}_N = -115$. Thus the g_N term dominates in Eq. (9.5).
2. This decrease in the voltage triggers the inhibition of the sodium channels (see the h -variable in Fig. 9.4 and Fig. 9.5), i.e., the g_N term loses its dominance and the voltage starts to recover.
3. Additionally, the potassium channels open (allowing a little K^+ to leave the cell). Because the g_K term now is dominant, the voltage approaches the Nernst equilibrium potential for potassium, $\bar{V}_K = 12$, which leads to a “undershoot” of the voltage to well below the resting potential.
4. Finally the voltage reverts to the resting potential.

The Hodgkin-Huxley model is unpleasantly complex, and in this given form one can little more than simulate the model on a computer to see its behavior in time. The output of the model is therefore almost as “flat” as the output of biological experiments. Several researchers have tried to simplify the model to obtain better insight into its behavior (and simultaneously into the behavior of the neurons we are modeling). Citing Fitzhugh (1960): “The usefulness of an equation to an experimental physiologist (...) depends on his understanding how it works.” Fitzhugh (1960) analyzed the Hodgkin-Huxley model and observed that the variables have quite different time scales: the V and m variables change more rapidly than h and n . For instance, during the first milli-second in Fig. 9.5, h and n have hardly changed. He exploited these different time scales to simplify the Hodgkin-Huxley model. In the exercises you will work with the much simpler Fitzhugh-Nagumo model, which is a phenomenological description of the Hodgkin-Huxley model.

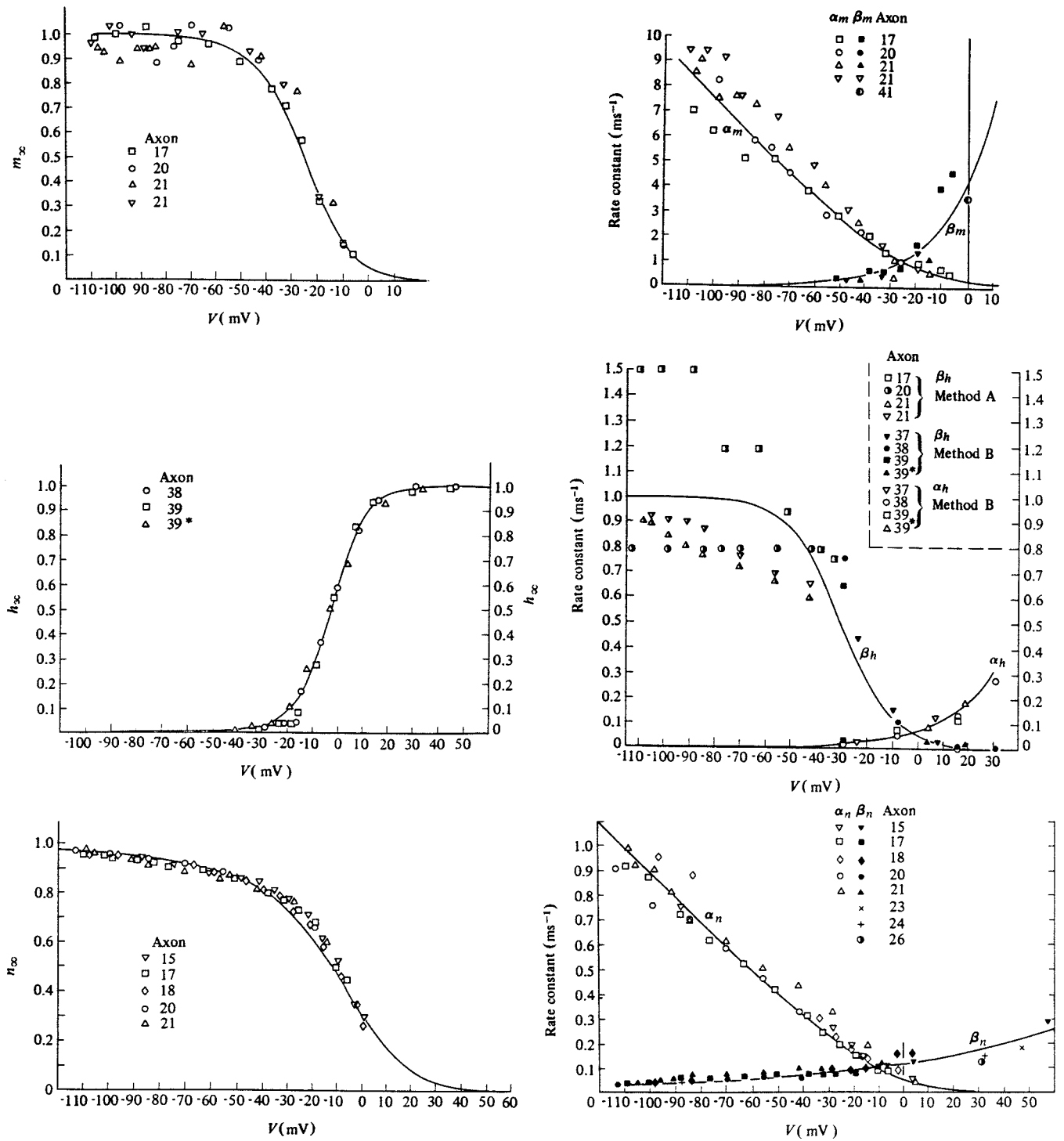


Figure 9.4: The data collected by Hodgkin and Huxley were fitted to a variety of functions. Left: the equilibrium values \bar{m} , \bar{h} and \bar{n} as functions of the voltage. Right: the functions $\alpha(V)$ and $\beta(V)$ for the three different channels. From: Hodgkin & Huxley (1952).

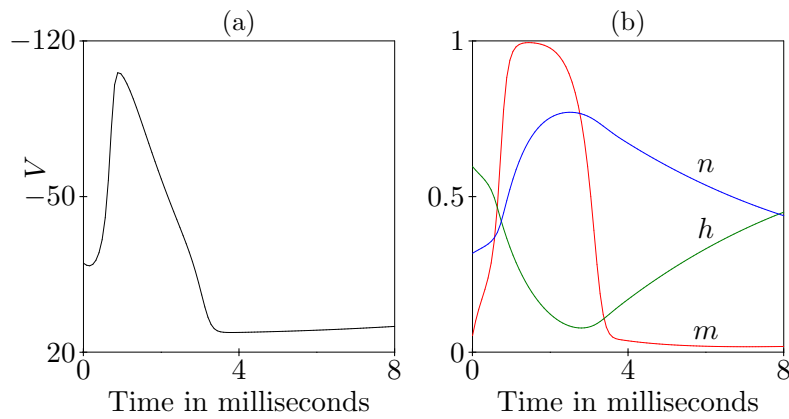


Figure 9.5: An action potential in the Hodgkin-Huxley model. Note that the vertical axis in panel (a) runs from positive to negative in order to have the usual picture of an action potential.

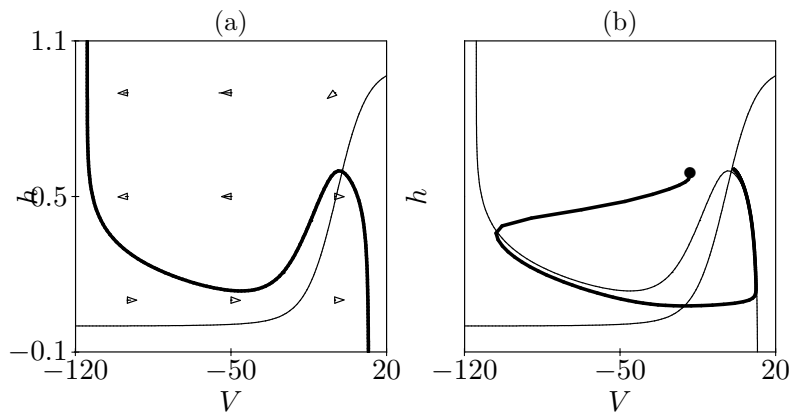


Figure 9.6: The nullclines of the Hodgkin-Huxley model for the QSS assumption $dm/dt = 0$ and the approximation $n = 0.91 - h$. The heavy line in (a) is the $dV/dt = 0$ nullcline and the heavy line in (b) is a trajectory of the complete 4-dimensional model. The trajectory of the full model appears to obey the nullclines of the simplified model.

9.2 Quasi steady state

Because dm/dt is so much faster than the h and n variables, we do the “quasi steady state” (QSS) approximation $dm/dt = 0$ (see Chapter 8). This means that we assume that m remains at steady state with the slow variables of the model. Thus, we set $dm/dt = 0$ in Eq. (9.6) and find that

$$m = \frac{\alpha_m}{\alpha_m + \beta_m}, \quad (9.10)$$

where α and β are the expressions given in Eq. (9.6). This quasi steady state equation provides for any value of V the corresponding equilibrium value of m . Replacing Eq. (9.6) with this algebraic expression simplifies the Hodgkin-Huxley models from a 4-dimensional model to a 3-dimensional QSS model.

There is another reasonable simplification. One can see in Fig. 9.5 that the behavior of the h and n variables is more or less complementary, i.e., $n + h \simeq 0.91$. One can therefore eliminate the dn/dt differential equation by substituting $n = 0.91 - h$ in Eq. (9.9). This then delivers a 2-dimensional model, which has the $dV/dt = 0$ and $dh/dt = 0$ nullclines depicted in Fig. 9.6. Fig. 9.6b depicts a trajectory of the full 4-dimensional model projected into the 2-dimensional phase space of the simplified model. One observes that the trajectory reasonably obeys the nullclines, i.e., our simplification seems fair. Summarizing, this simplification was achieved by a QSS assumption $dm/dt = 0$ and a “conservation equation” $n + h \simeq 0.91$. The $dV/dt = 0$ nullclines looks like the hysteresis diagrams we have seen before, with a steady state at the Nernst equilibrium potential of sodium ($\overline{V}_N = -115\text{mV}$), and one at the Nernst equilibrium potential of potassium ($\overline{V}_K = 12\text{mV}$).

In the phase space of the simplified model the resting state is a stable point. The resting state cannot be a saddle-point because there is no stable and unstable direction. Increasing V makes $dV/dt < 0$ and increasing h makes $dh/dt < 0$, which are both stabilizing. However, if one decreases the voltage beyond the unstable rising part of the V -nullcline, one enters an area where $dV/dt < 0$. The trajectory there goes to the left until it approaches the $\overline{V}_N = -115\text{mV}$ region of the $dV/dt = 0$ nullcline. Then it moves down along the V -nullcline until the nullcline reverses. The vector field points to the right, and the trajectory crosses to the $\overline{V}_K = 12\text{mV}$ branch of the V -nullcline. Finally, it slowly returns to the resting steady state along that branch of the nullcline.

According to this description an action potential is a large excursion through phase space that was triggered by a sufficiently large perturbation of the steady state. This nullcline configuration indeed defines an “excitable” system. A small microscopic disturbance (excitation) is blown up into a large macroscopic signal, that ultimately reverts back to rest. The shape of the $dV/dt = 0$ nullcline creates a threshold around the steady state that has to be breached to initiate the action potential.

During the final part of the action potential, i.e., when the trajectory moves upwards along the $\overline{V}_K = 12\text{mV}$ branch of the $dV/dt = 0$ nullcline, the system is refractory to new excitations. To excite the neuron within that time window one has to give a much larger stimulus. Because the distance to the threshold (i.e., to the unstable part of the V -nullcline) is much larger, a larger decrease in the voltage is required for excitation.

Background to the material covered in this chapter can be found in the books of Edelstein-Keshet (1988) and Keener & Sneyd (1998).

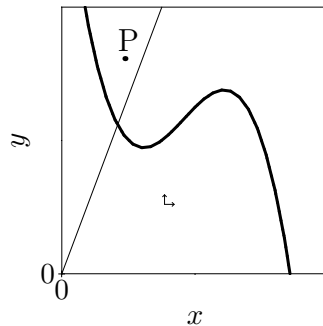
9.3 Exercises

Question 9.1. Time scales

Consider the following biochemical system

$$\frac{dx}{dt} = f(x, y) \quad \text{and} \quad \frac{dy}{dt} = \epsilon(ax - by) ,$$

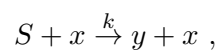
where $a, b > 0$ and $\epsilon \ll 1$ such that **the kinetics of y is much slower than that of x** . The phase space is:



where the heavy line represents the $dx/dt = 0$ nullcline, and the straight line is the $dy/dt = 0$ nullcline.

a. Sketch a trajectory from the point P.

Let y be produced from a substrate S by a reaction that is catalyzed by x :



and assume that the concentration of the substrate S declines

- b. Which parameter of the model will change due to this decrease of S ?
- c. How will the nullclines change?
- d. Sketch two qualitatively different nullcline configurations.
- e. Sketch trajectories for both of them.

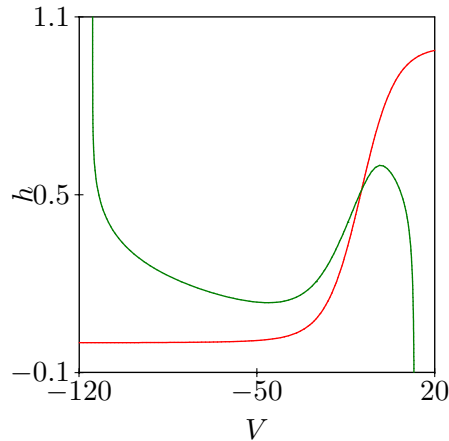
Question 9.2. Inhibition

The sigmoid $dh/dt = 0$ nullcline in Fig. 9.6 closely resembles the h_∞ line in Fig. 9.4.

a. How can this be?

Question 9.3. Hodgkin Huxley (Extra exercise for cool students)

We have simplified the Hodgkin-Huxley model and have found the nullclines depicted in Fig. 9.6. Changing the parameters of the model, one can also obtain the following nullclines:



After this (minor) change of the parameters the h variable has remained much slower than the V variable (like it is in Fig. 9.6).

- Determine the stability of the steady state.
- Sketch a trajectory and let it approach the final behavior of the system.
- Sketch the behavior in time.
- Give a biological interpretation of a neuron with these parameters.

Question 9.4. FitzHugh-Nagumo model (Extra exercise for cool students)

Instead of deriving a reasonable simplification of the Hodgkin-Huxley model, one can also define a “phenomenological” model that has essentially the same behavior. A famous phenomenological model is the FitzHugh-Nagumo model,

$$\frac{dV}{dt} = -V(V - a)(V - 1) - W \quad \text{and} \quad \frac{dW}{dt} = \epsilon(V - bW),$$

where V is some arbitrary variable representing the voltage, and W is a slow variable basically following W . The steady state of W is $W = V/b$ and the small ϵ parameter makes dW/dt a slow equation. Note that one can easily express the $dV/dt = 0$ nullcline as $W = -V(V - a)(V - 1)$, which is zero at three values of V .

- Sketch the nullclines of the model assuming that $a < 1$.
- Determine the stability of the steady state(s).
- Sketch a trajectory corresponding to an excitatory perturbation of this steady state.
- Does this resemble the action potential of the Hodgkin-Huxley model?
- Is this a good model for the action potential?

- f. Now add an external input, e.g., from a dendrite, $dV/dt = i - V(V - a)(V - 1) - W$ and sketch the nullclines for all qualitatively different possibilities.
- g. Determine the stability of all steady states.
- h. Sketch for each situation a representative trajectory.

Question 9.5. Computer exercise: Hodgkin Huxley model

The Hodgkin Huxley model is available as a GRIND model in the files `hh.*` and `hhq.*`, for the full model and the simplified model, respectively. For this exercise we have extended the Hodgkin Huxley model with such an input by adding a source parameter to dV/dt . We have also added one free parameter k .

- a. Study the Hodgkin Huxley for various values of the source and the new k parameter.
- b. Can one obtain a short burst, i.e., “spike train”, of action potentials by having the external input “on” for a short period of time?

Chapter 10

T cell vaccination

The aim of this chapter is to show how nullclines and phase space analysis can help the interpretation of complex phenomena. We make this point by elaborating an example of vaccination against autoimmune disease (Borghans *et al.*, 1998).

Paradoxically, many autoimmune diseases can be prevented or ameliorated by priming the immune system with autoreactive T cells. This priming evokes a regulatory T-cell response to the receptors on the autoreactive T cells, which induces resistance to autoimmunity. To prevent the autoreactive cells from inducing autoimmunity, they are given in a sub-pathogenic dose, or in an attenuated form. This vaccination method, termed T-cell vaccination (TCV), has been successful against several autoimmune diseases. In several autoimmune models, the regulatory cells responsible for resistance against autoimmunity are anti-idiotypic T cells. These cells, which recognize epitopes of the T-cell receptor (TCR) of the autoreactive cells, can for example be detected in mice recovering from experimental autoimmune encephalomyelitis (EAE) (Kumar & Sercarz, 1996). Transfer experiments have demonstrated that $CD4^+$ and $CD8^+$ anti-idiotypic T cells cooperate to down-regulate the autoreactive response. Based on these observations the regulatory circuitry depicted in Fig. 10.1 for the control of EAE has been proposed (Kumar & Sercarz, 1996).

This autoimmune disease, resembling human multiple sclerosis, can be induced in mice by giving myelin basic protein (MBP) or activated MBP-specific T cells. It has been shown that mice recovering from EAE harbor T cells that are specific for peptides from the TCR of an autoreactive clone. Such an anti-idiotypic T-cell response seems a normal physiological response, because it is also evoked if disease is induced by giving MBP. Cloned anti-idiotypic T cells were shown to be $CD4^+$ and recognize the framework region 3 peptide of the autoreactive TCR $V\beta 8.2$ chain in the context of MHC II. Since mouse T cells generally do not express MHC II molecules, it was proposed that antigen-

presenting cells (APCs), for example macrophages or B cells, pick up the $V\beta 8.2$ chain peptide and present it to the $CD4^+$ cells in the context of class II MHC molecules. On adoptive transfer, the cloned anti-idiotypic cells were shown to inhibit autoreactive responses and protect mice from MBP-induced EAE (Kumar & Sercarz, 1993). $CD8^+$ cells also appeared to play a role in the induction of resistance. When $CD8^+$ T cells in the recipient mouse were deleted by anti-CD8 monoclonal antibody treatment, the $CD4^+$ cells were unable to confer resistance (Kumar & Sercarz, 1993; Gaur *et al.*, 1993). It was therefore concluded that the $CD4^+$ cells exert their regulatory effect by recruiting anti-idiotypic $CD8^+$ cells down-regulating the autoreactive response (Kumar & Sercarz, 1993; Kumar *et al.*, 2001; Braciak *et al.*, 2003).

The essential assumption upon which our results are based, is that TCV involves T cells reactive to self epitopes for which T-cell tolerance is incomplete (e.g., T cells reactive to sub-dominant self determinants), and that these T cells are present in the mature peripheral repertoire. This seems a quite natural assumption because the simple fact that these mice can develop automimmunity confirms that the tolerance to MBP can be broken. Further, we assume that the presentation of these self epitopes is enhanced by the autoreactive immune response. T-cell stimulation induces $IFN-\gamma$ which up-regulates the presentation of MHC molecules on target cells. This stimulates the presentation of ignored or cryptic self peptides and hence the activation of autoreactive cells. Aberrant expression of MHC molecules on target cells has been demonstrated for several autoimmune diseases.

10.1 Model

We simplify this complicated regulatory circuitry into a simple mathematical model to study how TCV can be explained. For our model we consider three T-cell clones: an autoreactive clone A , a $CD4^+$ regulatory clone R_4 , and a $CD8^+$ regulatory clone R_8 . All clone sizes increase due to an influx of naive T cells from the thymus and by T-cell proliferation. The autoreactive cells proliferate in response to presented self peptides, whereas both regulatory clones proliferate in response to TCR peptides of the autoreactive cells. Since only little is known about the presentation of TCR peptides on MHC molecules, we do not explicitly model the dynamics of MHC-peptide complexes. Instead we assume that this presentation occurs on such a fast time scale compared to the T cell dynamics, that the proliferation of both regulatory clones can be approximated to be proportional to the number of autoreactive cells. All clones decrease in size due to natural cell death. The autoreactive clone is inhibited by the $CD8^+$ regulatory cells; the inhibition term is absent in the equations of the regulatory cells.

The full model for the regulatory circuitry as presented in Fig. 10.1 is modeled by the

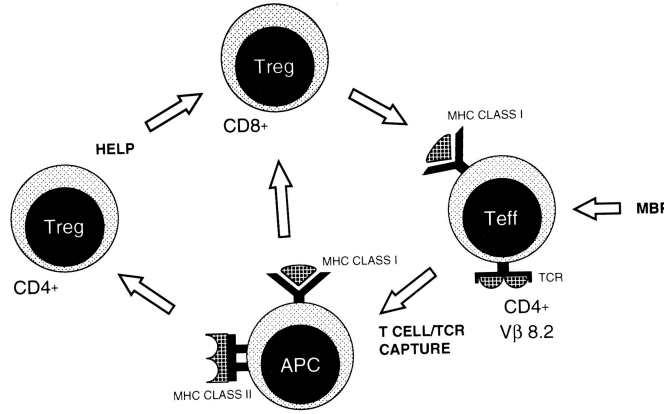


Figure 10.1: T-cell circuitry involved in the regulation of EAE (Kumar & Sercarz, 1996). Different TCR peptides are presented on APCs in the context of class I and class II molecules. These APCs prime $CD4^+$ and $CD8^+$ anti-idiotypic cells. The $CD4^+$ regulatory cells (R_4), specific for the framework region 3 peptide of the autoreactive TCR $V\beta 8.2$ chain, provide help for the $CD8^+$ regulatory cells (R_8). This help may be delivered indirectly through an APC which is activated by the regulatory cells. The regulatory $CD8^+$ cells recognize another determinant from the autoreactive TCR, which is presented on MHC class I molecules on the autoreactive cells (A). The inhibitory effect of the $CD8^+$ cells on the autoreactive cells is thought to be responsible for recovery from EAE. From: Kumar & Sercarz (1996).

following differential equations:

$$\begin{aligned}
 \frac{dA}{dt} &= m_A + pAf(A) - iAR_8 - dA - \epsilon_A A^2, \\
 \frac{dR_4}{dt} &= m_R + pR_4g(A) - dR_4 - \epsilon_R R_4^2, \\
 \frac{dR_8}{dt} &= m_R + pR_8g(A)h(R_4) - dR_8 - \epsilon_R R_8^2,
 \end{aligned} \tag{10.1}$$

where the Hill functions $f(A)$, $g(A)$, and $h(R_4)$ denote the stimulation of autoreactive cells by self epitopes, the stimulation of regulator cells by TCR epitopes from the autoreactive cells, and the help provided by R_4 cells to R_8 cells, respectively. The influxes of autoreactive and regulatory cells from the thymus are represented by m_A and m_R respectively. Because $0 \leq f(), g(), h() \leq 1$, the maximum proliferation rate of all T cells is p . Autoreactive cells are inhibited by $CD8^+$ regulatory cells at rate i . If clone sizes are small, cells die naturally at rate d . For large clone sizes, cells undergo an extra density-dependent cell death (the terms $\epsilon_N N^2$), which is supposedly due to competition, and accounts for a carrying capacity $(p - d)/\epsilon$ when T cells are maximally stimulated.

The presentation of self peptides is assumed to be reinforced by activated autoreactive cells. The presented self epitopes are therefore modeled as a saturation function of the number of autoreactive cells. The stimulation of the regulator cells is also assumed to

be a saturation function of the density of autoaggressive cells

$$f(A) = \frac{A}{k_A + A} \quad \text{and} \quad g(A) = \frac{A}{k_R + A} . \quad (10.2)$$

For their proliferation, CD8⁺ cells require both their specific ligand and T-cell help from CD4⁺ cells. T-cell help can be modeled by another saturation function, e.g., $h(R_4) = R_4/(k_h + R_4)$.

The equations of the CD4⁺ and the CD8⁺ regulatory populations given in Eq. (10.1) are very similar. The only difference pertains to the help the CD8⁺ population receives from the CD4⁺ regulatory population. Since we want to obtain basic, fundamental insights into the working of TCV, we simplify the model by lumping both regulatory populations into one regulatory population R . Such a simplification facilitates the analysis of the model because one can do phase space analysis. Our simplification in fact amounts to assuming that the proliferation of CD8⁺ cells is never limited by help from the CD4⁺ regulatory cells. The simplified model becomes

$$\begin{aligned} \frac{dA}{dt} &= m_A + pAf(A) - iAR - dA - \epsilon_A A^2 , \\ \frac{dR}{dt} &= m_R + pRg(A) - dR - \epsilon_R R^2 , \end{aligned} \quad (10.3)$$

where $f(A)$ and $g(A)$ are given by Eq. (10.2). The simplified model can be schematized by two coupled feedback loops (see Fig. 10.2): a negative loop between the regulatory cells R and the autoreactive cells A , and a positive loop between the autoreactive cells and the presented self peptides $f(A) = S_A$. Since both feedback loops are coupled, it is hard to predict intuitively what will happen if the model immune system is perturbed by giving autoreactive cells. Therefore we use a mathematical model to analyze the steady states and the dynamics of the system.

10.2 Steady states

Because so many parameters are unknown, time and all parameters have been scaled into arbitrary units. For the parameters chosen, the system defined by Eq. (10.3) has two stable steady states, denoted by the black squares in Fig. 10.3, and one unstable steady state, denoted by the open square in Fig. 10.3. The stability of the steady states can be determined from the vector field. In the lower left corner both populations increase by the source terms. Completing the vector field around the “normal” state of incomplete tolerance, in which both the autoreactive and the regulatory clone are small, therefore shows that this state is stable. Completing the vector field around the state in the upper right corner also shows that this state is stable. The state in the middle is saddle point because it has a stable and an unstable direction in the vector field. In the “normal”

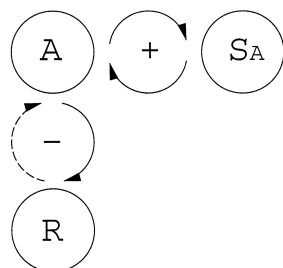


Figure 10.2: Schematic representation of the simplified model, as defined in Eq. (10.3). The autoreactive cells A recruit a regulatory population R which consists of both $CD4^+$ and $CD8^+$ cells. The regulatory cells R inhibit the autoreactive cells A (denoted by the dashed arrow). This results in a negative feedback loop between A and R . The autoreactive cells proliferate upon stimulation by presented self epitopes $f(A) = S_A$. Since the autoreactive cells stimulate the presentation of self epitopes on MHC molecules, for example by $IFN-\gamma$ production, there is a positive feedback loop between A and S_A .

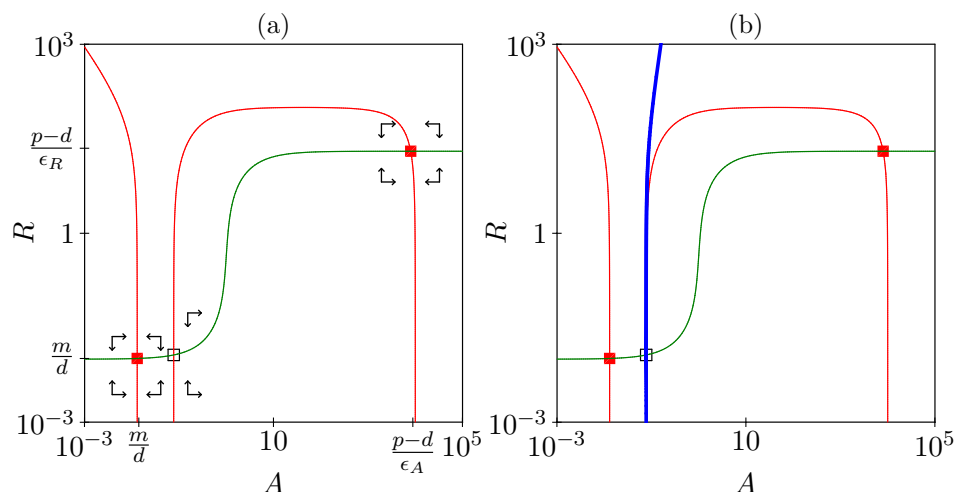


Figure 10.3: Nullclines (a) and separatrix (b) of the TCV model. All initial conditions to the right of the separatrix lead to the vaccinated state, while those to the left of the separatrix lead to the normal state. Parameters are: $m_A = m_R = 0.01$, $p = 2$, $i = 0.01$, $d = 1$, $k_A = 0.1$, $k_R = 1$, $\epsilon_A = 0.0001$, $\epsilon_R = 0.05$.

state of incomplete tolerance both feedback loops are non-functional. In the other stable steady state, the autoreactive cells are actively controlled by the regulatory cells. We interpret this state as the vaccinated state (V); the individual is healthy, and resistant to the autoimmune disease. The steady state in the middle is a saddle point that spans up a separatrix dividing the basins of attraction of the normal and the vaccinated state (Fig. 10.3b).

Since the system has only two stable steady states, the injection of cells into a normal individual will either lead to vaccination or to a return to the normal state. Although the system will always end up healthy, i.e., in the normal state or in the vaccinated state, the number of autoreactive cells can temporarily become very large. These transient high numbers of autoreactive cells can be interpreted as autoimmunity (see the shaded region in Fig. 10.4). Thus the intensity of autoimmunity is assumed to be proportional to the number of autoreactive cells.

10.3 TCV virtual experiments

EAE can be evoked in susceptible animals by giving MBP or by giving activated autoreactive T cells. Since both methods ultimately amount to increasing the number of autoreactive cells in the recipient, we model the induction of autoimmunity by introducing autoreactive cells into the naive state. Fig. 10.4a shows that this indeed evokes an autoimmune response. Initially (see *a* in Fig. 10.4a) the autoreactive cells respond vigorously, as they initiate their positive feedback loop, and reach the high levels that we interpret as autoimmune disease. During the second phase of the response (see *b* in Fig. 10.4a), however, the regulatory cells effectively control the autoreactive cells. The autoimmune disease vanishes and the system approaches the vaccinated state (see *c* in Fig. 10.4a). In this state the immune system is protected against autoimmunity; the number of regulatory cells is so high that a previously pathogenic dose of autoreactive T cells can no longer induce autoimmunity (Fig. 10.4b).

To protect animals against autoimmunity without inducing disease, one would have to attain the vaccinated state by giving a low dose of autoreactive cells. Fig. 10.3 shows that an injection of autoreactive cells can only lead to a switch to the vaccinated state if the injected dose is large enough to cross the separatrix. Too small a dose of autoreactive cells fails to initiate both feedback loops. Giving a dose of autoreactive cells that is small but sufficient (Fig. 10.4c), we observe that the vaccinated state is approached while no autoimmune disease is induced. The proliferation of autoreactive cells is so slow that the regulatory cells can keep up with them and control the autoreactive cells from the start.

T-cell vaccination has also been achieved with large doses of attenuated autoreactive cells. Since attenuation blocks cell division, the ultimate effect of an injection of attenuated autoreactive cells is a stimulation of the regulatory cells. This will obviously lead to protection against disease, because it is a way to stimulate the regulatory feedback loop without stimulating the disease-causing positive feedback loop. According to the separatrix of Fig. 10.3, however, it should be impossible to attain the vaccinated state by giving attenuated cells. Stimulating the regulatory cells only, one can never cross the separatrix, because the vaccinated state requires that the positive feedback loop

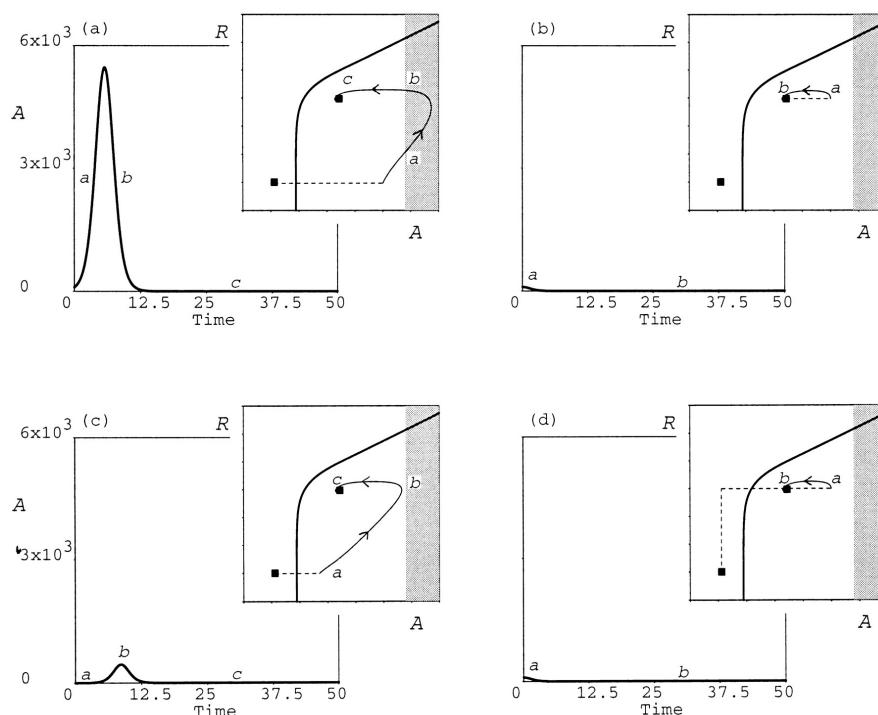


Figure 10.4: T cell vaccination virtual experiments. The large panels show the model behavior in conventional time plots; the insets show the same behavior in the state space of Fig. 10.3. The thin lines in these state spaces represent the trajectories. The letters in the figures denote corresponding time points in the state spaces and the time plots. Note that to be able to discriminate between the naive and the vaccinated state the state spaces have logarithmic axes, while the behavior in time is plotted on a linear axis in order to discriminate between autoimmunity and vaccination. The difference between the vaccinated state and the normal state is hardly visible in the time plots, which reflects the realistic notion that the number of autoreactive cells is small in both states. Panel (a): A large dose of autoreactive cells ($A = 100$) given in the normal state N (see dashed line) causes a vigorous autoreactive response which is interpreted as autoimmunity. Eventually the vaccinated state is approached, leaving the animal healthy and resistant to autoimmunity. Panel (b): If the same large dose of autoreactive cells ($A = 100$) is given in the vaccinated state V (see dashed line), the regulatory cells are able to control the autoreactive response. There is no autoimmune disease and the system returns to the vaccinated state. Panel (c): A small dose of autoreactive cells ($A = 0.5$) given in the normal state N leads to a switch to the vaccinated state V while no autoimmune disease is induced. Panel (d): Attenuated autoreactive cells or regulatory cells ($R = 10$) given in the normal state N (see the vertical line) are able to confer transient protection. If a previously pathogenic dose of live autoreactive cells ($A = 100$) is given when the concentration of regulatory cells is still large (see the horizontal line), the system switches to the vaccinated state while no autoimmunity is induced. From: Borghans *et al.* (1998).

between the autoreactive cells and the presented self epitopes is initialized. Thus as soon as the attenuated cells have disappeared, the regulatory population will gradually

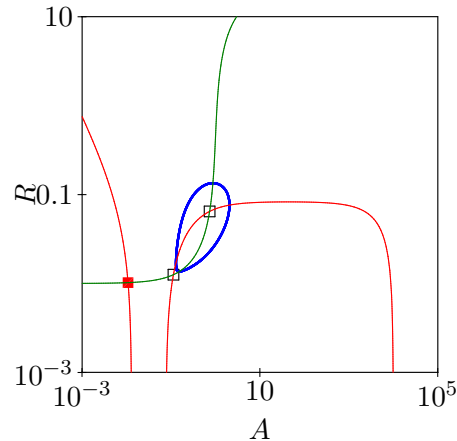


Figure 10.5: Relapsing disease: the nullclines of Eq. (10.3) for a stronger inhibition parameter $i = 12$.

decrease due to normal turnover. We conclude that, according to the model, long-term protection against autoimmunity can never be obtained by giving attenuated autoreactive cells only. Transiently, however, the attenuated cells can provide protection against disease and hence account for TCV. If the number of regulatory cells stimulated by the attenuated autoreactive cells (see the vertical line in Fig. 10.4d) is still high when live autoimmune cells are given to challenge an autoimmune disease (see the horizontal line in Fig. 10.4d), the latter cells proliferate less vigorously and approach the vaccinated state without reaching the high numbers required for autoimmunity (Fig. 10.4d).

In summary, the model predicts a qualitative difference between vaccination with normal and with attenuated autoreactive cells. A low dose of normal autoreactive cells can lead to a switch to the vaccinated steady state. Therefore it is an all-or-nothing phenomenon which gives rise to long lasting protection. Inoculation with attenuated cells, in contrast, can only confer transient protection. Since resistance reduces with time, the latter form of vaccination should be dose dependent.

Relapsing disease

While animals often spontaneously recover from autoimmunity, many human autoimmune diseases are characterized by relapses. The vaccinated state of our model need not be a stable steady state; instead for particular parameter combinations it can be unstable (denoted by the open square in Fig. 10.5 and Fig. 10.6a), and be surrounded by a stable limit cycle corresponding to oscillatory behavior. For the current parameter setting such oscillations are observed if the inhibitory effect of the regulatory cells i is

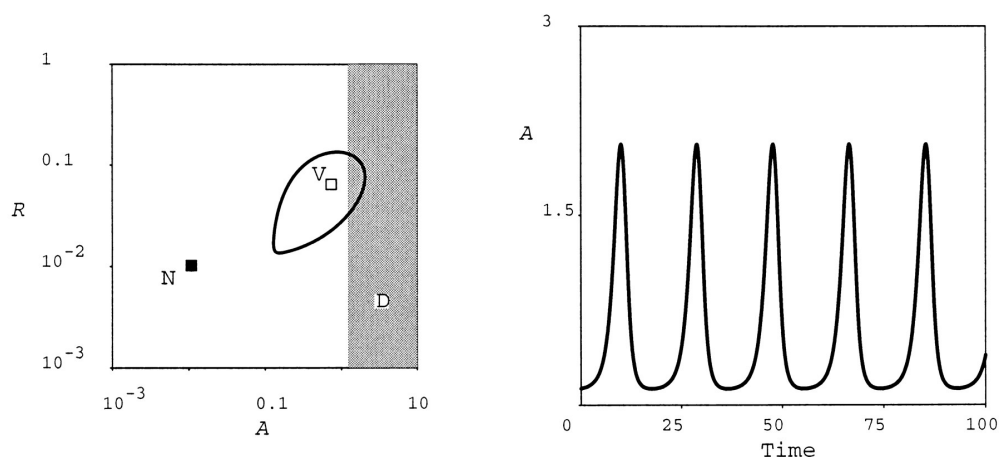


Figure 10.6: Relapsing autoimmunity. For $i = 12$ the vaccinated state V (denoted by the open square) is no longer an attractor of the system. Instead the system oscillates around the unstable vaccinated state. Here the oscillations are so large that the autoreactive cells repeatedly pass through the region of disease. This can be interpreted as a relapsing autoimmune disease. Note that, because of the parameter change, the axes had to be changed. From: Borghans *et al.* (1998).

increased (or the saturation constant for stimulation of regulatory cells k_r is decreased). The system will then oscillate around the vaccinated state. If the oscillations are sufficiently large, the autoreactive cells repeatedly pass through the region of disease, which would be observed as a relapsing disease (Fig. 10.6). Recent experiments showing that relapses in EAE do not require spreading determinants, but can be driven by T cells reactive to the initial dominant determinant of MBP (Kumar *et al.*, 1996), support this mechanism for relapsing disease.

According to the model, TCV should fail to provide protection against such a relapsing disease. If a large oscillation surrounds the vaccinated state, there is no state of protection the system can switch to. The only possibility of curing such a relapsing autoimmune disease, would be to induce a switch back to the normal state. Since this would require breaking the positive feedback loop of autoreactive cell-induced antigen presentation, this is probably too difficult. Moreover, if the cause of the autoimmune disease is still present, one would expect autoimmunity to recur.

10.4 Exercises

Question 10.1. Intraspecific competition

What happens with the steady states of Fig. 10.3 if one omits the intraspecific competition from the model?

Question 10.2. Relapsing disease

In Fig. 10.6 we obtained periodic behavior that can be interpreted as a relapsing autoimmune disease by increasing the inhibition parameter i .

- Can you obtain similar behavior by changing other parameters?
- Use the `continue` command in GRIND to find the parameter values for which the vaccinated state is stable.
- Is there always a stable limit cycle when the vaccinated state is unstable?
- Try various initial conditions to see what happens with trajectories starting outside of the limit cycle.
- What does this tell you about the separatrix?

Question 10.3. Normal steady state

The model has a normal “naive” steady state due to a balance between a small thymic production and normal turnover of the cells. The regulatory interactions are negligible in the normal state.

- What is the effect of increasing thymic production?
- What is the effect of decreasing thymic production?
- Some authors have argued that the normal state also involves active regulation because the regulator cells are primed by the common V β 8.2 TCR. Can you modify the model such that the normal state involves active regulation?

Question 10.4. Competitive proliferation

Try to find a phase space accounting for TCV with the following model:

$$\frac{dA}{dt} = m_A + \frac{p_A A^2}{h_A + A} - iAR - dA \quad \text{and} \quad \frac{dR}{dt} = m_R + \frac{p_R RA}{h_R + cR + A} - dR$$

- Give an interpretation of all terms in the model
- What is the meaning of the c parameter?
- Search for parameter values giving a phase space with two stable steady states and one saddle point.

Question 10.5. Segel *et al.* (1995)

TCV was also obtained by “reverse engineering”. Read the paper by Segel *et al.* (1995) and discuss similarities and differences between their model and the models presented in this Chapter.

Chapter 11

TCR rearrangement excision circles

The aim of this chapter is to show how an appropriate mathematical model helps the interpretation of experimental data. We here develop a model for the TREC content of naive T cells, and let you use the insights obtained with the model to interpret the paper on TRECs in HIV-1 infected patients by Douek *et al.* (1998).

When the TCR is formed in the thymus, fragments of DNA are excised from the T cell progenitor chromosome (see Fig. 11.1). These DNA fragments form circles that are called “TRECs”, for TCR rearrangement excision circles, and are not replicated in cell division, but are divided randomly over the two daughter cells. The average TREC content of T cells can be measured by specific PCR, and seems a reasonable marker for cells that have recently emigrated from the thymus (RTEs). Because thymocytes divide after rearranging the TCR, most novel T cells emigrating from the thymus contain no TRECs. Ye & Kirschner (2002) estimate that cells emigrating from the thymus have an average TREC content of 0.118 TRECs/cell. The TREC content of thymocytes is not changing with age (Jamieson *et al.*, 1999). Throughout life naive T cells therefore leave the thymus with the same average TREC content.

The TREC content of naive T cells decreases more than 10-fold occurs from 20-year-olds to 80-year-olds (see Poulin *et al.* (1999) and Fig. 11.2). Because RTEs have the highest TREC levels, the decline in the TREC content with age is thought to reflect the age-related thymic involution (Steinmann *et al.*, 1985). By developing a mathematical model we will discover that a decrease in thymic output decreases the influx of RTE with high TREC content, but that this alone does not influence the average TREC content of the naive population. The only way the TREC content of a naive T cell can decrease is by division or intracellular degradation. Here, we show that the decrease in the average

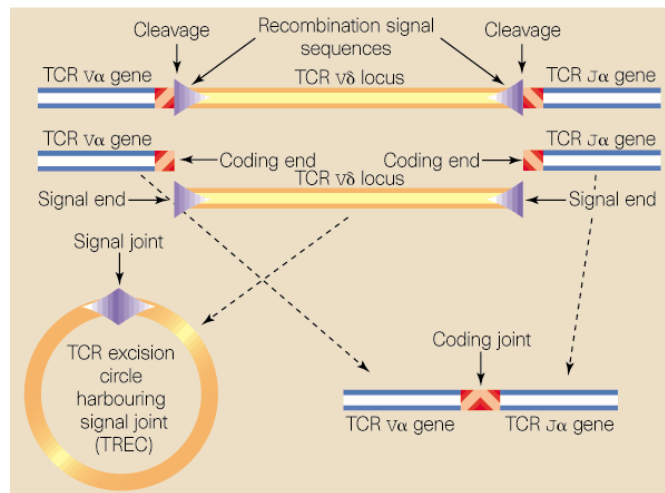


Figure 11.1: TRECs are formed in the thymus when TCRs are formed by somatic recombination. From: Rodewald (1998).

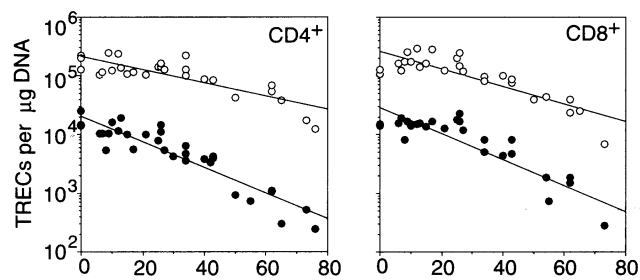


Figure 11.2: The average TREC content decreases with age. From: Douek *et al.* (1998).

TREC content of the naive population is determined by the decreasing thymic output, homeostatically countered by renewal and/or an increased lifespan of naive T cells.

11.1 Model

We develop a mathematical model of two ordinary differential equations describing the dynamics of naive T cells N (either CD4⁺ or CD8⁺ naive T cells) and the total number of TRECs T in the naive T cell population. Production of recent thymic emigrants (RTEs) in the thymus is represented by parameter $\sigma(t)$, and $\rho(N)$ is a renewal term. Setting $\rho(N) = 0$, we can study naive T cells without renewal. The cells are removed

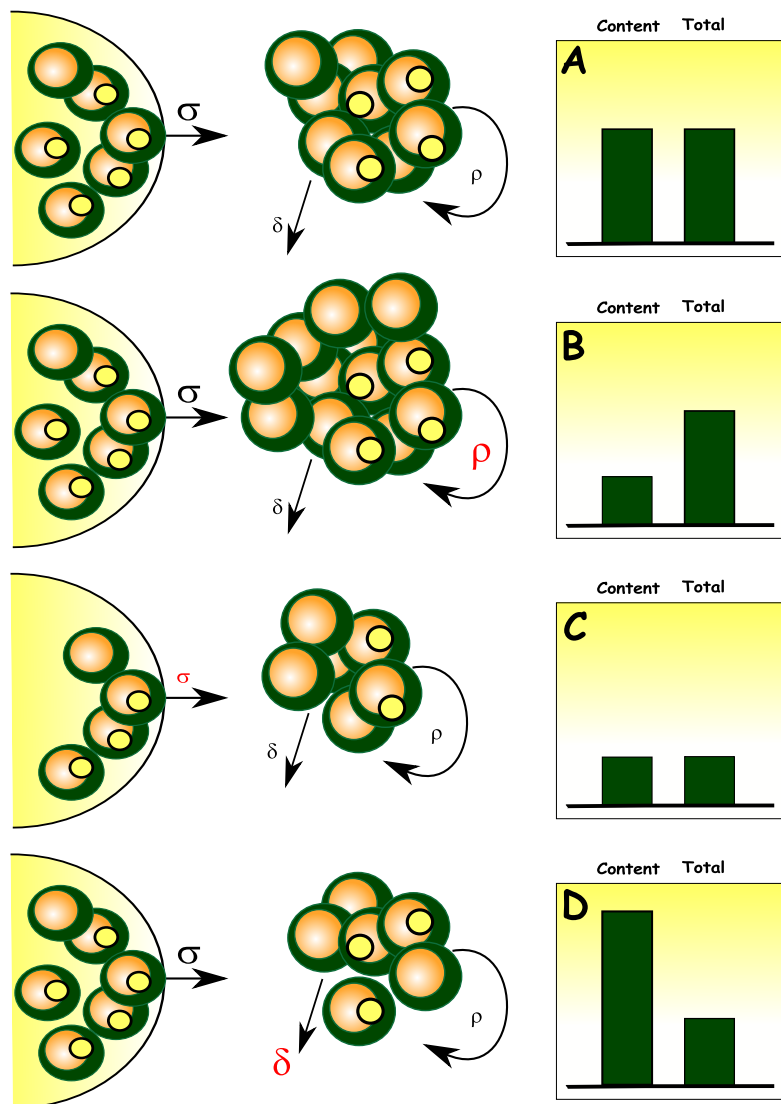


Figure 11.3: The predicted changes in TREC contents and the TREC total after changing the renewal rate (B), thymic production (C), or the death rate (D). Panel A depicts the normal situation. The cells on the left are thymocytes, that may contain a TREC (yellow circle). The cells in the middle depict peripheral naive T cells, that increase by increased renewal (ρ : B), decrease by decreased thymic production (σ : C), or increased death (δ : D). The histograms depict the TREC content and the total number of TRECs. From: De Boer (2006).

from the naive compartment at rate $\delta(N)$, which represents cell death plus priming by antigen (the latter changes the cells to the memory phenotype). For the total number of naive T cells we therefore write

$$\frac{dN}{dt} = \sigma(t) + \rho(N)N - \delta(N)N . \quad (11.1)$$

To describe the dynamics of the total number of TRECs T in the naive T cell population, we let c be the TREC level of an RTE. TRECs disappear from the population by intracellular degradation at rate δ_I , or, together with their host cell, by death or antigenic priming at rate $\delta(N)$. In cell division, the TRECs are not replicated, and are randomly divided over the two daughter cells, so the total number of TRECs in the naive population is not affected by the renewal parameter $\rho(N)$:

$$\frac{dT}{dt} = c\sigma(t) - (\delta(N) + \delta_I)T . \quad (11.2)$$

Since the experimental data suggest the average number of TRECs per naive T cell decreases with age and with HIV-1 infection, we rewrite Eq. (11.2) in terms of the average $A = T/N$. For the time derivative of $A(t)$ defined as the ratio $T(t)/N(t)$ we have to invoke the quotient rule of differentiation $(f(x)/g(x))' = (f(x)'g(x) - f(x)g(x)')/g(x)^2$, i.e.,

$$\begin{aligned} \frac{dA}{dt} &= \frac{[c\sigma(t) - (\delta(N) + \delta_I)T] - [\sigma(t) + (\rho(N) - \delta(N))N]A}{N} \\ &= \frac{\sigma(t)}{N}(c - A) - (\delta_I + \rho(N))A . \end{aligned} \quad (11.3)$$

One obtains a better understanding by considering the, probably quite realistic scenario, where the dynamics of the T cells and of the average TREC levels are much faster than the slow thymic involution of $\sigma(t)$. In such a regime A will approach a quasi steady state (QSS)

$$\bar{A} = \frac{c}{1 + \frac{N}{\sigma(t)}(\delta_I + \rho(N))} . \quad (11.4)$$

This QSS expression shows that in the absence of intracellular degradation and naive T cell renewal (i.e., $\delta_I + \rho(N) = 0$), there can be no decline in the average TREC content, i.e., $\bar{A} = c$. Further the expression shows that increasing the division rate $\rho(N)$ has a similar effect on the average TREC content A as decreasing the thymic production $\sigma(t)$. Further, if N were to decrease due to increased death, the average TREC content is expected to increase (see Fig. 11.3).

11.2 Homeostasis

The thymic output $\sigma(t)$ is an exponentially decreasing function of age t with a constant exponential rate v

$$\sigma(t) = \sigma_0 e^{-vt} , \quad (11.5)$$

where v is about 0.05 per year (Steinmann *et al.*, 1985). The density-dependent renewal rate $\rho(N)$ can be modeled by a sigmoid Hill function with steepness parameter k . By

setting $k = 0$, the renewal rate can be made non-homeostatic:

$$\rho(N) = \frac{\rho_0}{1 + (N/h)^k} . \quad (11.6)$$

The rate of death may increase with increasing naive T cell numbers. A possible way to model this is

$$\delta(N) = \delta_0 [1 + (\varepsilon N)^m] . \quad (11.7)$$

which can be made independent of the cell density by setting $m = 0$.

Before embarking on numerical analysis we approach the model analytically for the simple case where there is no homeostasis. Eq. (11.4) shows that we need at least renewal or intracellular degradation of TRECs to allow the average TREC levels to drop, so let us now allow for a non-homeostatic renewal at rate ρ , and intracellular degradation δ_I . Similarly, the cell death and antigenic priming occurs at a fixed rate δ . The naive lymphocyte population will approach

$$\bar{N} = \frac{\sigma(t)}{\delta - \rho} . \quad (11.8)$$

Substitution of \bar{N} into the general QSS solution of the average TRECs (Eq. (11.4)) yields

$$\bar{A} = \frac{c}{1 + (\delta_I + \rho)/(\delta - \rho)} . \quad (11.9)$$

Thus, in the absence of homeostasis, the average TREC content of the naive T cells will go to a fixed level, which is independent of the thymic output $\sigma(t)$, and is only determined by the (fixed) renewal and death rates. Thanks to our analytical approach this result is independent of the values of the parameters ρ , δ or δ_I . The model demonstrates that the continued decline in the average number of TRECs per cell with age can only be observed in a system with homeostasis, even if $\delta_I + \rho > 0$. Thus, renewal and/or death rates of naive T cells have to be density-dependent.

11.3 Parameters

To set the parameters of this model one could consider the steady state for a healthy 30-year-old individual. On the basis of blood T cell numbers, blood volume and the percentage of T cells residing in the blood, Clark *et al.* (1999) calculate that a human adult has of the order of 10^{11} naive CD4⁺ and CD8⁺ T lymphocytes, and a thymic output of about 10^8 naive CD4⁺ and CD8⁺ T cells per day. At low naive T cell counts, a maximum of 10 % of the naive T cells was found to divide (Hazenberg *et al.*, 2000), setting a maximum of $\rho_0 = 0.1/\text{day}$. But in a normal healthy individual less than

0.1% of the naive T cells is in division. Because thymic production decreases about 5% per year, i.e., $v \approx 0.05/\text{year}$, throughout life (Steinmann *et al.*, 1985), we need to set $\sigma_0 = 4.48 \cdot 10^8$ cells/day to obtain the estimated thymic output of 10^8 cells/day in a healthy 30-year-old adult. Ye & Kirschner (2002) estimate an average TREC content of $c = 0.118$ TRECs/cell.

The numerical analysis of the model will be left to you. Fill in all parameters using the estimates provided above. Test if you can get a realistic 10-20 fold decline in the TREC content A over 100 years. Test what happens if you would perform a thymectomy at various ages. Test what would happen when HIV infection would change σ , ρ , and/or δ . Study the model when homeostasis is due to density dependent proliferation, and when homeostasis is brought about by density dependent death. Answers to these questions can be found in various papers (Hazenberg *et al.*, 2000; Dutilh & De Boer, 2003; De Boer, 2006).

11.4 Exercises

Question 11.1. Average TREC content

The ODE for the average TREC content dA/dt was obtained by rewriting a model in terms of total naive T cells and total TRECs.

- Would you, in retrospect, be able to directly write down the dA/dt equation?
- What is the average TREC content if we had made the stronger quasi steady state assumption (QSSA) $dN/dt = dT/dt = 0$?
- What is the difference between these two QSSA?

Question 11.2. Douek *et al.* (1998)

The Douek *et al.* (1998) paper was the first paper to report that the TREC content of T cells was decreased in HIV-1 infected patients, like it is in thymectomized individuals. The authors therefore conclude that HIV-1 infection ameliorates thymic production.

- Read the paper and use the equilibrium results derived above to facilitate the interpretation of the data.
- The authors discuss the effect of an increased death rate of $CD4^+$ T cells on their TREC content. If naive $CD4^+$ T cells have a shortened expected life span in HIV-1 infected patients, what would you predict for their TREC content?
- HIV-1 infection induces generalized immune activation, which involves increased division of naive T cells. Given this generalized immune activation, do the data allow one to conclude that thymic production is decreased in HIV-1 infected patients?
- Study the model numerically, and so this separately for density dependent renewal and death. See if you can obtain a realistic 10-20 fold decline in the TREC content with age.
- Study the effect of a decreased thymic production, or thymectomy, for different ex-

pected life spans of the naive T cells.

f. More than 20 years after thymectomy healthy individuals still have TREC⁺ T cells. How can this be, and what does this tell you about the intra-cellular decay of TRECs?

Question 11.3. Ye & Kirschner (2002)

A more complicated/realistic TREC model was developed by Ye & Kirschner (2002). The authors also address the TREC content of T cells in HIV-1 infected patients, and conclude that thymic production is affected by HIV-1.

a. Why do they reach this conclusion, while you were unable to do so in the previous question?

b. What are the advantages and disadvantages of analyzing a more complicated/realistic model?

Question 11.4. Lewin *et al.* (2002)

A model writing the dynamics of TREC⁺ and TREC⁻ T cells was developed by Lewin *et al.* (2002). Read the paper and discuss the similarities and differences between their results and the results obtained in this Chapter.

Chapter 12

Diversity of the Immune system

Diversity is a hallmark of the immune system. The repertoires of B cells and of CD4⁺ and CD8⁺ T cells each consist of more than 10^8 different clonotypes each characterized by a unique receptor. Each immune response is characterized by a large panel of different cytokines with –partly overlapping– functions. Each individual is characterized by a unique combination of MHC molecules that play an essential role in the selection of peptides presented to the cellular immune system. MHC loci are the most polymorphic genes known for vertebrates, i.e., for most loci several hundreds of alleles have been identified at the population level. However, each individual inherits only a limited number of MHC genes from its parents, and expresses no more than 10-20 different MHC molecules. We will here address the question why lymphocytes are so diverse within an individual, and why MHC molecules are diverse at the population level, and not diverse within an individual. The consensus explanation of the enormous diversity of lymphocyte repertoires is the improved recognition of pathogens with a large diversity of lymphocytes. The consensus explanation for the limited diversity of MHC molecules within an individual is the excessive negative deletion by self tolerance processes when the number of presented self peptides is increased by increasing the diversity of MHC molecules.

12.1 Diversity of the immune repertoire

We start with a simple toy model revealing some novel expectations for the relationships between lymphocyte specificity p , the number of self epitopes S , and the initial repertoire size R_0 (De Boer & Perelson, 1993). Defining the lymphocyte specificity p as the probability that a lymphocyte responds to a randomly chosen epitope, we have a definition that remains close to the conventional concept of the “precursor frequency”

of an epitope. A typical viral epitope activates about one in 10^5 naive $CD8^+$ T cells (Blattman *et al.*, 2002), which also says that the probability that a lymphocyte recognizes a randomly chosen epitope is about $p = 10^{-5}$. It is difficult to estimate the number of self epitopes in general. For the peptides of nine amino acids (9-mers) that are used as epitopes by $CD8^+$ T cells, we have recently made an estimate by enumerating all unique 9-mers in the human genome (Burroughs *et al.*, 2004). Given that there are approximately 10^7 unique 9-mers in the human self, and that MHC molecules typically present about 1% of these, we would have an estimate of $S = 10^5$ self epitopes per T cell restricted to one particular MHC (Burroughs *et al.*, 2004). Fortunately, for the arguments presented here the precise number of self epitopes turns out to be unimportant, we only need to know that it is large. The diversity of the repertoire before tolerization R_0 is also a large number. Because the size of the functional $CD4^+$ T repertoire R in man is at least 10^8 different receptors (Arstila *et al.*, 1999; Keşmir *et al.*, 2000), the diversity of the pre-tolerance repertoire should at least be an order of magnitude higher, i.e., $R_0 > 10^9$.

Having these concepts at hand we write a simple mathematical model. The diversity of the functional repertoire R is determined by the chance that a clonotype fails to recognize all self epitopes S , i.e.,

$$R = R_0(1 - p)^S . \quad (12.1)$$

Similarly, the chance that an individual fails to respond to a foreign epitope is the probability that none of its clonotypes in the functional repertoire R recognize the epitope. Expressing one minus the chance of failure as the probability of mounting an immune response to a foreign epitope we obtain

$$P_i = 1 - (1 - p)^R = 1 - (1 - p)^{R_0(1-p)^S} . \quad (12.2)$$

Plotting P_i as a function of the lymphocyte specificity p gives Fig. 12.1a which has a very wide region of specificities where the chance of mounting a successful immune response is close to one. If lymphocytes are too specific, i.e., at the left, epitopes remain unrecognized. If they are too cross-reactive, too many clonotypes are deleted by self tolerance processes, and the functional repertoire becomes too small.

Because $(1 - x)^n \simeq e^{-xn}$ whenever $x \ll 1$, we can approximate this model by

$$R \simeq R_0 e^{-pS} \quad \text{and} \quad P_i \simeq 1 - e^{-pR} . \quad (12.3)$$

When plotted for the same parameters as those of Fig. 12.1 the approximation is indistinguishable from the original curve (not shown). The approximation allows us to compute the ‘‘optimal’’ value of P_i by taking the derivative $\partial_p P_i$ of Eq. (12.3) and solving $\partial_p P_i = 0$ to find that the maximum is at $\hat{P}_i = 1/S$. This optimum suggests that the lymphocyte specificity is largely determined by the number of self epitopes the immune system has to be tolerant to. Thus, the specificity is not determined by the

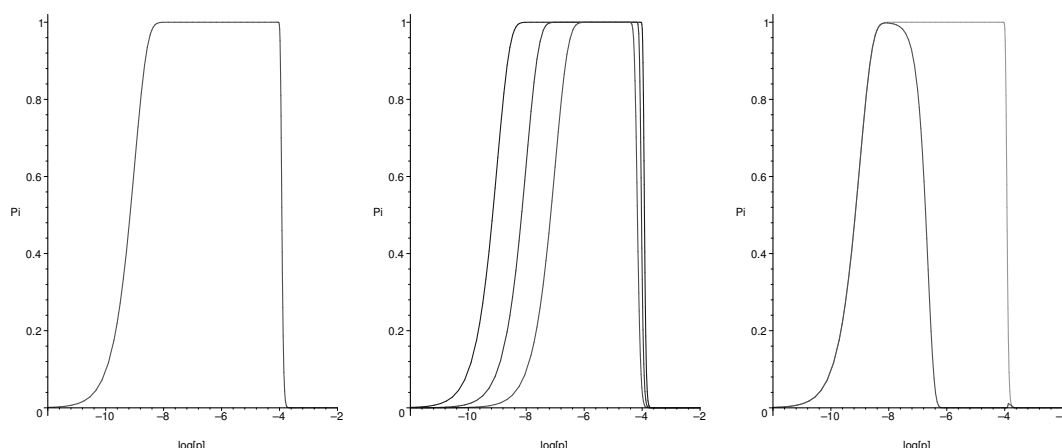


Figure 12.1: The probability of mounting an immune response P_i from Eq. (12.2) as a function of the specificity p of the lymphocytes. Parameters $S = 10^5$ and $R_0 = 10^9$. Panel (b) depicts the effect of decreasing the initial repertoire size from $R_0 = 10^9$, $R_0 = 10^8$, to $R_0 = 10^7$. Panel (c) depicts the effect of incomplete tolerance induction, i.e., $f = 1$ and $f = 0.8$ in Eq. (12.6).

recognition of pathogens, but by the demand to remain tolerant to a large number of self epitopes. Once lymphocytes are specific the repertoire has to be sufficiently diverse to guarantee recognition of foreign epitopes (Fig. 12.1b).

Incomplete tolerance

Although there is promiscuous expression of self antigens in the thymus, it remains unlikely that self tolerance is complete. Healthy individuals do harbor lymphocytes that can recognize self epitopes (see Chapter 10). To study how the results change when tolerance is incomplete we define a new parameter f for the fraction of self epitopes that manage to induce tolerance. For $f = 1$ the new model should be identical to the previous one. For a foreign epitope we now require that it is recognized, but that none of the clonotypes recognizing the foreign epitope also recognize one of the $(1 - f)S$ self epitopes that fail to induce tolerance. Otherwise the clone will be held responsible for auto-immunity. Following Borghans *et al.* (1999) we let α be the fraction of clonotypes recognizing at least one ignored self epitope, i.e.,

$$\alpha = 1 - (1 - p)^{(1-f)S} . \quad (12.4)$$

The chance that the system remains tolerant when stimulated with a foreign epitope is the probability that none of the clones in the functional repertoire R will respond (with chance p) and is potentially auto-reactive (with chance α), i.e.,

$$P_t = (1 - p\alpha)^R \quad \text{where} \quad R = R_0(1 - p)^{fS} . \quad (12.5)$$

Now the chance of a “successful immune response” is the probability that the system remains tolerant and responds to the foreign epitope, which is the chance to remain tolerant minus the chance to not respond at all:

$$P_s = P_t - (1 - p)^R, \quad (12.6)$$

where the functional repertoire R is given in Eq. (12.5). To study how incomplete tolerance affects the results we plot Eq. (12.6) for $f = 0.8$ and $f = 1$ in Fig. 12.1c.

Fig. 12.1c demonstrates that the effect of incomplete tolerance is enormous. The region of specificity values where the chance of a successful response P_s approaches one is much narrower. Moreover the optimum has shifted leftwards, i.e., towards a specificity much smaller than $p = 1/S$. Thus the $p = 1/S$ estimate (De Boer & Perelson, 1993) is an upper bound for the lymphocyte crossreactivity: when the initial repertoire is sufficiently large the immune system operates even better when lymphocytes are more specific (Borghans *et al.*, 1999). The conclusion remains that lymphocytes are specific to avoid auto-immunity, and not to recognize many pathogens.

12.2 MHC diversity within the individual

Since individual MHC diversity increases the presentation of pathogens to the immune system, one may wonder why the number of MHC genes is not much higher than it is. The argument that is mostly invoked is that more MHC diversity within the individual would lead to T cell repertoire depletion during self tolerance induction. This argument is incomplete, however, because more MHC diversity could also increase the number of clones in the T cell repertoire through positive selection. In order to be rescued in the thymus, lymphocytes need to recognize MHC–self peptide complexes with sufficient avidity. A high MHC diversity thus increases both the number of lymphocyte clones that are positively selected and the number of clones that are negatively selected. To calculate the net effect of these two opposing processes we develop a simple mathematical model (Borghans *et al.*, 2003).

Consider an individual with M different MHC molecules and an initial T lymphocyte repertoire consisting of R_0 different clones. Let p and n denote the (unconditional) chances that a clone is positively selected by a single MHC type, because its avidity is higher than a threshold T_1 , or negatively selected because its avidity exceeds a higher threshold T_2 , respectively (see Fig. 12.2). By this definition, thymocytes can only be negatively selected by MHC molecules by which they are also positively selected, i.e. $n < p$. Since T cell clones need to be positively selected by *at least one* of the MHC molecules, and avoid negative selection by *all* of the MHC molecules, the number of clones in the functional repertoire R can be expressed as

$$R = R_0 \left((1 - n)^M - (1 - p)^M \right), \quad (12.7)$$

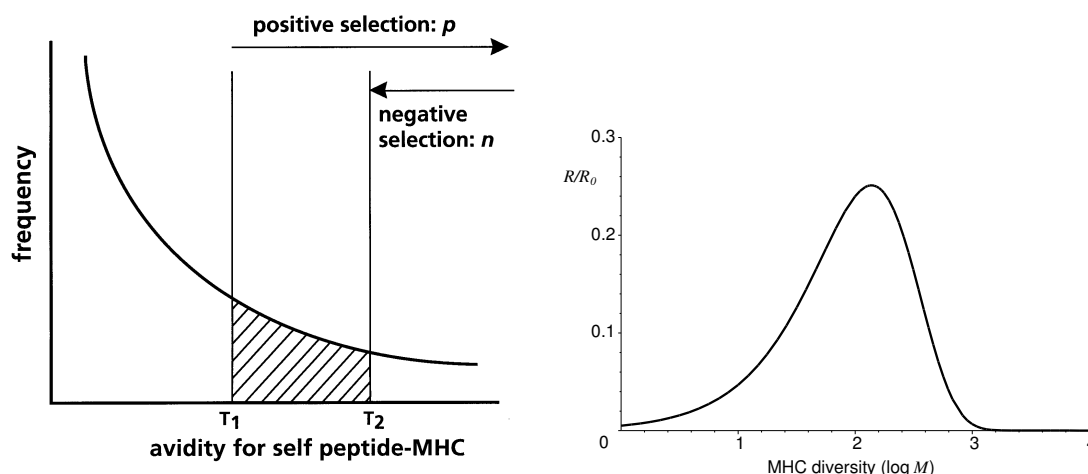


Figure 12.2: Positive and negative selection according to the avidity model (Janeway & Katz, 1984). The curve in (a) depicts the distribution of thymocyte avidities for self peptide–MHC complexes. In our model, the chance p to be positively selected by a single MHC type is the chance that the avidity between the thymocyte T cell receptor and any of the self peptide–MHC complexes exceeds threshold T_1 . Thymocytes with avidities for self peptide–MHC complexes exceeding the upper threshold T_2 are negatively selected (with chance n per MHC type). Panel (b) depicts the size of the T cell repertoire as a function of MHC diversity. The number of clones in the functional repertoire R is plotted as a fraction of the total initial lymphocyte repertoire R_0 . Parameters are: $p = 0.01$, and $n = 0.005$.

(Borghans *et al.*, 2003). The functional repertoire R thus contains all T cell clones that fail to be negatively selected, minus the ones that also fail to be positively selected by any of the M different MHC molecules of the host.

Experimental estimates for the parameters of this model have recently become available. In mice, around 3% of the T cells produced in the thymus end up in the mature T cell repertoire, and at least 50% of all *positively selected* T cells have been shown to undergo negative selection in the thymus (Van Meerwijk *et al.*, 1997). Thus, 94% of all thymic T cells fail to be positively selected by any of the MHC molecules in the host (Van Meerwijk *et al.*, 1997). These estimates can be used to calculate the chances p and n of a T cell clone to be positively or negatively selected by a single type of MHC molecule. Taking into account that inbred mice are homozygous and therefore express 3 types of class I MHC and 3 types of class II MHC molecules, p and n follow from: $(1 - p)^6 = 0.94$ and $(1 - n)^6 = 0.97$. This yields $p = 0.01$ and $n = 0.005$.

Using these experimental estimates, the number of clones in the functional T cell repertoire R increases with the number of different MHC molecules M in an individual until $M = 140$ (see Fig. 12.2b). In other words, the size of the functional T cell repertoire would increase if the MHC diversity M were to exceed its normal value of ten to twenty

in heterozygous individuals. The intuitive reason is that only a very small part of the T cell repertoire has sufficient avidity for self peptides presented by a single MHC type to be positively selected by that MHC. As long as additional MHC types positively select hardly overlapping parts of the T cell repertoire, negative selection will only waste T cells that were not even positively selected in the absence of those MHC molecules. A net negative effect of MHC diversity on the size of the functional T cell repertoire is only attained once the individual MHC diversity is so large that thymocytes are selected by multiple MHC types, *i.e.* when $M > 140$. Summarizing, the consensus explanation that the MHC diversity per individual is limited to avoid repertoire depletion is untenable.

12.3 Exercises

Question 12.1. Probability of response

Plot Eq. (12.2) for several values of S and R_0 using Maple.

- a. How do the results explained above depend to the precise values of S and R_0 ?
- b. What do you learn from this?

Question 12.2. Incomplete tolerance

Write the approximation of Eq. (12.6) using $(1 - x)^n \simeq e^{-xn}$.

- a. Plot the approximation and the original equation with Maple to test the validity of the approximation.
- b. See if you can find the optimal specificity with Maple.

Question 12.3. Epitopes

In Eq. (12.2) we calculated the probability of an immune response to one single epitope. Each pathogen obviously consists of a large number of epitopes.

- a. How would you extend the model to calculate the probability to respond to a pathogen with a number of epitopes?
- b. Use Maple to study how this affects the results derived above.

Question 12.4. Pathogens

An organism has to survive infection with many different pathogens. In the “Epitopes” project you calculated the chance to respond to a single pathogen consisting of a number of epitopes.

- a. Try to write an expression for the probability to respond to k different (and unrelated) pathogens.
- b. Use Maple to study how this affects the results derived above.

Question 12.5. Optimal #MHC

Nowak *et al.* (1992) also addressed the question of the optimum number of MHC molecules within an individual with a mathematical model. According to their model the functional repertoire is given by

$$R = R_0(1 - (1 - p)^M)(1 - n^*)^M, \quad (12.8)$$

where n^* is the *conditional* probability that a positively selected clone is negatively selected by a random MHC molecule, *i.e.* $n^* = n/p$.

- a. Discuss the interpretation of each term.
- b. What is wrong with this model?
- c. Study the model with Maple for the same parameters as used in Fig. 12.2b.

Question 12.6. MHC polymorphism

Having considered the evolution of the number of MHC loci per individual, it is tempting to speculate about the reasons for the enormous polymorphism at the population level.

- a. Why do you think the MHC is so polymorphic?
- b. Can you think of an approach to study these speculations?

Chapter 13

Theoretical immunology projects

Question 13.1. Early and Late antigens

Consider a pathogen with two developmental stages. During each stage there is one immunodominant antigen evoking one specific immune response. Let E be the early phase, that is recognized by immune response X , and let L be the late phases recognized by immune response Y :

$$\frac{dE}{dt} = rL \left(1 - \frac{E + L}{k} \right) - mE - k_x XE, \quad \frac{dL}{dt} = mE - k_y YL - \delta L,$$

$$\frac{dX}{dt} = p_x XE - dX \quad \text{and} \quad \frac{dY}{dt} = p_y YL - dY.$$

- a. Give a short interpretation of each term in the model.
- b. Can the two responses coexist at steady state?

Question 13.2. Ho *et al.* (1995)

Read the classical Ho *et al.* (1995) paper estimating the half life of CD4⁺ T cells infected by HIV-1.

- a. Make sure you understand the model they use for fitting the data. What criticism(s) do you have?
- b. Suppose the treatment is not 100% effective. How would that influence the estimates?
- c. Suppose there is a time delay before the drug enters the cells and becomes effective. How would that influence the estimates?
- d. They conclude that the production of CD4⁺ T cells is increased due to the HIV-1 infection. How do they reach this conclusion, and how do they compare it to the normal production rate?

Question 13.3. Diversity threshold

Nowak *et al.* (1991) argue that increasing the diversity of the HIV-1 quasi species within a host is sufficient for to drive disease progression (see also the book on viral dynamics by Nowak & May (2000)). Each novel strain of the virus elicits a new immune response, but all strains can infect and lyse CD4⁺ T cells independent of their specificity. This asymmetry is sufficient for having a “diversity threshold”, above which the immune system deteriorates despite having clonotypes available to respond to novel variants. A model to study this is the pair of one viral strain I with its specific helper T cell clone H ,

$$\frac{dI}{dt} = rI - kIH \quad \text{and} \quad \frac{dH}{dt} = s + \frac{pHI}{h+I} - dH - nIH ,$$

where the n parameter incorporates the diversity of the viral quasi species, i.e., each helper cell can be infected by all n strains.

- a. Explain each term of the model.
- b. Analyze the model, draw the nullclines, etcetera.
- c. Does this model have a diversity threshold?

Question 13.4. Th1 versus Th2

Helper T cell responses come in at least two types. Responses to intracellular pathogens are of the Th1 type, which characterized by IL-12 produced by dendritic cells, and IFN- γ produced by the Th1 cells. Immune responses to worms and other extracellular parasites are typically of the Th2 type, which is characterized by IL-4 production. Th1 and Th2 phenotypes exclude eachother because the two types reinforce themselves and downregulate eachother. A naive T cell stimulated in the presence of IL-12 or IFN- γ express the transcription factor T-bet which acts to remodel the repressed IFN- γ locus. Later HLX is expressed which maintains the expression of the IFN- γ locus. This is a positive feedback loop. If naive T cells are stimulated in the presence of IL-4, the GATA3 transcription factor induces heritable remodeling of the IL-4 locus, which is also a positive feedback loop. This scheme has recently been reviewed by Murphy & Reiner (2002).

- a. Develop a simple mathematical model of a single ODE for the heritable remodeling of repressed loci. Analyze the model to study its validity.
- b. Is heritable remodeling sufficient for the exclusive phenotypes?
- c. Extend your model into two ODEs, for for Th1 and one for Th2, and add a cross down regulatory effect. Analyze the model to study its validity.
- d. Read the paper by Hofer *et al.* (2002) and discuss differences and similarities between their model and the one you devised yourself.

Chapter 14

GRIND

The phase portraits in this book are made with a computer program called GRIND, for GReat INtegrator Differential equations. The user interface of GRIND is not as fancy as that of similar programs (like Berkeley Madonna), but GRIND has phase plane analysis as its major additional feature. GRIND allows you to study differential equation models by means of numerical integration, steady state analysis, and phase space analysis (e.g., nullclines and separatrices). The model equations are defined in a very natural formalism, and one can easily change parameters and initial conditions. The user interface to GRIND is based upon a simple command language. The best way to learn more about GRIND is to walk through the example listed below. Table 14.1 lists the most important GRIND commands. GRIND commands have a help function to remind you of their syntax.

GRIND is publically available from theory.bio.uu.nl/rdb/grind.html and operates under Microsoft Windows, Macintosh Unix, and Linux. Windows should know that a `model.grd` file has to be executed by `C:\mingw\grind\windows\grind.bat` (this path depends on where GRIND was installed for you), and in Linux one just calls the `grind` script on a text file containing the model.

All models described in this Chapter can be downloaded from theory.bio.uu.nl/rdb/tb/models.

14.1 Lotka Volterra model

A Lotka Volterra model with a density dependent growth rate can be studied with GRIND by typing the following text file, and saving it, for instance, under the name

lotka.grd:

```
R ' = r*R*(1-R/k) - a*R*N;
N ' = c*a*R*N - d*N;
```

The model has two differential equations, $R' =$ and $N' =$, and five parameters a , c , d , k , and r . Note that r is different from R !

Beforehand one can create a parameter file `lotka.txt` containing a parameter setting belonging to this model. Alternatively, one can make such a file from GRIND with the parameter `lotka.txt` command.

After firing up GRIND, by clicking the `lotka.grd` file in Windows, or typing `grind lotka` in Lunix, you start typing commands and parameter values as soon as you get the `GRIND>` prompt. For example:

```
display lotka.grd
a=1
c=1
d=.5
r=1;k=1
R=0.01;N=0
```

This first displays the model equations of the `lotka.grd` file. The following lines set the parameters, and then gives an initial condition with a little bit of prey and no predators. Note again that GRIND is case sensitive.

Now you are ready to go. To obtain a numerical solution say that you want twenty time steps and give the `run` command:

```
finish 20
run
timeplot
where
```

On your screen you get a listing of the predator and prey values obtained by “running” the model and solving the differential equations numerically. Timeplot makes a nice graph on your screen. The `where` command gives the final state.

The curve on the screen depicts the logistic growth of the prey.

Next we become interested in the predator:

```
N=0.01
run
ti
fin 50 50
run
ti
```

Which first sets the initial condition of the predator, runs, and makes a new timeplot. Then the integration time is changed to 50 time steps asking for all 50 time points. The model is solved and timeplot is called.

The main feature of GRIND is phase plane analysis:

```
2d
nullcline
vector
run
d=0.9
nu
```

Which depicts a 2-dimensional phase space, draws nullclines, shows the vector field, and the trajectory. Finally, the phase space is redrawn for $d = 0.9$.

GRIND can do local stability analysis for you:

```
axis x R 0 0.9
d=0.5
parameter lotka.txt
2d
nu
cursor
newton
eigen
```

Illustrates the usage of the `axis` command. Parameter values are listed and saved into a file `lotka.txt`. Such a file can later be read with the `read` command. Redraw the nullclines for $d = 0.5$ and click with the mouse close to the non-trivial intersection point of the two nullclines. Then do a “Newton Raphson” iteration to approach a nearby equilibrium point, and display the eigenvalues.

To set Gaussian variation on a parameter:

```
noise k 1 0.2
run
fin 500 500
run
ti
bye
```

Noise draws new values for k every time step from a Gaussian distribution with mean 1 and standard deviation 0.2. The model is solved. The time length is increased, the model is run, and the solution is plotted.

14.2 Exercises

Question 14.1. Tutorial

Here is a set of questions to test if you understood the tutorial you just made:

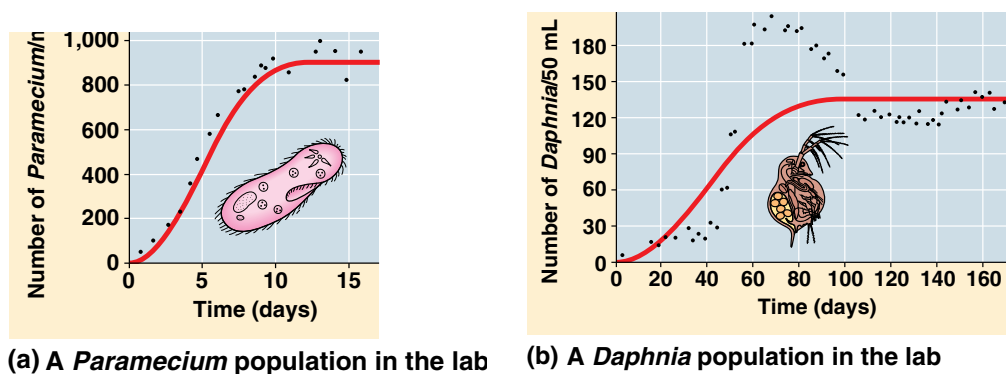
- When you called `run;timeplot` you got a nice graph on your screen. What is the meaning of this graph?
- How is the system of ODEs defining this graphs?
- When you called `2d>nullcline` you also got nice graphs on your screen. What do these mean?
- With the Newton Raphson command you just jump to a nearby steady state, whether it is stable or unstable. What do the eigenvalues mean that you get after issuing the `eigen` command?

Question 14.2. The Monod functional response

In Chapter 4 we analyzed the following predator prey model with a saturated functional response:

2d	make a 2-dimensional phase space
axis	define the identity and scaling of an axis
bye	leave GRIND
bifurcate	make a series of Poincaré sections
continue	follow a steady state as a function of a parameter
cursor	ask for a mouse click to set the initial condition
display filename	show the contents of a text file
eigen	compute eigenvalues
finish	set the time span and number of points reported
grid	start many trajectories
help	get help
keepvar	copy the final state into the initial state
newton	approach a close-by equilibrium point
noise	set white noise on a parameter
nulcline	draw nulclines
parameter	list parameter setting and/or save them into a file
poincare	make a poincaré section
read filename	read a file with parameters and/or commands
run	solve the model numerically
timeplot	depict the solutions
vector	show the vector field
where	where am I?

Table 14.1: A sample of the most important GRIND commands. Note that GRIND commands can be abbreviated to the first two letters.

(a) A *Paramecium* population in the lab(b) A *Daphnia* population in the lab

Copyright © Pearson Education, Inc., publishing as Benjamin Cummings.

Figure 14.1: Logistic growth of *Paramecium* and non-logistic growth of *Daphnia*. From: Campbell & Reece (2008)52.13.

$$F = R/(h + R);$$

$$R' = r \cdot R \cdot (1 - R/K) - b \cdot N \cdot F;$$

$$N' = b \cdot N \cdot F - d \cdot N;$$

The algebraic expression F defines the functional response, and is used in the differential equations $R' =$ and $N' =$.

This model is available from theory.bio.uu.nl/rdb/tb/models as a file `monod.grd` with the corresponding parameter file `monod.txt`.

- Double click the monod model and start with `read monod.txt`. Check the equations (`display`) and its parameter values (`par`).
- Make a time plot showing the logistic growth of the prey by starting with zero predators and few prey. Explain in words what this curve represents.
- Now study the 2-dimensional system by making a phase space. List the parameter values and make qualitatively different phase spaces. Sketch trajectories for each of these systems.
- When is the non-trivial steady state stable and when is it unstable? What is the behavior when it is unstable?
- What is the effect of changing the carrying capacity of the prey? Can you repeat Rosenzweig's paradox of enrichment?
- Which population increases most when you increase the carrying capacity of the prey?
- In Figure 52.13 of Campbell & Reece (2005) the growth of *Daphnia* is compared with logistic growth of *Paramecium* (see Fig. 14.1). A striking difference is that *Paramecium* asymptotically approaches its carrying capacity, whereas *Daphnia* has an oscillatory approach to its steady state. As *Daphnia* feeds on algae you can use this Monod saturated predator prey model to see if you can understand *Daphnia*'s growth curve depicted in Fig. 14.1b. Simulate the experimental curves in Fig. 14.1 by adding a few predators to a prey population at carrying capacity. Can you obtain the oscillatory approach of *Daphnia*?
- Can you also obtain the asymptotic approach of *Paramecium* with the same model

for other parameter values?

Question 14.3. Viral rebound

Consider an HIV-1 infected patient that is treated with an anti-retroviral drug. Use the following extension of Eq. (7.5):

$$\frac{dT}{dt} = \sigma - \delta_T T - \alpha_1 \beta T I_1 - \alpha_2 \beta T I_2, \quad \frac{dI_1}{dt} = \alpha_1 \beta T I_1 - \delta I_1, \quad \frac{dI_2}{dt} = \alpha_2 \beta T I_2 - \delta I_2,$$

where I_1 are cells infected with the wild-type virus, and I_2 are cells infected with a pre-existing drug resistant mutant. The $0 < \alpha_i \leq 1$ parameter represents the effect of treatment (where setting $\alpha_i = 1$ means absence of treatment). Because I_2 is a drug resistant mutant, $\alpha_2 < \alpha_1$ before treatment, and $\alpha_2 \gg \alpha_1$ during treatment. Help yourself when setting parameter values by noting that the wild type virus requires $R_0 = \frac{\beta\sigma}{\delta\delta_T} > 1$. The model is available as `hiv.*`.

- a.** First study viral rebound in the absence of drug resistant virus. Set $\alpha_1 = 1$ and $I_2 = \alpha_2 = 0$ and let the model approach a state corresponding to a chronic viral infection. Then give a mild “treatment” that decreases α_1 several-fold. Can the wild type virus rebound, and what is the new steady state?
- b.** Which population is most strongly affected by the treatment?
- c.** Now allow for the drug resistant virus, e.g., set $\alpha_2 = 0.95$ and see if the viruses can coexist in the absence of treatment.
- d.** Assume that drug resistant virus is continuously created by mutation, i.e., study treatment with drug resistant virus by giving I_2 a small initial value at the onset of treatment. Can the two viruses coexist under continuous treatment?

Chapter 15

Simple Maple examples

Maple is a system for doing mathematics with a computer. Maple has an excellent help function with lots of examples. Start maple by typing `xmaple` to the Linux-prompt. Then try the following examples:

Solve an algebraic equation:

```
solve(3*x=2,x);
```

Solve a quadratic equation with free parameters:

```
sol:=solve(a*x^2+b*x+c=0,x);
```

Later you can set `a:=3`; etcetera.

Get the second root:

```
sol2:=sol[2];
```

Solve a differential equation (i.e., Eq. (2.2)):

```
dsolve({diff(x(t),t)=s-d*x(t),x(0)=x0},x(t));
```

Plot a function:

```
plot(x*exp(-x),x=0..10);
```

Substitution of functions:

```
r:=(1-p)^s;y:=1-(1-p)^r;plot(subs(s=10^5,p=10^m,y),m=-8..-3);
```

Find maximum of the function:

```
simplify(solve(diff(y,p)=0,p));
```

Approximate a function by a Taylor series:

```
series(y,s=infinity);
```

Take the limit of a function:

```
limit(y,s=infinity);
```

Undefine all definitions:

```
restart;
```

Chapter 16

Appendix: mathematical prerequisites

16.1 Sketching functions

Most models in this course are analyzed graphically by sketching nullclines in phase space. Some experience with sketching functions is therefore required. To fresh up these techniques we here discuss the general approach, and give a few examples. Since most of the models have free parameters, we also have to sketch functions with free parameters. This implies that one cannot simply resort to a computer program or a graphical calculator.

The general procedure is:

1. Determine the intersects with the horizontal and vertical axis.
2. Check for vertical asymptotes, i.e., x values leading to division by zero.
3. Check for horizontal asymptotes by taking the limit $x \rightarrow \infty$ and $x \rightarrow -\infty$.
4. Check where the function has positive values where negative values.
5. We typically **do not need** to determine minimum values, maximum values, or inflexion points.

Example 1

Sketch the function

$$y = \frac{ax}{b-x} \tag{16.1}$$

in a graph plotting y as a function of x :

- a. For $x = 0$ one finds $y = 0$ as the intersect with the y -axis. This is the only intersect with the horizontal axis.

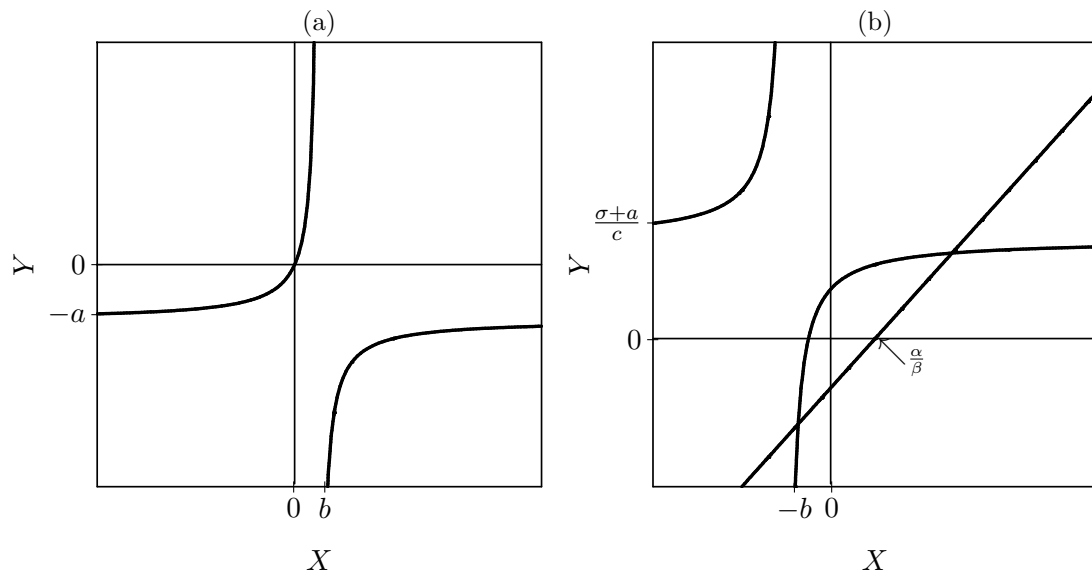


Figure 16.1: Two examples for **qualitatively** sketching functions.

- b.** There exists a vertical asymptote at $x = b$. When $x \uparrow b$ one finds that $y \rightarrow \infty$, when $x \downarrow b$ one sees that $y \rightarrow -\infty$.
- c.** To find horizontal asymptotes one rewrites the function into

$$y = \frac{a}{b/x - 1} . \quad (16.2)$$

Both for $x \rightarrow \infty$ and for $x \rightarrow -\infty$ one sees $y \rightarrow -a$. Thus, we find one horizontal asymptote at $y = -a$.

- d.** When $x < 0$ one sees that $y < 0$, when $0 \leq x < b$ one sees that $y \geq 0$, and when $x > b$ one finds $y < 0$. The function is sketched in Fig. 16.1a.

Example 2

Sketch the system

$$0 = \sigma + \frac{aX}{b+X} - cY , \quad (16.3)$$

$$0 = -\alpha + \beta X - \gamma Y \quad (16.4)$$

in one graph. Because both equations can easily be solved for the Y variable, it is most easy to draw Y as a function of X . For the second equation one finds

$$Y = -\alpha/\gamma + (\beta/\gamma)X , \quad (16.5)$$

which is a straight line with slope β/γ .

- a.** The intersect with the Y -axis $-\alpha/\gamma$, and that with horizontal axis $X = \alpha/\beta$.
- b.** No vertical asymptotes.

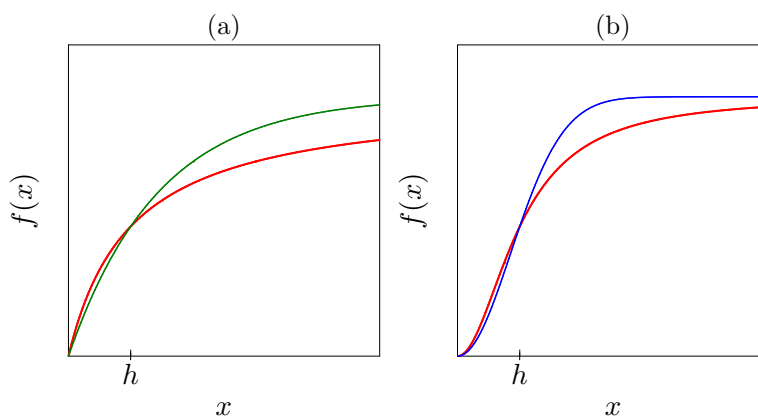


Figure 16.2: The increasing saturation functions defined by Eq. (16.15). The left panel depicts $f(x) = x/(h+x)$ and $f(x) = 1 - e^{-\ln[2]x/h}$ which both have the convenient property that $0 \leq f(x) < 1$ and $f(x) = 0.5$ when $x = h$. In the panel on the right we draw their corresponding sigmoid variants $f(x) = x^2/(h^2 + x^2)$ and $f(x) = 1 - e^{-\ln[2](x/h)^2}$.

- c. No horizontal asymptotes.
- d. When $X < \alpha/\beta$ one finds $Y < 0$, otherwise $Y \geq 0$.

For the first equation we also write Y as a function of X

$$Y = \sigma/c + \frac{(a/c)X}{b+X}. \quad (16.6)$$

- a. The intersect with the vertical axis is $Y = \sigma/c$. That with the X axis is $X = -b\sigma/(\sigma+a)$.
- b. There exists a vertical asymptote at $X = -b$. When $X \downarrow -b$ one finds that $Y \rightarrow -\infty$ and when $X \uparrow -b$ we see $Y \rightarrow \infty$.
- c. For the horizontal asymptotes one first writes

$$Y = \sigma/c + \frac{(a/c)}{b/X + 1}, \quad (16.7)$$

to see that for $X \rightarrow \infty$ and for $X \rightarrow -\infty$, $Y \rightarrow (\sigma+a)/c$.

- d. One finds that $Y > 0$ if $X > -b\sigma/(\sigma+a)$ or if $X < -b$.

Although one does not know the parameters of this system, one can be sure that in the positive quadrant the two curves have to intersect. Thus, qualitatively, there is only one unique situation, which is depicted in in Fig. 16.1b.

16.2 Mathematical background

Useful mathematical formulas

To fresh up your memory of earlier education in mathematics we provide a few standard formulas

$$\ln 1 = 0, \quad \ln xy = \ln x + \ln y, \quad \ln x/y = \ln x - \ln y, \quad e^{ix} = \cos x + i \sin x, \quad (16.8)$$

and the two roots of the quadratic equation

$$ax^2 + bx + c = 0 \quad \text{are} \quad x_{\pm} = \frac{-b \pm \sqrt{b^2 - 4ac}}{2a}. \quad (16.9)$$

The standard rules of differentiation are

$$[cx]' = c, \quad [cx^n]' = ncx^{n-1}, \quad [f(x) + g(x)]' = f'(x) + g'(x), \quad (16.10)$$

where the $'$ means ∂_x , and

$$[f(x)g(x)]' = f'(x)g(x) + f(x)g'(x), \quad \left[\frac{f(x)}{g(x)} \right]' = \frac{f'(x)}{g(x)} - \frac{f(x)g'(x)}{g(x)^2}, \quad (16.11)$$

and the famous chain rule

$$f[g(x)]' = f'(g) g'(x) \quad , \text{ e.g., } \quad \sqrt{1+ax}' = \left[\frac{1}{2}(1+ax)^{-\frac{1}{2}} \right]' a = \frac{a}{2\sqrt{1+ax}}. \quad (16.12)$$

Linearization

Complicated non-linear functions, $f(x)$, can be approximated by a local linearization around any particular value of x . Fig. 16.3 shows that the local tangent at some point linearizes the function such that nearby function values can be estimated. The underlying formula is

$$f(x+h) \simeq f(x) + \partial_x f h, \quad (16.13)$$

where $h \rightarrow 0$ is a small distance to the x value for which $f(x)$ is known. Basically, one estimates the vertical displacement by multiplying the local slope with the horizontal displacement. The same can be done for 2-dimensional functions, i.e.,

$$f(x+h_x, y+h_y) \simeq f(x, y) + \partial_x f h_x + \partial_y f h_y. \quad (16.14)$$

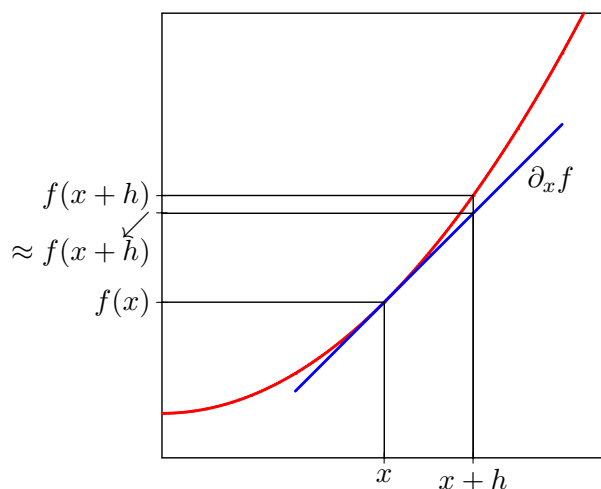


Figure 16.3: Linearization of a non-linear function. The heavy line is the local tangent at $f(x)$.

16.3 Convenient functions

Once we have a sketch of how some process should depend on a variable of the model, we need to translate this graph into a mathematical function. We here let you become familiar with a few families of convenient functions, i.e., Hill-functions and exponential functions. These will be used to formulate positive and negative effects of populations onto each other. Because these functions are dimensionless and remain bounded between zero and one, i.e., $0 \leq f(x) \leq 1$, one can easily multiply any term in a model (corresponding to some biological process) with such a function. We here define two families of functions $f(x)$ that increase with x , are zero when $x = 0$, and approach a maximum $f(x) = 1$ when $x \rightarrow \infty$. Whenever one would need a different maximum in the model, one could simply multiply $f(x)$ with some parameter. Having increasing functions $0 \leq f(x) \leq 1$, one can easily define decreasing functions by taking $g(x) = 1 - f(x)$.

A very conventional and convenient family of functions are the **Hill-functions**

$$f(x) = \frac{x^n}{h^n + x^n} \quad \text{and} \quad g(x) = 1 - f(x) = \frac{1}{1 + (x/h)^n}, \quad (16.15)$$

in which you may recognize the classical Michaelis-Menten saturation function for $n = 1$ (see Fig. 16.2a). The “saturation constant” h is the value of x where $f(x)$ or $g(x)$ attains half of its maximal value. The exponent n determines the steepness of the function. Whenever $n > 1$ the function is sigmoid (see Fig. 16.2b), and for $n \rightarrow \infty$ both $f(x)$ and $g(x)$ become step functions switching between zero and one at $x = h$. The slope of $f(x)$

in the origin is determined from its derivative, which for $n = 1$ equals

$$\partial_x f(x) = \frac{1}{h+x} - \frac{x}{(h+x)^2}, \quad (16.16)$$

which delivers a slope of $1/h$ for $x = 0$. For $n > 1$ the derivative is

$$\partial_x f(x) = \frac{nx^{n-1}}{h^n + x^n} - \frac{nx^{2n-1}}{(h^n + x^n)^2}, \quad (16.17)$$

which means that for $x = 0$ the slope is zero. An advantage of using Hill functions in mathematical models is that solving steady states corresponds to solving polynomial functions.

The exponential functions

$$f(x) = 1 - e^{-\ln[2]x/h} \quad \text{and} \quad g(x) = e^{-\ln[2]x/h}. \quad (16.18)$$

are as conventional as Hill functions. They may be more convenient for finding solutions of equations, but they are more cumbersome when it comes to finding steady states. Like Hill functions we have $f(0) = 0$. For finding the half maximal value of $f(x)$ one solves $0.5 = e^{-\ln[2]x/h}$ to find that $x = h$. The slope in the origin is determined from the derivative $\partial_x [1 - e^{-\ln[2]x/h}] = (\ln[2]/h)e^{-\ln[2]x/h}$ which for $x = 0$ gives a slope of $\ln[2]/h$. Like the Michaelis-Menten function this exponential function is not sigmoid (see Fig. 16.2a). The sigmoid form of the exponential function is known as the Gaussian distribution

$$f(x) = 1 - e^{-\ln[2](x/h)^2}, \quad \text{and} \quad g(x) = e^{-\ln[2](x/h)^2}. \quad (16.19)$$

Thanks to our scaling with $\ln[2]$ these sigmoid functions are also half maximal when $x = h$ (and $x = -h$); see Fig. 16.2b.

16.4 Phase plane analysis

Most mathematical models in biology have non-linearities and can therefore not be solved explicitly. One can nevertheless obtain insight into the behavior of the model by numerical (computer) analysis, and/or by sketching nullclines and solving for steady states. One determines the stability of the steady states from the vector field, and by linearization around the steady states.

The long-term behavior of a model typically approaches a stable steady state, a stable limit cycle, or a chaotic attractor. Phase plane analysis is a graphical method to analyze a model to investigate these behavioral properties of a model. Consider a model of two variables x and y ,

$$\frac{dx}{dt} = f(x, y) \quad \text{and} \quad \frac{dy}{dt} = g(x, y). \quad (16.20)$$

One can define a “phase space” with x on the horizontal axis and y on the vertical axis where each point in this space is one particular “state” of the model. To obtain further insight in the model one sketches the “nullclines” $f(x, y) = 0$ and $g(x, y) = 0$. This is useful because at the former nullcline dx/dt switches sign, and at the latter dy/dt switches sign. Two simple nullclines therefore typically define four regions with qualitatively different signs of the two differential equations. Nullclines enable one to localize all steady states of the model because these correspond to the intersections of the nullclines (i.e., $f(x, y) = g(x, y) = 0$). This is very useful because models may have a number of steady states.

For each steady state one has to determine whether it is an attractor, i.e., a stable steady state, or a repeller, i.e., an unstable equilibrium. The local vector field around a steady state in a phase space with nullclines often provides sufficient information to see whether the steady state is stable or unstable. In 2-dimensional phase spaces there are three classes of steady states: nodes, saddles, and spirals. Nodes and spirals are either stable or unstable, and a saddle point is always unstable because it has a stable and an unstable direction. The two nullclines intersecting at the equilibrium point define four regions of phase space, each with its unique local vector field. The four vector local fields define the nature of the steady state.

A simple example is a “stable node”, for which all four vector fields points towards the steady state (see Fig. 16.4a). A stable node is therefore approached by trajectories from all four directions (Fig. 16.4b). When the vector fields point outwards in all four regions the equilibrium is an “unstable node” (Fig. 16.4c), and trajectories are repelled in all four directions (Fig. 16.4d). The local vector fields in Fig. 16.4e define a “saddle point”, which has a stable and an unstable direction (Fig. 16.4f). The stable direction of a saddle point defines a “separatrix” because all trajectories starting at either side of this line end up in another attractor (i.e., a separatrix defines different basins of attractions).

The local vector field can also suggest rotation (see Fig. 16.5). Rotating vector fields are typical for spiral points. The local vector field fails to provide sufficient information to determine with absolute certainty whether a spiral point is stable or unstable. However, one can get some good suggestion for the stability from the vector field. In Fig. 16.5c, for instance, and one can see that increasing y from its steady state value makes $dy/dt > 0$. Locally, there must be some positive feedback allowing y to increase further when y increases. This is definitely destabilizing, and the trajectory in Fig. 16.5d confirms that this is an “unstable spiral” point. Conversely, the spiral point in Fig. 16.5a is stable, and locally has negative feedback for both x and y (i.e., increasing x makes $dx/dt < 0$ and increasing y makes $dy/dt < 0$), which has a stabilizing influence. Because the stability of spiral points also depends on the local difference in time scales of the horizontal (x) and vertical (y) variables, the local vector field is not always sufficient to determine the stability of the steady state. Even the suggestion of rotation in a local vector field is not sufficient to determine with certainty that the steady state is a spiral. Fig. 16.5e &

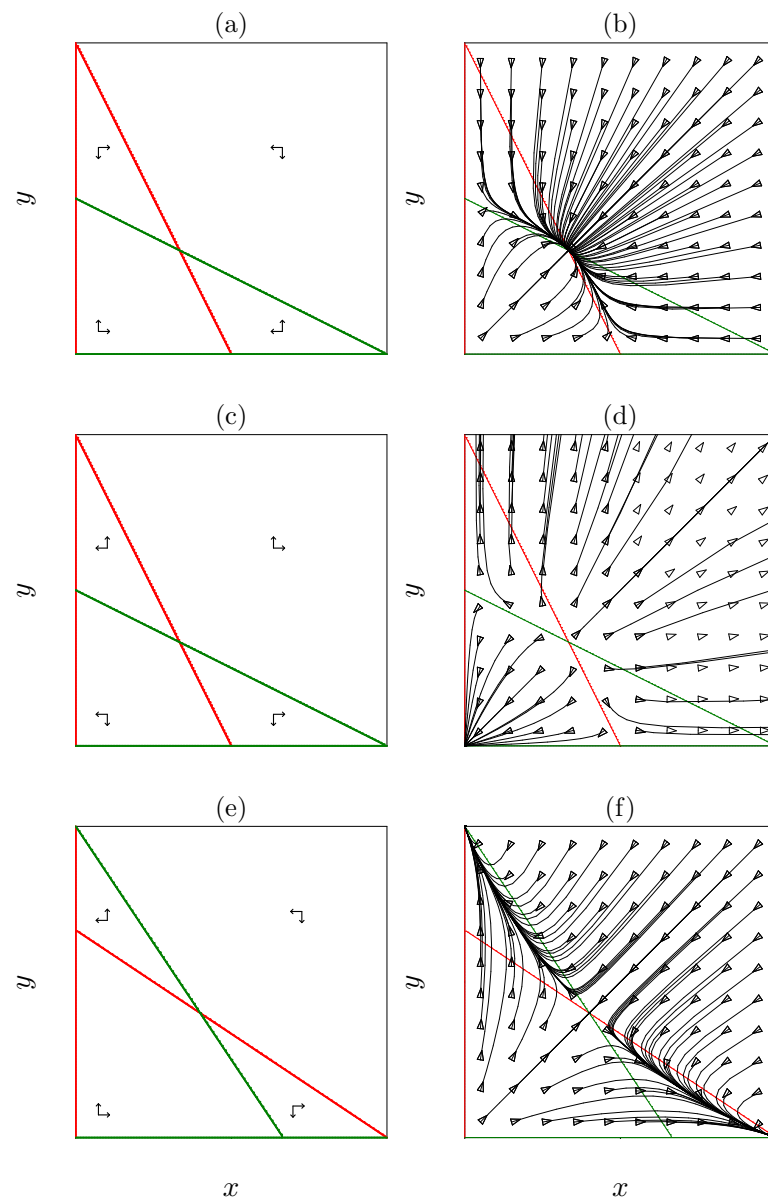


Figure 16.4: Qualitatively different steady states determined by the local vector field in the four regions defined by the nullclines. Stable node (a,b): the vector field points inwards in all four sections. Unstable node (c,d): the vector field points outwards in all four sections. Saddle point (e,f): the vector field points inwards in two sections, and outwards in the other two regions. A saddle point is an unstable steady state with a stable and an unstable direction.

f show that the same vector field defining a stable spiral point in Fig. 16.5a can actually also correspond to a stable node.

Example: Lotka Volterra model

Using the famous Lotka Volterra model as an example we review a few methods for analyzing systems of non-linear differential equations. The Lotka-Volterra predator prey model can be written as:

$$\frac{dR}{dt} = aR - bR^2 - cRN \quad \frac{dN}{dt} = dRN - eN, \quad (16.21)$$

where a, b, c, d, e are positive constant parameters, and R and N are the prey and predator densities. The derivatives dR/dt and dN/dt define the rate at which the prey and predator densities change in time.

A first step is to sketch nullclines (0-isoclines) in phase space. A nullcline is the set of points (R, N) for which the corresponding population remains constant. Thus, the R -nullcline is the set of points at which $dR/dt = 0$. Setting $dR/dt = 0$ and $dN/dt = 0$ in Eq. (16.21) one finds

$$R = 0, \quad N = \frac{a - bR}{c} \quad \text{and} \quad N = 0, \quad R = \frac{e}{d}, \quad (16.22)$$

for the prey nullcline and the predator nullclines, respectively. These four lines are depicted in Fig. 16.6. For biological reasons we only consider the positive quadrant.

A second step is to determine the vector field. Not knowing the parameter values, one considers extreme points in phase space. In the neighborhood of the point $(R, N) = (0, 0)$, for example, one can neglect the quadratic bR^2 , cRN , and dRN terms, such that

$$\frac{dR}{dt} \approx aR, \quad \frac{dN}{dt} \approx -eN. \quad (16.23)$$

Since the former is strictly positive, and the latter strictly negative, we assign $(+ -)$ to the local direction of the vector field (see Fig. 16.6). This means that $dR/dt > 0$ below the R -nullcline, i.e., we sketch arrows to the right, and that at the left hand side of the N -nullclines $dN/dt < 0$, i.e., we sketch arrows pointing to the bottom. At the R and N -nullclines the arrows are vertical and horizontal, respectively. The derivatives switch sign, and the arrows switch their direction, when one passes a nullcline. Nullclines therefore separate the phase space into regions where the derivatives have the same sign.

An important step is to determine the steady states of the system. A steady state, or equilibrium, is defined as $dR/dt = dN/dt = 0$. Graphically steady states are the intersects of the nullclines. Analytically, one finds

$$(R, N) = (0, 0), \quad (R, N) = (a/b, 0) \quad \text{and} \quad (R, N) = \left(\frac{e}{d}, \frac{da - eb}{dc} \right) \quad (16.24)$$

as the three steady states of this system. Note that the non-trivial steady state only exists when $\frac{da - eb}{dc} > 0$. We will further analyze the model for the parameter condition that all three steady states exist, i.e., we consider $da > eb$.

Finally, one has to determine the nature of the steady states. For the steady states $(0, 0)$ and $(a/b, 0)$ one can read from the vector field that they are saddle points. Around $(a/b, 0)$ the vertical component is the unstable direction, and around $(0, 0)$ the horizontal component is the unstable direction. This is not so simple for the non-trivial point. Because there is no stable and unstable direction in the vector field the non-trivial steady state cannot be a saddle point, and it has to be a node or a spiral point. To determine its stability one can check for local feedback. Increasing R in the steady state makes $dR/dt < 0$, and increasing N in the steady state keeps $dN/dt = 0$ because one lands exactly on the $dN/dt = 0$ nullcline (see Fig. 16.6). Because there is no positive feedback we suggest that the non-trivial steady state is stable.

16.5 Exercises

Question 16.1. Sketch a few functions

In this course we sketch nullclines from models with free parameters. It is very important therefore to know how to sketch arbitrary functions with free parameters.

- Sketch $y = \frac{h}{h+x}$.
- Sketch $y = \frac{x}{h+x}$.
- Sketch $aA - bLA - cL = 0$ plotting L as a function of A , and plotting A as a function of L .
- Sketch $0 = aY(1 - Y) - \frac{bYX}{c+Y}$. Hint: think beforehand which variable can best be expressed as a function of the other variable.
- Sketch $y = a \frac{k-x}{q+k-x} - d$ assuming that $a > d$.
- Sketch $y = a\sqrt{x}(b-x)$. What is the derivative when $x = 0$? At what value of x will y have a maximal value?

Question 16.2. Linearization

Consider the function $f(x) = x^2$.

- What is the derivative $\partial_x f(x)$?
- What is the function value at $x = 3$?
- Use linearization to estimate the function value at $x = 3.1$. What is the true value at $x = 3.1$?

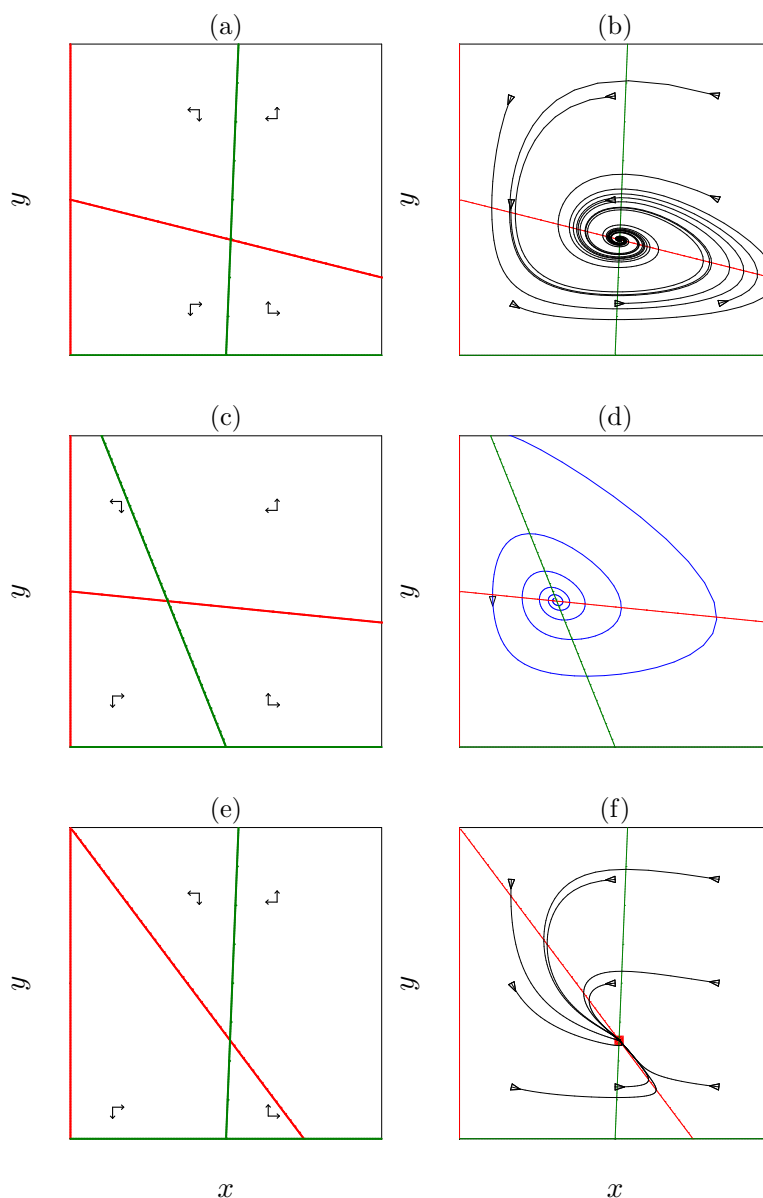


Figure 16.5: Qualitatively different steady states determined by the local vector field in the four regions defined by the nullclines. Spiral points (a-d): the vector field suggests rotation. The spiral point in (a,b) is stable which can be guessed because increasing x at the steady states makes $dx/dt < 0$ and increasing y at the steady states makes $dy/dt < 0$ (which is stabilizing). The spiral in (c,d) is unstable which can be guessed because increasing y at the steady states makes $dy/dt < 0$ (which is stabilizing). Panels (e & f) illustrate that nodes can also have a rotating vector field, i.e., that one cannot tell with certainty from the local field whether or not a steady state is a spiral point.

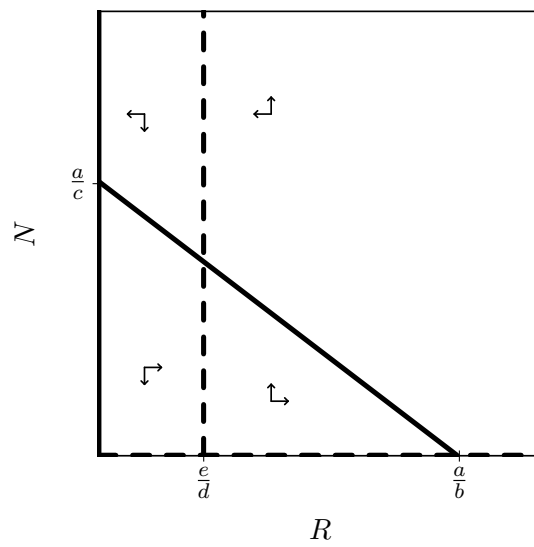


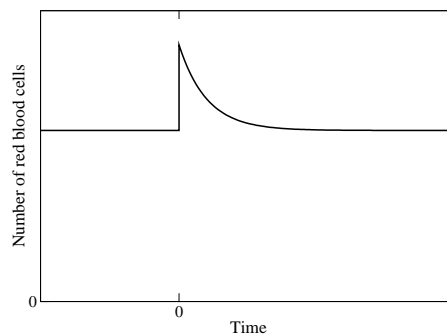
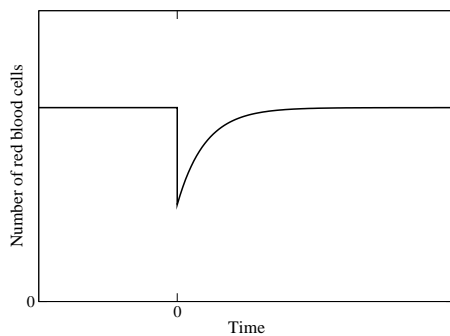
Figure 16.6: The phase space of the Lotka Volterra model with the vector field indicated by the arrows.

Chapter 17

Answers to the exercises

Question 1.1. Red blood cells

A possible good answer has the following sketches:



- a. $dN/dt = m - dN$.
- b. See the sketch in Panel (a)
- c. See the sketch in Panel (b)

Question 1.2. SARS

- a. First count the total number of infected patients $I(t)$. $R_0 = 3$ in two weeks means that $\beta = 1.5$ per week. For a time scale of weeks the model therefore is $dI/dt = 1.5I - 0.5I = I$. The equation to solve is $3 \times 10^9 = I(0)e^{rt}$, where $r = (\beta - \delta) = 1$, and where one starts with one infected individual, i.e., $I(0) = 1$. Solving $3 \times 10^9 = e^t$

yields $t = 22$ weeks for the time required to have $I(t) = 3 \times 10^9$.

One could argue that it is more interesting to calculate the time required to have killed half of the population, but this is more difficult. For that one also should keep track of the total number of dead individuals $dD/dt = \delta I$. With $I(t) = e^{(\beta-\delta)t}$ and $D(0) = 0$ the solution of $dD/dt = \delta e^{(\beta-\delta)t}$ is $D(t) = \frac{\delta[e^{(\beta-\delta)t}-1]}{\beta-\delta}$. Solving $I(t) + D(t) = 3 \times 10^9$ for $\beta = 1.5$ and $\delta = 0.5$ per week gives a total time of $t = 21$ weeks. The difference is small because the number of dead patients approaches a fixed fraction $\frac{\delta}{\beta-\delta} = 0.5$ of the total number of patients that are alive.

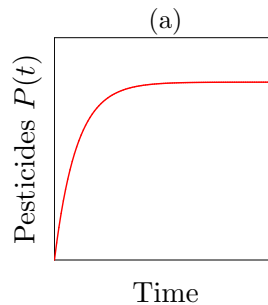
- b. No, it will go slower because the epidemic will limit itself by depleting the number of susceptibles. A better model is to add an ODE for the susceptibles, S , where $S(0) = 6 \times 10^9$ is the initial population size. Redefining β as the chance to meet and infect a susceptible person the model becomes

$$\frac{dI}{dt} = \beta IS - \delta I \quad \text{and} \quad \frac{dS}{dt} = -\beta IS .$$

Another improvement of the model that would slow down the epidemic is to allow for an incubation period, i.e., to introduce a time lag in the two week period during which patients are not yet infective.

Question 1.3. Pesticides on apples

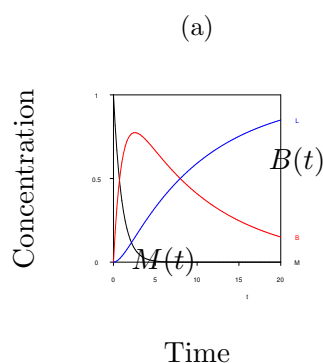
A possible good answer has the following sketch:



- a. See the sketch in Panel (a)
 b. $\bar{P} = \sigma/\delta$.
 c. The model becomes $dP/dt = -\delta P$ with the initial condition $P(0) = \sigma/\delta$. Solving $P(0)/2 = P(0)e^{-\delta t}$ yields $t_{1/2} = \ln[2]/\delta$.
 d. From $dP/dt = 2\sigma - \delta P$ with $\bar{P} = 2\sigma/\delta$, one obtains the same $\ln 2/\delta$ days for the half life.
 e. From $50 = \ln 2/\delta$ one obtains $\delta = 0.014$ per day.

Question 1.4. Injecting anesthesia

A possible good answer has the following sketch:



- See the sketch in Panel (a)
- $\ln 2/e$ time steps
- No, it all depends on the clearance rate from the blood. If c is small one should wait longer than $\ln 2/e$ time steps.
- For $\delta = 0$ everything ends up in the liver: $L(\infty) = M(0)$.

Question 1.5. Chemical reactions

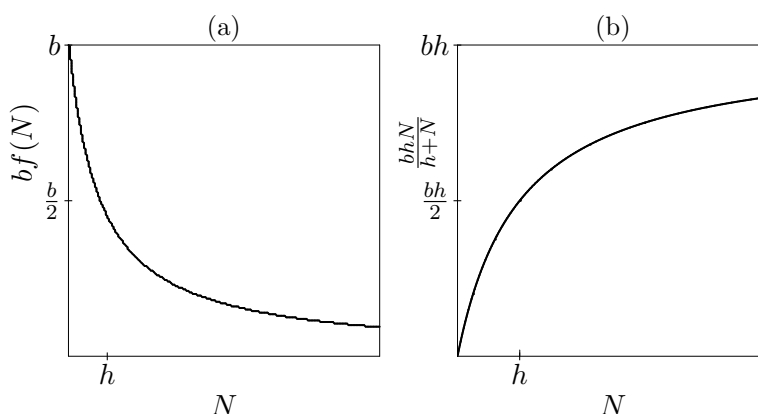
- $dA/dt = k_1AS - k_2AB - 2k_3E_1A^2$ and $dB/dt = k_2AB - k_4BE_2$.

Question 1.6. Physics

- The dimension of v is m/s and that of a is m/s^2 .
- The derivative of the $v(t)$ solution is $dv/dt = a$ and that of the $x(t)$ solution is $dx/dt = at + v(0)$.
- The amount of nitrogen in the moorland obeys $dN/dt = cA$ where A is the amount of nitrogen in the air, and c is the fraction that drops out onto the moorland. The amount of nitrogen in the air is given by $dA/dt = \alpha$ or $A(t) = A(0) + \alpha t$, where α is the slope with which nitrogen in the air increases.

Question 2.1. Density dependent growth

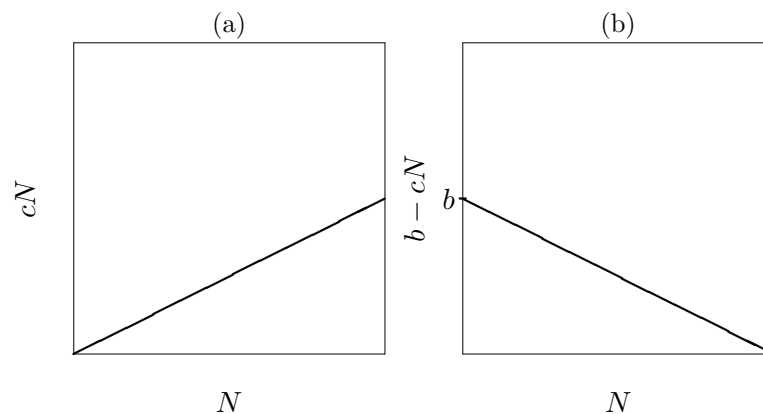
A possible good answer has the following sketches:



- a. See the sketch in Panel (a).
 b. The population growth is $\frac{bN}{1+N/h} = \frac{bhN}{h+N}$, which approaches the horizontal asymptote bh . See the sketch in Panel (b).
 c. $N = 0$ and $N = h(b-d)/d$
 d. $R_0 = b/d$ and $N = h(R_0 - 1)$.
 e. Yes: $1/(1 + N/h)$ is the same as $h/(h + N)$ which is a declining Hill function with for $n = 1$.

Question 2.2. Density dependent death

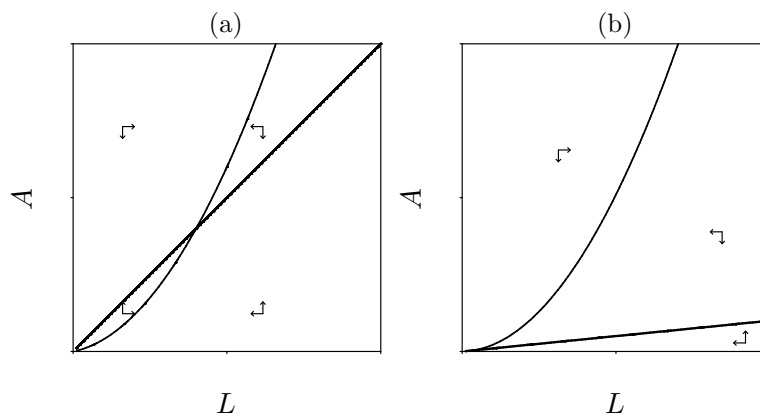
A possible good answer has the following sketches:



- a. See the sketch in Panel (a)
 b. See the sketch in Panel (b)
 c. $\bar{N} = b/c$.
 d. Because there is no generation time.
 e. The derivative with respect to N is $b - 2cN$. Substituting $N = b/c$ yields $\lambda = -b < 0$. Thus the return time $T_R = 1/b$ is fully determined by the birth rate and is independent of the density dependent death rate c .

Question 2.3. Growth of insects

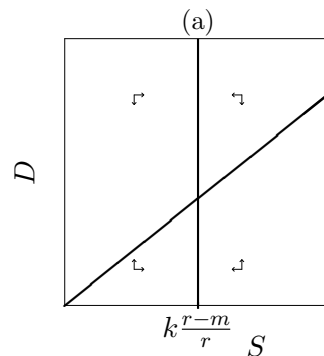
A possible good answer has the following sketches:



- a. aA : adults reproducing into larvae, $dL(1+eL)$: density dependent death of the larvae, cL : larvae mature into adults, δA : death of the adults.
- b. $dL/dt = 0$ gives the parabola $A = \frac{d+c}{a}L + \frac{de}{a}L^2$, and $dA/dt = 0$ gives the straight line $A = (c/\delta)L$. There are two possibilities; see Panels (a) and (b).
- c. Panel (a) $(0,0)$: unstable, non-trivial: stable node, Panel (b) $(0,0)$: stable.

Question 2.4. Stem cells

A possible good answer has the following sketch:



- a. $dS/dt = rS(1 - S/k) - mS$
- b. $dD/dt = mS - \delta D$
- c. The $dS/dt = 0$ nullcline is independent of D , and is a line at $S = k(r - m)/r$. The $dD/dt = 0$ nullcline is a diagonal line through the origin: $D = (m/\delta)S$. See the sketch in Panel (a). The vector field shows that the equilibrium is stable.

Question 2.5. Freitas

- a. No, the steady state of $dB/dt = m - dB$ is $\bar{B} = m/d$. In such a model the number of peripheral B cells is proportional to the number of bone marrow precursors (which determines m).

- b. For instance with density dependent death, $dB/dt = m - dB(1 + eB)$, or with density dependent production, $dB/dt = m/(1 + eB) - dB$.
- c. Yes clearly, in the absence of homeostasis the steady number of peripheral B cells is proportional to the number of bone marrow precursors.
- d. No, it is accounting for a steady state, but not for density dependent population regulation.

Question 2.6. Negative birth

In the text we derived that the non-trivial steady state is located at $\bar{N} = k(1 - 1/R_0)$ which is less than k . At the equilibrium point we therefore have a positive birth rate. Note that this should always be the case because there can be no equilibrium point when both the birth rate and the death rate have a negative contribution to the population size.

Question 2.7. Logistic growth

- a. $N = K$
- b. $rN(1 - N/K) = rN - (r/K)N^2$ and $[b(1 - N/k) - d]N = (b - d)N - (b/k)N^2$. Setting $r = (b - d)$ and $r/K = b/k$ (i.e., $K = kr/b$) makes the two models identical.
- c. $[b - d(1 + N/k)]N = (b - d)N - (d/k)N^2$. Setting $r = (b - d)$ and $r/K = d/k$ (i.e., $K = kr/d$) makes the two models identical.

Question 2.8. Red blood cells

- a. If P is the erythropoietin concentration, it should drop with the number of erythrocytes, i.e., with the oxygen level. One could model this with a simple decreasing function and write $P = 1/(1 + [B/h]^k)$. For simplicity we could assume that the daily production is proportional to P , and write $dB/dt = mP - dB$, where $d = 1/120$ per day.
- b. For $k = 1$, i.e., $P = 1/(1 + B/h)$ the model is identical to Eq. (2.2). The steady state is the positive root of the quadratic equation solved in the text.
- c. The dependence of the steady state level on the bone marrow production m is less than linear because m is part of the $\sqrt{\quad}$ term. For higher Hill-coefficients the dependence becomes even weaker.

Question 2.9. Naive T cell renewal

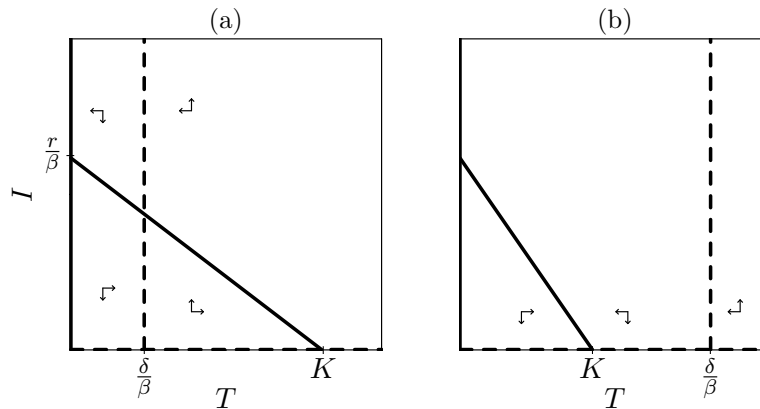
- a. $dN/dt = s(t) + \frac{pN}{1 + N/k} - dN$
- b. Solving $0 = s + (s/k)N + pN - dN - (d/k)N^2$ yields $N = \frac{s + pk - dk \pm \sqrt{(s + pk - dk)^2 - 4dsk}}{2d}$. The negative root is not physically meaningful. The fact that the model has a unique steady state level for the naive T cell counts supports its feasibility.

Question 2.10. Tumor growth

- a. $dT/dt = b\sqrt{T} - dT$
- b. $\sqrt{T} = b/d$.
- c. plot $b\sqrt{T}/T = b/\sqrt{T}$ as a function of T . This is a hyperbolic graph having the x-axis and the y-axis as asymptotes. Per capita growth thus goes to infinity when the tumor is small.

Question 3.1. Lotka Volterra model

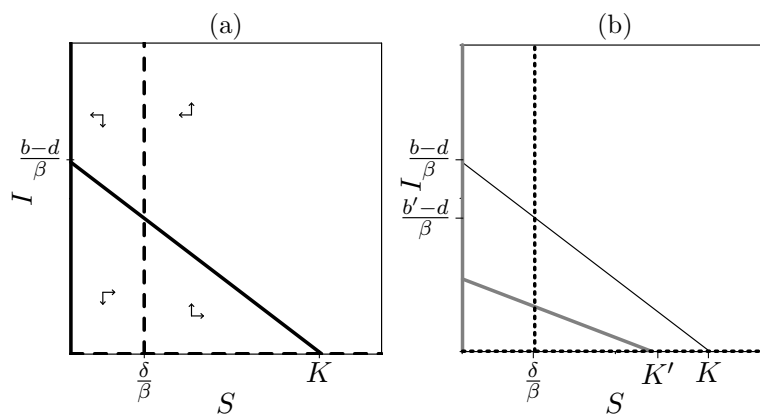
A possible good answer has the following sketches:



- $\frac{dT}{dt} = rT(1 - T/K) - \beta TI$ and $\frac{dI}{dt} = \beta TI - \delta I$ The R_0 of the infection is $R_0 = (\beta K)/\delta_I$
- $(0, 0)$, $(K, 0)$ and $(K/R_0, \frac{r}{\beta}(1 - \frac{1}{R_0}))$.
- See the sketches in Panel (a) and (b).

Question 3.2. Seals

This is basically a Lotka-Volterra model with explicit parameter for the death of the seals. A possible good answer has the following sketches:



- $S = 0$ and $S = K = k(1 - d/b)$.
- $R_0 = b/d$. For the infection $R_0 = \beta K/\delta$ where $K = k(1 - d/b)$ is the carrying capacity of the seals.
- $S = 0$ and $S = k(1 - 1/R_0)$
- Let $b' = b/2$ then $S = k(1 - d/b')$ is the new steady state.
- $S = \delta/\beta$

- f. Not changed: b' is not influencing $S = \delta/\beta$
- g. The situation with a chronic infection is sketched in Panel (a). These are the Lotka-Volterra nullclines: stability is the same.
- h. The nullclines in the presence and absence of PCBs are sketched in Panel (b).

Question 3.3. Solving the steady state

First find the equation from which can solve B most easily. This is $dC/dt = 0 = eBC - fC$ yielding $\bar{B} = f/e$.

Question 3.4. Viral fitness

The steady state is the same as that of Eq. (3.1) when one substitutes $\beta' = f\beta$.

- a. $\bar{T} = \frac{\delta_I}{f\beta}$ and $\bar{I} = \frac{\sigma}{\delta_I} - \frac{\delta_T}{f\beta}$.
- b. The viral load obeys the function $y = a - b/x$, which approach the asymptote $a = \sigma/\delta_I$ when the fitness is low. We need not expect a large change in viral load when the fitness changes.
- c. Changing viral fitness has a much larger effect on the target cell density. Viruses with a poor fitness cause less target cell depletion and therefore approach higher loads than would intuitively be expected.

Question 4.1. Host-parasite model

Question 4.2. Immune control

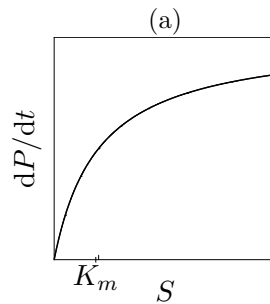
- a. the steady state of I does not contain the β parameter. Ultimately the viral load should return the pretreatment level.
- b. Yes, Eq. (3.5) shows that the target cell levels go up.

Question 4.3. Oscillations

- a. Yes this model is capable of periodic oscillations when the steady state is stable. It can give transient oscillations when the equilibrium point is a stable spiral.
- b. The simpler model can also account for transient oscillations because the steady state can also be a stable spiral.

Question 5.1. Michaelis Menten

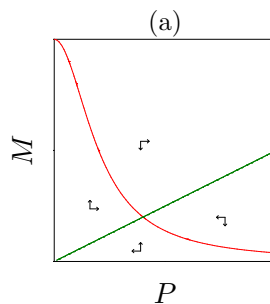
A possible good answer has the following sketch:



- a. $dC/dt = k_1ES - (k_{-1} + k_2)C = k_1(E_0 - C)S - (k_{-1} + k_2)C$ and $dP/dt = k_2C$
 b. $dC/dt = 0 = k_1E_0S - (k_1S + k_{-1} + k_2)C$ and $C = \frac{E_0S}{K_m + S}$ where $K_m = \frac{k_{-1} + k_2}{k_1}$.
 c. $dP/dt = \frac{k_2E_0S}{K_m + S}$
 d. See the sketch in Panel (a).
 e. $dS/dt = -\frac{k_2E_0S}{K_m + S}$

Question 5.2. mRNA

A possible good answer has the following sketch:



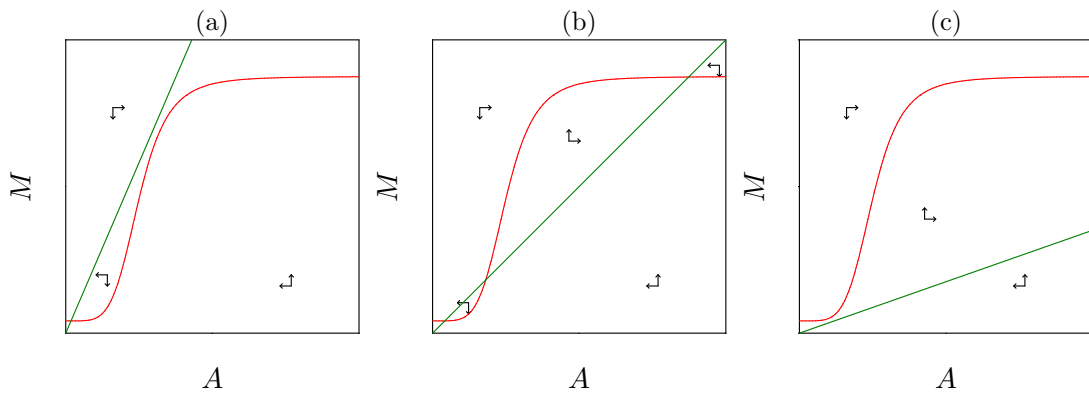
The new model is

$$\frac{dM}{dt} = \frac{c}{1 + P^2} - dM \quad \frac{dP}{dt} = lM - \delta P$$

- a. The $dM/dt = 0$ nullcline now is $M = \frac{c/d}{1 + P^2}$ which is a decreasing sigmoid function. The $dP/dt = 0$ nullclines remains the same. See the sketch in Panel (a).
 b. The vector field shows that it is a stable node
 c. $dP/dt = \frac{lc/d}{1 + P^2} - \delta P$

Question 5.3. Lac-operon

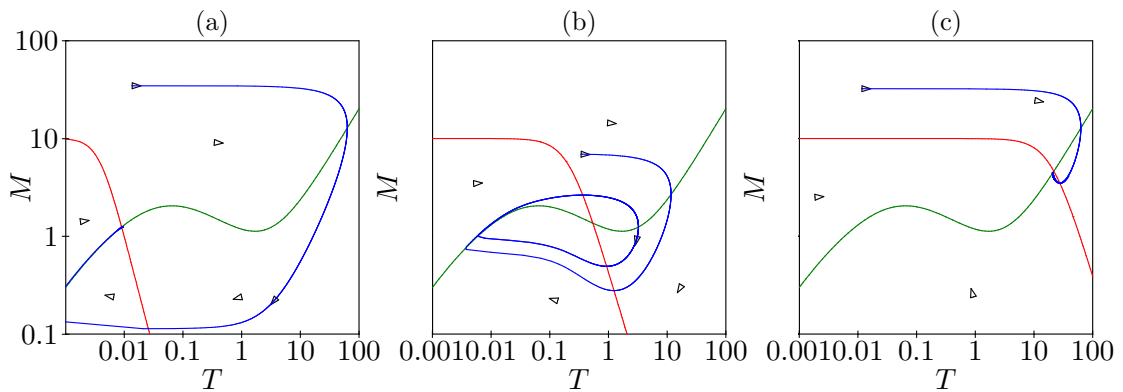
A possible good answer has the following sketches:



- a. The model becomes $dA/dt = ML - \delta A$, which has $M = (\delta/L)A$ as the allolactose nullcline. This is a diagonal line through the origin. The mRNA nullcline remains the same. There are three possibilities; see Panels (a-c).
- b. Left panel: stable node; Middle panel: two stable nodes one saddle point. Right panel: stable node (sorry: not visible).
- c. $dA/dt = \frac{c_0L}{d} + \frac{(c/d)LA^n}{1+A^n} - \delta A$

Question 6.1. Tyson model

A possible good answer has the following sketches:



- a. Three situations, made by setting $P_c = 0.001, P_c = 0.1$ and $P_c = 10$ are depicted in Panels (a)–(c).

- b. None of the steady states is a saddle point. The steady state in the middle can be unstable because of the positive feedback of T on itself. The steady states in the left and right panels are stable because the feedbacks of T and M on themselves are negative.
- c. See the phase spaces.

Question 6.2. Goldbeter

As yet, no answer is available.

Question 6.3. Michaelis-Menten

- a. For $i = 1, 2$ one writes

$$\frac{dC_i}{dt} = k_i S_i (E_0 - C_1 - C_2) - C_i (k_{-i} + p_i) \quad \text{and} \quad \frac{dS_i}{dt} = -k_i S_i (E_0 - C_1 - C_2) + k_{-i} C_i,$$

- b. Solving $dC_i/dt = 0$ yields

$$C_1 = \frac{S_1(E_0 - C_2)}{S_1 + K_1} \quad \text{and} \quad C_2 = \frac{S_2(E_0 - C_1)}{S_2 + K_2}$$

where $K_i = \frac{k_{-i} + p_i}{k_i}$. Substituting C_1 into the C_2 equation yields:

$$\begin{aligned} C_2(S_2 + K_2) &= S_2 E_0 - \frac{S_1 S_2 (E_0 - C_2)}{S_1 + K_1} \\ C_2(S_2 + K_2)(S_1 + K_1) &= S_2 E_0 (S_1 + K_1) - S_1 S_2 E_0 + S_1 S_2 C_2 \\ C_2 &= \frac{K_1 S_2 E_0}{K_1 K_2 + S_2 K_1 + S_1 K_2} \\ C_2 &= \frac{S_2 E_0}{K_2 + S_2 + S_1 K_2 / K_1}. \end{aligned}$$

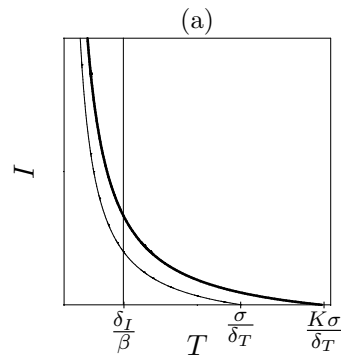
Because of the symmetry of the problem this implies

$$C_1 = \frac{S_1 E_0}{K_1 + S_1 + S_2 K_1 / K_2}.$$

For the substrates one adds dC_i/dt to dS_i/dt to obtain $dS_i/dt = -p_i C_i$.

Question 7.1. CD4⁺ T cells

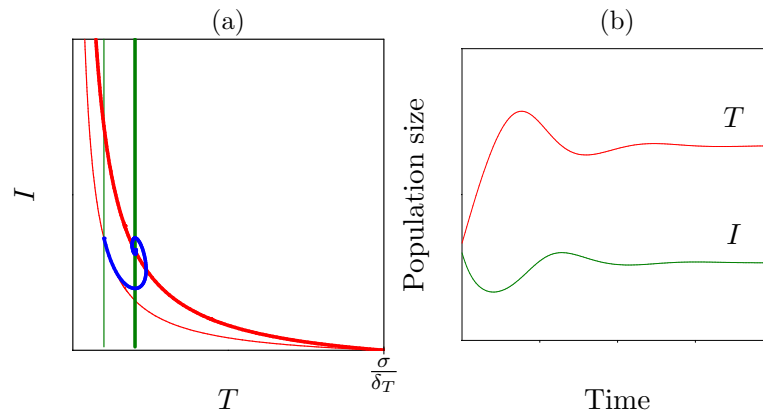
A possible good answer has the following sketch:



- a. $dT/dt = K\sigma - \delta_T T - \beta TI$, $dI/dt = \beta TI - \delta_I I$, where $K > 1$ implements an increase in $CD4^+$ T cell production.
- b. we base our expectation on the nullclines shown in Panel (a), where the heavy lines denote the nullclines during treatment. One can see that the new steady state lies at the same $CD4^+$ T cell count.
- c. Reduce (!) $CD4^+$ T cell production to $K\sigma/\delta_T = \delta_I/\beta$.
- d. The count remains $T = \delta_I/\beta$.

Question 7.2. Rebound

A possible good answer has the following sketches:



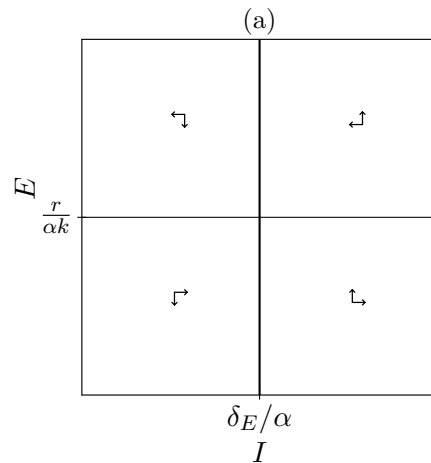
- a. See the sketch in Panel (a): light nullclines before and heavy nullclines during treatment.
- b. See the phase space in Panel (a).
- c. See the sketch in Panel (b)
- d. No

Question 7.3. Immune control

- a. the steady state of I does not contain the β parameter. Ultimately the viral load should return the pretreatment level.

- b. Yes, target cell levels go up.

Question 7.4. Ogg *et al.*, 1998

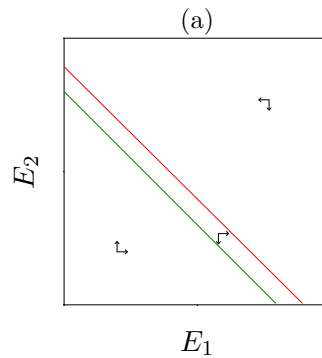


- a. $V = (p/\delta_V)I$ which by substitution yields $dI/dt = rI - \alpha kEI$, where $r = p\beta/\delta_V - \delta_I$.
 b. See the sketch in Panel (a). The heavy line is the $dE/dt = 0$ nullcline; the light the $dI/dt = 0$ nullcline.
 c. $I = \delta_E/\alpha$ and $E = r/(\alpha k)$
 d. Because both are inversely related to α they should be positively correlated when α varies between patients.

Question 7.5. Competitive exclusion

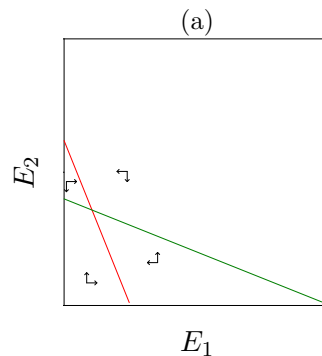
- a. $\bar{I} = \delta_E/\alpha_1$.
 b. $\bar{I} = \delta_E/\alpha_2$.
 c. No.
 d. $dE_2/dt = \delta_E E_2 (\alpha_2/\alpha_1 - 1) < 0$ because $\alpha_2/\alpha_1 < 1$. The second immune response declines when $dE_1/dt = 0$.

Question 8.1. Saturated proliferation



- a. $dE_1/dt = \frac{pE_1A}{h_1+A} - dE_1 = 0$ yields $E_1 = 0$ and $pA - dh_1 - dA = 0$ or $A = \frac{dh_1}{p-d} = 1 - kE_1 - kE_2$. Solving for E_2 yields $E_2 = 1/k - \frac{dh_1}{k(p-d)} - E_1$. Repeating this for $dE_2/dt = 0$ yields $E_2 = 1/k - \frac{dh_2}{k(p-d)} - E_1$. Thus, both nullclines have a slope of -1 in the phase space depicted in Panel (a).
- b. No, parallel nullclines cannot intersect
- c. Hardly any difference: competitive exclusion

Question 8.2. Competitive proliferation



- a. Solving $dE_1/dt = \frac{pE_1A}{1+c_1E_1} - dE_1 = 0$ yields $E_1 = 0$ and $p(1 - kE_1 - kE_2) = d + dc_1E_1$. Expressing this in terms of E_2 gives $E_2 = \frac{p-d}{pk} - \frac{pk+dc_1}{pk} E_1$. The $dE_2/dt = 0$ nullcline yields $p(1 - kE_1 - kE_2) = d + dc_2E_2$ or $E_2 = \frac{p-d}{pk+dc_2} - \frac{pk}{pk+dc_2} E_1$. In a phase space with E_2 on the vertical axis, the slope of the $dE_2/dt = 0$ nullcline is larger than -1 , and the slope of the $dE_1/dt = 0$ nullcline is less than -1 . The nullclines in Panel (a) are straight lines with different slopes.
- b. Yes, the nullclines can intersect in a stable node.
- c. Due to the intra-specific competition coexistence is possible: T cells are directly competing for APCs.

Question 8.3. Virus competition experiments

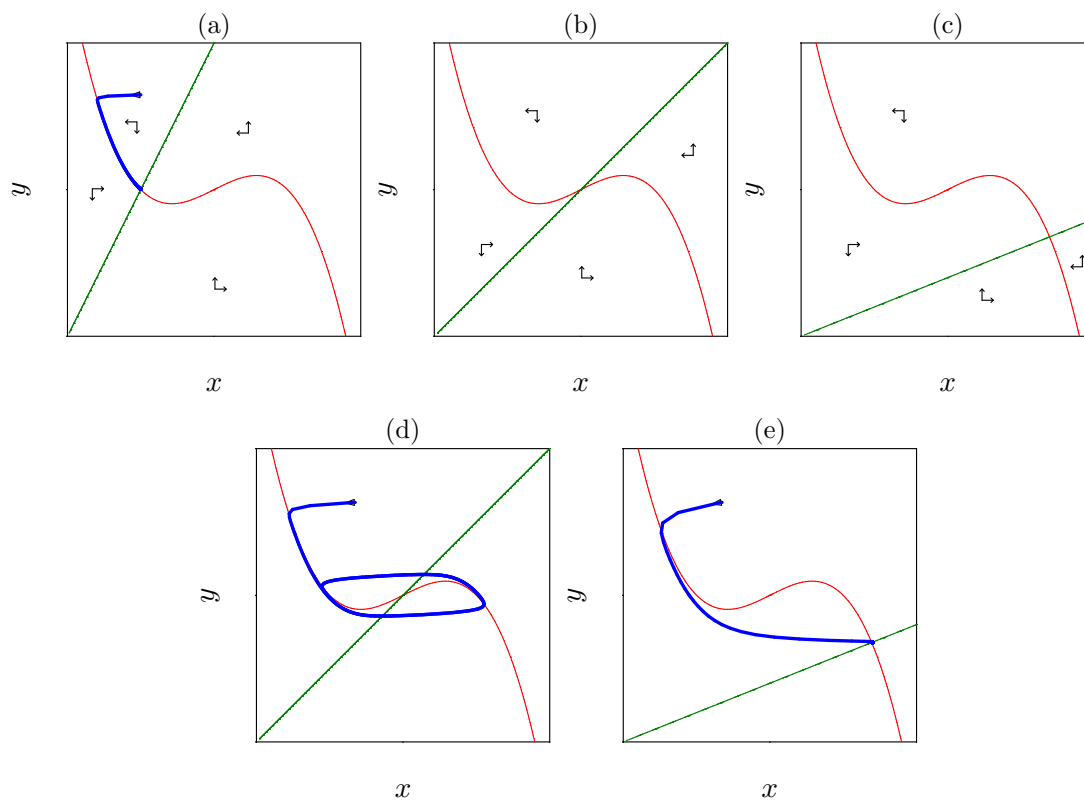
a. When $\rho(t) \equiv V_2(t)/V_1(t)$, the derivative $d\rho/dt \equiv \rho'$ obeys

$$\begin{aligned} \frac{d\rho}{dt} &= \frac{V_2'V_1 - V_1'V_2}{V_1^2}, \\ &= \frac{r(1+s)V_2V_1 - rV_1V_2}{V_1^2}, \\ &= r s \rho. \end{aligned}$$

b. Since $d\rho/dt = r s \rho$ has the solution $\rho(t) = \rho(0)e^{rst}$, the natural logarithm of the ratio plotted in time should be a straight line with slope rs . Note that this slope is not reflecting the relative fitness, s , but the difference in the growth rate, rs (Marée *et al.*, *J. Virol.*, 2001).

Question 9.1. Time scales

A possible good answer has the following sketches:



a. For the stability of the steady state we note that $dx/dt < 0$ when we increase x , and that $dy/dt < 0$ when we increase y . Since this cannot be a saddle point, it should be stable.

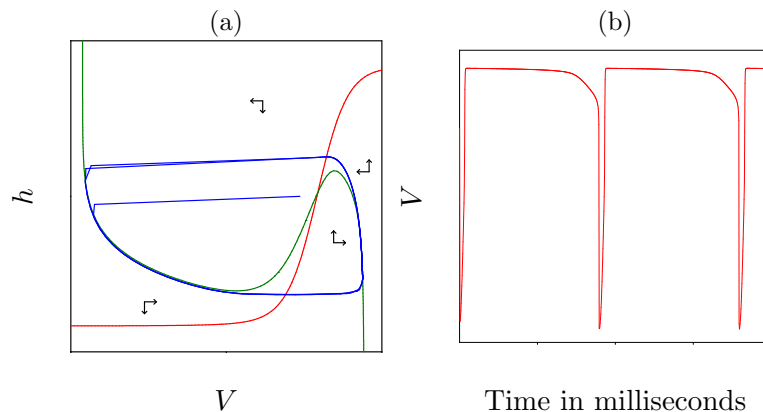
- b. The a parameter: note that $dy/dt = kSx$, and hence $a = kS$.
- c. Because the $dy/dt = 0$ nullcline is given by $y = (a/b)x$, its slope is proportional to a . The $dx/dt = 0$ nullcline is independent of a .
- d. The two possibilities are depicted in Panels (b) and (c).
- e. Increasing x now makes $dx/dt > 0$ which is a destabilizing local positive feedback. Indeed, due to the large difference in time scales we can conclude from the vector field that the steady state is unstable. In the right panel increasing x or y makes $dx/dt < 0$ or $dy/dt < 0$, respectively. Since this cannot be a saddle point, the steady state should be stable.
- f. The trajectories are depicted in Panels (d) and (e).

Question 9.2. Inhibition

The h_∞ line gives for every voltage the equilibrium value of h . The $dh/dt = 0$ nullcline is the set of h and V values where $dh/dt = 0$. That is the same.

Question 9.3. Hodgkin Huxley

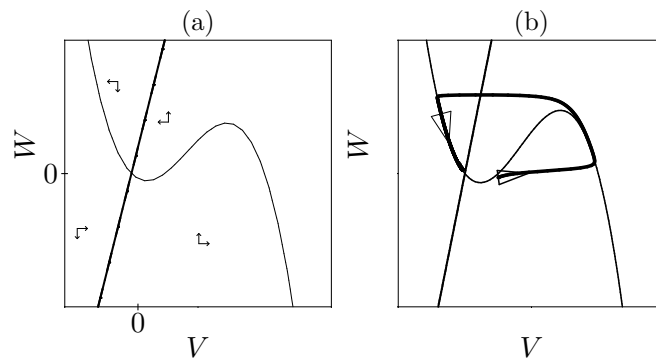
A possible good answer has the following sketches:



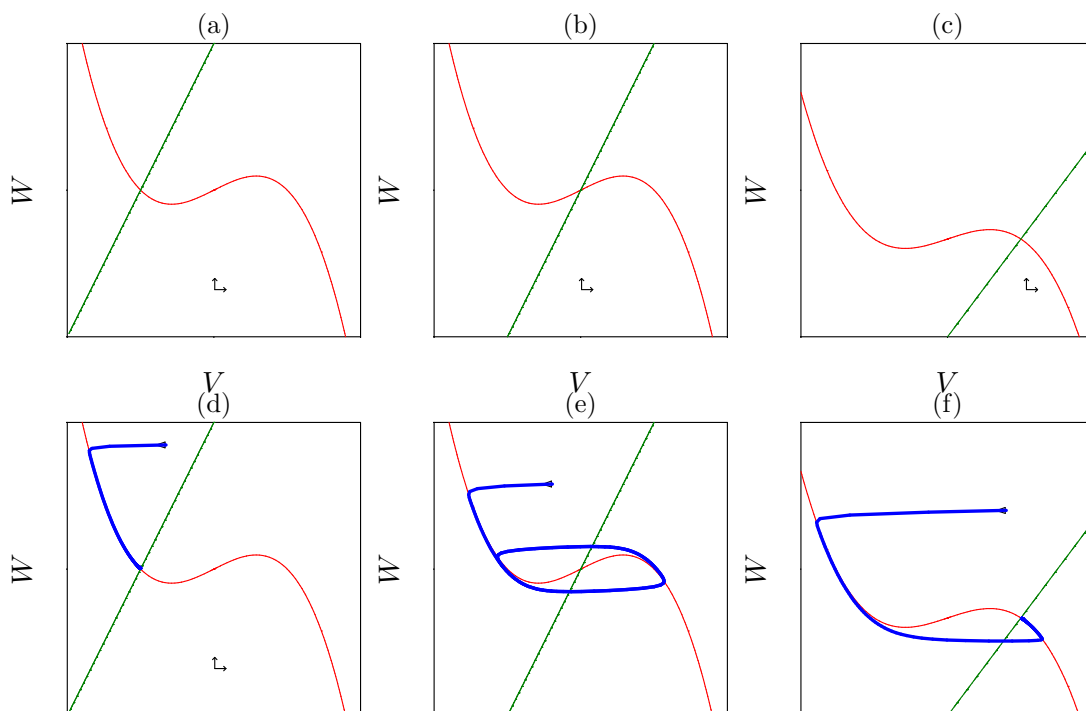
- a. The vector field is indicated in the phase space in Panel (a). This is not a saddle-point, and increasing V makes $dV/dt > 0$, which is a destabilizing positive feedback. Because we know that h is slow one can see from the vector field that the steady state is unstable.
- b. See the sketch in Panel (a).
- c. See the sketch in Panel (b).
- d. A neuron firing spontaneously

Question 9.4. FitzHugh-Nagumo model

A possible good answer has the following sketches:



- See the sketch in Panel (a).
- This is not a saddle-point and both in the horizontal (V) and vertical (W) direction there is a negative feedback: the steady state should be stable.
- See the sketch in Panel (b).
- Yes, very much.
- Yes, although it is not mechanistic, the model is attractively simple, and has very similar behavior.
- With an external input the nullclines become:



For $a = 0.5$, $b = 1$, $\epsilon = 0.01$ we get for $i = 0$ the phase space of Panels (a) and (d). For $i = 0.5$ we get those of Panels (b) and (e), and for $i = 1$ one gets those of Panels (c) and (f).

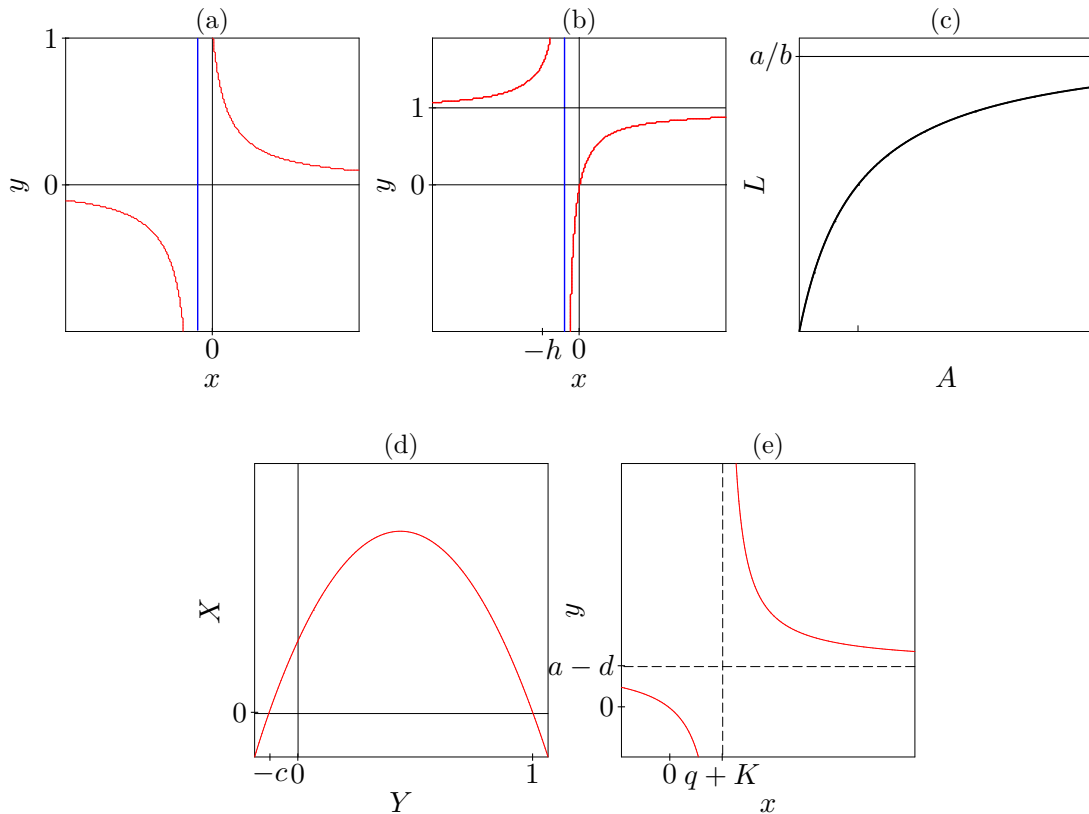
- No of the three steady states is a saddle-point. Only in the middle picture (b,e) there

is a positive feedback because increasing V makes $dV/dt > 0$. This is not so in the other two. Because of the large difference in time scales one can see that the steady state is unstable.

h. See Panels (d)–(f).

Question 16.1. Sketch a few functions

A possible good answer has the following sketches:



- $y = \frac{h}{h+x} = 1$ when $x = 0$. For $x \rightarrow \infty, y \rightarrow 0$. For $x \rightarrow -\infty, y \rightarrow 0$. There is a vertical asymptote at $x = -h$. See the sketch in Panel (a).
- $y = \frac{x}{h+x} = 0$ when $x = 0$. For $x \rightarrow \infty, y \rightarrow 1$. For $x \rightarrow -\infty, y \rightarrow 1$. There is a vertical asymptote at $x = -h$. See the sketch in Panel (b).
- $L = \frac{aA}{c+bA}$ with horizontal asymptote $L = a/b$ or $A = \frac{cL}{a-bL}$ with vertical asymptote $L = a/b$. See the sketch in Panel (c).
- Write $Y = 0$ and $X = (a/b)(1 - Y)(c + Y)$. See the sketch in Panel (d).
- Intersection with x -axis: $x = \frac{ak-dq-dk}{a-d}$, intersection with y -axis: $y = \frac{ak}{q+k} - d$. Horizontal asymptote: $y = a - d$, and vertical asymptote: $x = q + k$. See the sketch in Panel (e), where the dashed lines denote the two asymptotes.

f.

Question 16.2. Linearization

a. $\partial_x x^2 = 2x$

b. For $x = 3$ one obtains $x^2 = 9$

c. $y = 9 + 0.1 \times 2 \times 3 = 9.6$. The true value is $3.1^2 = 9.61$.

Chapter 17

Credits

The first part of Chapter 6 describes the stable limit cycles occurring in classical predator-prey, or host-parasite models; the second part describes the model by Tyson *et al.* (1999). Chapter 9 is copied from our Theoretical Biology course given to biology students. Chapter 11 was based upon the work of Hazenberg *et al.* (2000) and Dutilh & De Boer (2003). Chapter 10 is based upon the work of Borghans *et al.* (1998). The first part of Chapter 12 was largely based upon the work of Borghans *et al.* (1999); the second part on MHC diversity comes from an unpublished manuscript by Borghans *et al.* (2003).

Bibliography

- ADLER, F. R. (1997). *Modeling the Dynamics of Life. Calculus and Probability for Life Scientists*. Pacific Grove: Brooks/Cole.
- AGENES, F., ROSADO, M. M. & FREITAS, A. A. (1997). Independent homeostatic regulation of B cell compartments. *Eur. J. Immunol.* **27**, 1801–1807.
- ARSTILA, T. P., CASROUGE, A., BARON, V., EVEN, J., KANELLOPOULOS, J. & KOURILSKY, P. (1999). A direct estimate of the human alphabeta T cell receptor diversity. *Science* **286**, 958–961.
- BARKAI, N. & LEIBLER, S. (2000). Circadian clocks limited by noise. *Nature* **403**, 267–268.
- BELAIR, J., MACKEY, M. C. & MAHAFFY, J. M. (1995). Age-structured and two-delay models for erythropoiesis. *Math. Biosci.* **128**, 317–346.
- BLATTMAN, J. N., ANTIA, R., SOURDIVE, D. J., WANG, X., KAECH, S. M., MURALI-KRISHNA, K., ALTMAN, J. D. & AHMED, R. (2002). Estimating the precursor frequency of naive antigen-specific CD8 T cells. *J. Exp. Med.* **195**, 657–664.
- BONHOEFFER, S., COFFIN, J. M. & NOWAK, M. A. (1997). Human immunodeficiency virus drug therapy and virus load. *J. Virol.* **71**, 3275–3278.
- BORGHANS, J. A. M., DE BOER, R. J. & SEGEL, L. A. (1996). Extending the quasi-steady state approximation by changing variables. *Bull. Math. Biol.* **58**, 43–63.
- BORGHANS, J. A. M., DE BOER, R. J., SERCARZ, E. & KUMAR, V. (1998). T cell vaccination in experimental autoimmune encephalomyelitis: a mathematical model. *J. Immunol.* **161**, 1087–1093.
- BORGHANS, J. A. M., NOEST, A. J. & DE BOER, R. J. (1999). How specific should immunological memory be? *J. Immunol.* **163**, 569–575.
- BORGHANS, J. A. M., NOEST, A. J. & DE BOER, R. J. (2003). Thymic selection does not limit the individual MHC diversity. *Eur. J. Immunol.* **33**, 3353–3358.

- BRACIAK, T. A., PEDERSEN, B., CHIN, J., HSIAO, C., WARD, E. S., MARICIC, I., JAHNG, A., GRAHAM, F. L., GAULDIE, J., SERCARZ, E. E. & KUMAR, V. (2003). Protection against experimental autoimmune encephalomyelitis generated by a recombinant adenovirus vector expressing the V β 8.2 TCR is disrupted by coadministration with vectors expressing either IL-4 or -10. *J. Immunol.* **170**, 765–774.
- BURROUGHS, N. J., DE BOER, R. J. & KESMIR, C. (2004). Discriminating self from nonself with short peptides from large proteomes. *Immunogenetics.* **56**, 311–320.
- CAMPBELL, N. A. & REECE (2002). *Biology, sixth edition*. Redwood city CA: Benjamin/Cummings.
- CAMPBELL, N. A. & REECE (2005). *Biology, Seventh edition*. San Francisco, CA: Pearson/BenjaminCummings.
- CAMPBELL, N. A. & REECE, J. B. (2008). *Biology, Eighth edition*. San Francisco, CA: Pearson/BenjaminCummings.
- CLARK, D. R., DE BOER, R. J., WOLTERS, K. C. & MIEDEMA, F. (1999). T cell dynamics in HIV-1 infection. *Adv. Immunol.* **73**, 301–327.
- DE BOER, R. J. (2006). Estimating the role of thymic output in HIV infection. *Curr. Opin. HIV AIDS* **1**, 16–21.
- DE BOER, R. J., FREITAS, A. A. & PERELSON, A. S. (2001). Resource competition determines selection of B cell repertoires. *J. theor. Biol.* **212**, 333–343.
- DE BOER, R. J. & PERELSON, A. S. (1993). How diverse should the immune system be? *Proc. R. Soc. Lond., B, Biol. Sci.* **252**, 171–175.
- DE JONG, M. D., VEENSTRA, J., STILIANAKIS, N. I., SCHURMAN, R., LANGE, J. M., DE BOER, R. J. & BOUCHER, C. A. (1996). Host-parasite dynamics and outgrowth of virus containing a single K70R amino acid change in reverse transcriptase are responsible for the loss of human immunodeficiency virus type 1 RNA load suppression by zidovudine. *Proc. Natl. Acad. Sci. U.S.A.* **93**, 5501–5506.
- DOUEK, D. C., MCFARLAND, R. D., KEISER, P. H., GAGE, E. A., MASSEY, J. M., HAYNES, B. F., POLIS, M. A., HAASE, A. T., FEINBERG, M. B., SULLIVAN, J. L., JAMIESON, B. D., ZACK, J. A., PICKER, L. J. & KOUP, R. A. (1998). Changes in thymic function with age and during the treatment of HIV infection. *Nature* **396**, 690–695.
- DUTILH, B. & DE BOER, R. J. (2003). Decline in excision circles is no evidence for homeostatic renewal of naive T cells. *J. theor. Biol.* **224**, 351–358.
- EDELSTEIN-KESHET, L. (1988). *Mathematical Models in Biology*. New York: Random House.

- FITZHUGH, R. (1960). Thresholds and plateaus in the Hodgkin-Huxley nerve equations. *J. Gen. Physiol.* **43**, 867–896.
- GAUR, A., RUBERTI, G., HASPEL, R., MAYER, J. P. & FATHMAN, C. G. (1993). Requirement for CD8⁺ cells in T cell receptor peptide-induced clonal unresponsiveness. *Science* **259**, 91–94.
- GOLDBETER, A. (1996). *Biochemical Oscillations and cellular Rhythms. The molecular bases of periodic and chaotic behaviour*. Cambridge: Cambridge U.P.
- GOLDBETER, A. (2002). Computational approaches to cellular rhythms. *Nature* **420**, 238–245.
- GOLDING, I. & COX, E. C. (2006). Eukaryotic transcription: what does it mean for a gene to be 'on'? *Curr. Biol.* **16**, R371–R373.
- GOLDING, I., PAULSSON, J., ZAWILSKI, S. M. & COX, E. C. (2005). Real-time kinetics of gene activity in individual bacteria. *Cell* **123**, 1025–1036.
- GRIFFITH, J. S. (1968). Mathematics of cellular control processes. II. Positive feedback to one gene. *J. theor. Biol.* **20**, 209–216.
- HAZENBERG, M. D., OTTO, S. A., STUART, J. W., VERSCHUREN, M. C., BORLEFFS, J. C., BOUCHER, C. A., COUTINHO, R. A., LANGE, J. M., DE WIT, T. F., TSEGAYE, A., VAN DONGEN, J. J., HAMANN, D., DE BOER, R. J. & MIEDEMA, F. (2000). Increased cell division but not thymic dysfunction rapidly affects the T-cell receptor excision circle content of the naive T cell population in HIV-1 infection. *Nat. Med.* **6**, 1036–1042.
- HO, D. D., NEUMANN, A. U., PERELSON, A. S., CHEN, W., LEONARD, J. M. & MARKOWITZ, M. (1995). Rapid turnover of plasma virions and CD4 lymphocytes in HIV-1 infection. *Nature* **373**, 123–126.
- HODGKIN, A. L. & HUXLEY, A. F. (1952). A quantitative description of membrane current and its application to conduction and excitation in nerve. *J. Physiol.* **117**, 500–544. Reprinted in *Bull. Math. Biol.* 1990, 52, 25–71.
- HOFER, T., NATHANSEN, H., LOHNING, M., RADBRUCH, A. & HEINRICH, R. (2002). GATA-3 transcriptional imprinting in Th2 lymphocytes: a mathematical model. *Proc. Natl. Acad. Sci. U.S.A.* **99**, 9364–9368.
- HOLLAND, J. J., DE LA TORRE, J. C., CLARKE, D. K. & DUARTE, E. (1991). Quantitation of relative fitness and great adaptability of clonal populations of RNA viruses. *J. Virol.* **65**, 2960–2967.
- JACOB, F. & MONOD, J. (1961). Genetic regulatory mechanisms in the synthesis of proteins. *J. Mol. Biol.* **3**, 318–356.

- JAMIESON, B. D., DOUEK, D. C., KILLIAN, S., HULTIN, L. E., SCRIPTURE-ADAMS, D. D., GIORGI, J. V., MARELLI, D., KOUP, R. A. & ZACK, J. A. (1999). Generation of functional thymocytes in the human adult. *Immunity* **10**, 569–575.
- JANEWAY, JR, C. A. & KATZ, M. E. (1984). Self Ia-recognizing T cells undergo an ordered series of interactions with Ia-bearing substrate cells of defined function during their development: a model. *Surv. Immunol. Res.* **3**, 45–54.
- KEENER, J. & SNEYD, J. (1998). *A mathematical introduction to medical physiology*. New York: Springer.
- KEŞMİR, C., BORGHANS, J. A. M. & DE BOER, R. J. (2000). Diversity of human $\alpha\beta$ T cell receptors. *Science* **288**, 1135a.
- KUMAR, V. & SERCARZ, E. (1996). Dysregulation of potentially pathogenic self reactivity is crucial for the manifestation of clinical autoimmunity. *J. Neurosci. Res.* **45**, 334–339.
- KUMAR, V., SERCARZ, E., ZHANG, J. & COHEN, I. (2001). T-cell vaccination: from basics to the clinic. *Trends Immunol.* **22**, 539–540.
- KUMAR, V. & SERCARZ, E. E. (1993). The involvement of T cell receptor peptide-specific regulatory CD4⁺ T cells in recovery from antigen-induced autoimmune disease. *J. Exp. Med.* **178**, 909–916.
- KUMAR, V., STELLRECHT, K. & SERCARZ, E. (1996). Inactivation of T cell receptor peptide-specific CD4 regulatory T cells induces chronic experimental autoimmune encephalomyelitis (EAE). *J. Exp. Med.* **184**, 1609–1617.
- LEWIN, S. R., RIBEIRO, R. M., KAUFMANN, G. R., SMITH, D., ZAUNDERS, J., LAW, M., SOLOMON, A., CAMERON, P. U., COOPER, D. & PERELSON, A. S. (2002). Dynamics of T cells and TCR excision circles differ after treatment of acute and chronic HIV infection. *J. Immunol.* **169**, 4657–4666.
- LIPSITCH, M., COHEN, T., COOPER, B., ROBINS, J. M., MA, S., JAMES, L., GOPALAKRISHNA, G., CHEW, S. K., TAN, C. C., SAMORE, M. H., FISMAN, D. & MURRAY, M. (2003). Transmission dynamics and control of severe acute respiratory syndrome. *Science* **300**, 1966–1970.
- MAY, R. M. (1977). Thresholds and breakpoints in ecosystems with a multiplicity of stable states. *Nature* **269**, 471–477.
- MELLORS, J. W., RINALDO, JR, C. R., GUPTA, P., WHITE, R. M., TODD, J. A. & KINGSLEY, L. A. (1996). Prognosis in HIV-1 infection predicted by the quantity of virus in plasma. *Science* **272**, 1167–1170.
- MÜLLER, V., MARÉE, A. F. & DE BOER, R. J. (2001). Small variations in multiple parameters account for wide variations in HIV-1 set-points: a novel modelling approach. *Proc. R. Soc. Lond. B. Biol. Sci.* **268**, 235–242.

- MURPHY, K. M. & REINER, S. L. (2002). Decision making in the immune system: The lineage decisions of helper T cells. *Nat. Rev. Immunol.* **2**, 933–944.
- NEUMANN, A. U., LAM, N. P., DAHARI, H., GRETCH, D. R., WILEY, T. E., LAYDEN, T. J. & PERELSON, A. S. (1998). Hepatitis C viral dynamics in vivo and the antiviral efficacy of interferon- α therapy. *Science* **282**, 103–107.
- NOVICK, A. & WEINER, M. (1957). Enzyme induction as an all-or-none phenomenon. *Proc. Natl. Acad. Sci. U.S.A.* **43**, 553–566.
- NOWAK, M. A., ANDERSON, R. M., MCLEAN, A. R., WOLFS, T. F., GOUDSMIT, J. & MAY, R. M. (1991). Antigenic diversity thresholds and the development of AIDS. *Science* **254**, 963–969.
- NOWAK, M. A. & BANGHAM, C. R. (1996). Population dynamics of immune responses to persistent viruses. *Science* **272**, 74–79.
- NOWAK, M. A. & MAY, R. M. (2000). *Virus dynamics. Mathematical principles of immunology and virology*. Oxford: Oxford U.P.
- NOWAK, M. A., TARCZY-HORNOCH, K. & AUSTYN, J. M. (1992). The optimal number of major histocompatibility complex molecules in an individual. *Proc. Natl. Acad. Sci. U.S.A.* **89**, 10896–10899.
- OGG, G. S., JIN, X., BONHOEFFER, S., DUNBAR, P. R., NOWAK, M. A., MONARD, S., SEGAL, J. P., CAO, Y., ROWLAND-JONES, S. L., CERUNDOLO, V., HURLEY, A., MARKOWITZ, M., HO, D. D., NIXON, D. F. & MCMICHAEL, A. J. (1998). Quantitation of HIV-1-specific cytotoxic T lymphocytes and plasma load of viral RNA. *Science* **279**, 2103–2106.
- OZBUDAK, E. M., THATTAI, M., LIM, H. N., SHRAIMAN, B. I. & VAN OUDENAARDEN, A. (2004). Multistability in the lactose utilization network of *Escherichia coli*. *Nature* **427**, 737–740.
- PERELSON, A. S., NEUMANN, A. U., MARKOWITZ, M., LEONARD, J. M. & HO, D. D. (1996). HIV-1 dynamics in vivo: virion clearance rate, infected cell life-span, and viral generation time. *Science* **271**, 1582–1586.
- POULIN, J. F., VISWANATHAN, M. N., HARRIS, J. M., KOMANDURI, K. V., WIEDER, E., RINGUETTE, N., JENKINS, M., MCCUNE, J. M. & SEKALY, R. P. (1999). Direct Evidence for Thymic Function in Adult Humans. *J. Exp. Med.* **190**, 479–486.
- RAJ, A., PESKIN, C. S., TRANCHINA, D., VARGAS, D. Y. & TYAGI, S. (2006). Stochastic mRNA synthesis in mammalian cells. *PLoS. Biol.* **4**, e309.
- RODEWALD, H. R. (1998). The thymus in the age of retirement [news; comment]. *Nature* **396**, 630.

- SCHEFFER, M., CARPENTER, A., FOLEY, J. A., FOLKE, C. & WALKER, B. (2001). Catastrophic shifts in ecosystems. *Nature* **413**, 591–596.
- SEGEL, L. A. (1988). On the validity of the steady state assumption of enzyme kinetics. *Bull. Math. Biol.* **50**, 579–593.
- SEGEL, L. A., JAGER, E., ELIAS, D. & COHEN, I. R. (1995). A quantitative model of autoimmune disease and T-cell vaccination: does more mean less? *Immunol. Today* **16**, 80–84.
- STEINMANN, G. G., KLAUS, B. & MULLER-HERMELINK, H. K. (1985). The involution of the ageing human thymic epithelium is independent of puberty. A morphometric study. *Scand. J. Immunol.* **22**, 563–575.
- TYSON, J. J., HONG, C. I., THRON, C. D. & NOVAK, B. (1999). A simple model of circadian rhythms based on dimerization and proteolysis of PER and TIM. *Biophys. J.* **77**, 2411–2417.
- VAN HOEK, M. J. & HOGEWEG, P. (2006). In silico evolved lac operons exhibit bistability for artificial inducers, but not for lactose. *Biophys. J.* **91**, 2833–2843.
- VAN MEERWIJK, J. P., MARGUERAT, S., LEES, R. K., GERMAIN, R. N., FOWLKES, B. J. & MACDONALD, H. R. (1997). Quantitative impact of thymic clonal deletion on the T cell repertoire. *J. Exp. Med.* **185**, 377–383.
- VILAR, J. M., KUEH, H. Y., BARKAI, N. & LEIBLER, S. (2002). Mechanisms of noise-resistance in genetic oscillators. *Proc. Natl. Acad. Sci. U.S.A.* **99**, 5988–5992.
- WEI, X., GHOSH, S. K., TAYLOR, M. E., JOHNSON, V. A., EMINI, E. A., DEUTSCH, P., LIFSON, J. D., BONHOEFFER, S., NOWAK, M. A., HAHN, B. H. *et al.* (1995). Viral dynamics in human immunodeficiency virus type 1 infection. *Nature* **373**, 117–122.
- WINFREE, A. T. (1986). *The timing of biological clocks*. New York: Scientific American Library.
- YE, P. & KIRSCHNER, D. E. (2002). Reevaluation of T cell receptor excision circles as a measure of human recent thymic emigrants. *J. Immunol.* **168**, 4968–4979.